ABSTRACT

DEVELOPMENT OF ANALYTICAL SYSTEMS AND MONITORING OF VOCS EMISSIONS DURING POLYMER PROCESSING

by

Qin Xiang

A method using direct flame ionization detector (FID) measurement was developed to study total volatile organic compounds (VOCs) emissions during thermal degradation of polymers. This was used to estimate organic emissions from both virgin polymer resins and commingled plastics. The effects of process parameters, i. e., temperature, heating rate and residence time, were also studied. Significant VOCs emissions were observed at normal processing temperatures, particularly from recycled polymers. Each polymer showed a distinct evolution pattern during its thermal degradation. Kinetics of VOCs emissions were also studied using a non-isothermal technique. The kinetic parameters were in agreement with data from the literature.

Polypropylene, as a commodity recyclable thermoplastic, was studied in this research to evaluate the potential environmental impact resulting from VOCs emitted during multiple melt reprocessing. Unstabilized and stabilized PP homopolymers, referred to as U-PP and S-PP, were used to simulate recycled materials prone to degradation. They were evaluated for total VOCs emissions generated during multiple melt reprocessing by injection molding and extrusion respectively. Results show that the maximum amount of total VOCs from each cycle (up to six cycles for extrusion and up to ten for injection molding) did not significantly change, while the cumulative VOCs increased with increasing processing cycle for both materials. A good correlation was obtained between the cumulative VOCs increase and the Melt Flow Index increase for

the U-PP, and the MW decrease for the S-PP. Reprocessing in all cases was accompanied by decreases in molecular weight and melt viscosity as a result of thermo-oxidative degradation. Corresponding structural changes were investigated using FTIR, and the data showed increases in carbonyl content and degree of unsaturation with the increase of processing cycle number. At equivalent cycle numbers, degradation appeared to be more severe for the extruded material in spite of the longer oxidative induction time of the "as received" pellets used in extrusion. The onset and type of structural changes was shown to depend on cycle number and reprocessing method. A simulation study was also performed by multiple heating and cooling of a single U-PP sample under static conditions, and under different gaseous atmospheres. The results indicate that the actual reprocessing conditions generated emissions whose levels, and rate of generation were closer to a mild thermo-oxidative degradation rather than a pure thermal one.

Continuous nonmethane organic carbon (C-NMOC) analysis was considered to be a more accurate and on-line method for monitoring emissions during polymer processing. An improved version of the C-NMOC system was developed in this research. A multi-bed microtrap was developed to prevent the breakthrough of small molecules such as propane and methanol. Two novel sampling configurations were also developed, and were referred to as sequential valve with backflushed microtrap (SV-BM) and multi-injection sequential valve with backflushed microtrap (MSV-BM). By combining the multi-bed microtrap with the SV-BM and MSV-BM configurations, ideal performances were obtained in terms of linearity, reproducibility of multiple injections and separation of background gases. Both small molecules and large molecules could be effectively collected and desorbed with the optimized microtrap.

DEVELOPMENT OF ANALYTICAL SYSTEMS AND MONITORING OF VOCS EMISSIONS DURING POLYMER PROCESSING

by
Qin Xiang

A Dissertation
Submitted to the Faculty of
New Jersey Institute of Technology and
Rutgers, The State University of New Jersey - Newark
In Partial Fulfillment of the Requirements for
the Degree of Doctor of Philosophy

Department of Chemistry and Environmental Science

January 2002

APPROVAL PAGE

DEVELOPMENT OF ANALYTICAL SYSTEMS AND MONITORING OF VOCS EMISSIONS DURING POLYMER PROCESSING

Qin Xiang

Dr. Somenath Mitra, Dissertation Advisor — Date
Professor of Chemistry
Director of Environmental Science Program, NJIT

Dr. Barbara Kebbekus, Committee Member — Date
Professor of Chemistry
Associate Chair for Environmental Science, NJIT

Dr. Marino Xanthos, Committee Member — Date
Professor of Chemical Engineering, NJIT

Dr. Richard Trattner, Committee Member — Date
Professor of Chemistry, NJIT

Dr. Nicholas Snow, Committee Member — Date
Associate Professor of Chemistry
Associate Chair of Department of Chemistry and Biochemistry
Seton Hall University, South Orange, NJ

BIOGRAPHICAL SKETCH

Author: Qin Xiang

Degree: Doctor of Philosophy

Date: December 2001

Undergraduate and Graduate Education:

- Doctor of Philosophy in Environmental Science,
  New Jersey Institute of Technology, Newark, New Jersey, 2001
- Master of Science in Chemistry
  Sichuan University, Sichuan, P. R. China, 1994
- Bachelor of Science in Chemistry
  Sichuan University, Sichuan, P. R. China, 1991

Major: Environmental Science

Presentations and Publications:

Xiang, Q., Mitra, S., Xanthos, M. and Dey, S. K.,
"Evolution and Kinetics of Volatile Organic Compounds (VOCs) Generated During Low-Temperature Polymer Degradation", Journal of the Air & Waste Management Association, in press, 2001.

Xiang, Q., Xanthos, M., Mitra, S., Patel, S. H. and Guo, J.,
"Effects of Melt Reprocessing on Volatile Emissions and Structural/Rheological Changes of Unstabilized Polypropylene", submitted to Polymer Degradation and Stability, 2001.

Xiang, Q., Xanthos, M., Mitra, S., and Patel, S. H.,
"Effects of Material Type and Reprocessing Conditions on Volatile Emissions of Melt Degraded Polypropylene", submitted to Advances in Polymer Technology, 2001.

Xiang, Q., Xanthos, M., Mitra, S., and Patel, S. H.,
"VOC Emissions and Structural Changes of Polypropylene During Multiple Melt Processing", Annual Technical Conference - Society of Plastics Engineers, 59th SPE ANTEC, Vol. 2, pp. 1806-1810, 2001.

Xiang, Q., Mitra, S., Xanthos, M., and Dey, S. K.,
"Kinetic Analysis of VOC Emissions Thermally Generated from Polymers at Processing Temperatures", National Meeting of the American Chemical Society, Extended Abstract, Vol. 41, No.1, pp. 59-61, 2001.

Xanthos, M., Xiang, Q. and Mitra, S.,
"Relationships between VOC Emissions and Structural Changes during Reactive Degradation of Polypropylene", The Seventeenth Annual Meeting of the Polymer Processing Society (PPS-17), Montreal, Canada, May, 2001.

Xiang, Q., Mitra, S., Dey, S. and Xanthos, M.,
"Analytical System for Measuring Thermally Generated VOC Emissions from Polymers", 58th SPE ANTEC, Vol. 2, pp. 2168-2172, 2000.

Xiang, Q., Mitra, S., Dey, S. and Xanthos, M.,
"Continuous On-line Monitoring of VOC Emissions Generated During Polymer Processing", the 39th Annual Eastern Analytical Symposium, Atlantic City, NJ, October 29 - November 3, 2000.

To my beloved family

ACKNOWLEDGMENT

I would like to express my deepest appreciation to Dr. Somenath Mitra, who served as my research advisor, and Dr. Marino Xanthos for his guidance as the co-advisor in the polymer segment of this research. Special thanks are given to Dr. Barbara Kebbekus, Dr. Richard Trattner, and Dr. Nicholas Snow for actively participating in my thesis committee.

Financial support for this work was provided by the Multi-Lifecycle Engineering Research Center (MERC) of NJIT, which is partially funded by the New Jersey Commission on Science and Technology (NJCST). Thanks are also due to Department of Chemistry and Environmental Science for providing financial support through the teaching assistantships during the first two years of graduate studies.

Special thanks are also extended to Dr. S. H. Patel, Polymer Processing Institute (PPI), for his support in the FTIR analysis in this research, Dr. J. Guo (PPI) who provided the multiple injection molded PP samples and conducted the measurement of MFI, Dr. V. Tan (PPI) and Mr. C. Wan for their help in the DSC experiment. Samples of stabilized PP after reprocessing were supplied by Professor S. Canevarolo of the University of Sao Carlos, Brazil. I also would like to thank Dr. S. K. Dey, Dr. Q. Zhang, Dr. M. Young and Mr. D. Conti in PPI for their assistance and suggestions. Mr. Y. Gandhi (Department of Chemistry and Environmental Science), Ms. L. Barnes (MERC), and many of my fellow graduate students are deserving of recognition for their support.

TABLE OF CONTENTS

TABLE OF CONTENTS
(Continued)

Chapter **Page**

TABLE OF CONTENTS
(Continued)

Chapter **Page**

LIST OF TABLES

LIST OF FIGURES

LIST OF FIGURES
(Continued)

LIST OF FIGURES
(Continued)

LIST OF FIGURES
(Continued)

Figure **Page**

CHAPTER 1

INTRODUCTION

1.1 Importance of VOCs Measurement and Analysis

Volatile organic compounds (VOCs) include a variety of organic molecules with different functional groups. Many of them are classified as hazardous air pollutants (HAPs) by the United States Environmental Protection Agency (US EPA), and regulated by the Clean Air Act Amendments (CAAA) of 1990. They can cause eye, nose, and throat irritation, headaches, nausea, and damage to liver, kidney, and central nervous system. Some VOCs, such as benzene, methylene chloride and perchloroethylene, are known to cause cancer in animals and in humans [1]. Furthermore, VOCs cause serious health problems by photochemical reactions that form ground-level ozone, which is the principal component of smog [2]. Ozone pollution (smog) causes severe health and environmental problems, such as respiratory problems, damaging crops and plants, ruining the city landscape [3]. In addition, some VOCs play an important role in global warming and in destruction of the stratospheric good ozone [4].

VOCs are encountered virtually everywhere. The consumer items, the energy sources, and the drink water (because of the reaction between chlorine used for water disinfection and organic matter in water) all increase human exposure to these compounds [5,6]. The combination of ubiquitous exposure and possible serious health effects has long been making VOCs a major public health issue. In 1997, the US government approved strong new clean air standards for smog and soot, which could prevent up to 15,000 premature deaths a year and improve the lives of millions of Americans who suffer from respiratory illnesses [7]. To achieve this goal, the US EPA

implemented emission factors and emission inventories as fundamental tools/concepts in air quality management. These tools are important for developing emission control strategies, determining the applicability of permitting and control programs, and ascertaining the effects of sources and appropriate mitigation strategies [8]. Policies on reduction of pollution can only be designed when the extent and identity of the pollutants is known. Emissions can only be regulated based on accurate and reliable methods for monitoring the emitted materials. Therefore, measurement and analysis of VOCs is the cornerstone for protecting public health and the environment.

1.2 Developments in Sampling of VOCs from Air

VOCs are omnipresent, existing in air, water and soil. Extensive research and developments in measuring and analyzing these VOCs have been performed by environmental analytical and occupational health professionals [9]. In the last two decades, major advances have been made, and these were partially summarized by Clement, et al. [10] in their reviews. The measurements are necessary for exposure assessment, and also to understand ozone-precursor relationships on urban and regional scales. Moreover, there has been an increasing demand for improved air sampling and analysis methods due to the: (1) increasing number of regulated sources and pollutants; (2) recognition of toxicity for chemicals that were thought to be relatively harmless (e.g. formaldehyde); (3) recognition of toxic effects of more chemicals at even lower concentrations, and (4) increasing public awareness of both indoor and outdoor air quality [11]. In recent years, novel sampling and analytical methods have been developed, and applied to the characterization and analysis of toxic airborne pollutants

(including VOCs). These include sampling (design, phase distribution, sector sampling, and specific sampling devices), spectroscopy/chemometrics (optical spectroscopy, mass spectrometry, postdata processing, and data interpretation algorithms), automated analysis, faster and miniaturized instrumentation [10].

The collection of representative air samples for laboratory analysis remains as the most challenging part in air monitoring and analysis [10]. Proper sampling and sample storage procedures are essential to ensure that laboratory data are representative of the sampling site and comply with applicable technologies and regulations.

1.2.1 Developments in the Conventional Methods

In 1984, the US EPA issued a compendium of methods for monitoring VOCs in ambient air [12]. Prior to that, the National Institute for Occupational Safety and Health (NIOSH), and the Occupational Safety and Health Administration (OSHA) published analytical methods for monitoring volatiles in workplace [13,14]. These conventional methods involve collecting a grab sample, transporting the sample to a laboratory, concentrating the VOCs from a large enough quantity of air to obtain enough material to measure, and, finally, separating and identifying the individual compounds using GC, GC/MS or other analytical techniques.

Compared to the GC analysis of VOCs, which was clearly described in the methods published by EPA and other regulatory agencies, sample collection and concentration may be troublesome, and can be approached in several different ways. The two most common methods use canister or sorbent sampling. EPA Method 18, TO-14 and TO-15 employ the canister sampling [12,15], whereas, EPA Method TO-1, TO-2,

TO-3, and many NIOSH and OSHA methods use sorbent sampling [12,13,14]. The respective advantages and limitations of these two techniques have been widely discussed in the literature [16-25].

Both methods are still broadly applied to the analysis of VOCs in air [16,21, 25-29]. Meanwhile, developments have also been made to these conventional methods. For example, special canisters were developed in EPA Method TO-15 to analyze polar VOCs [30]. They were used to study the analysis, stability and recovery of aldehydes and terpenes [21]. Sorbent-based sampling methods have been developed as active samplers (pumped sorbent tubes) and passive (diffusive) samplers. Active sampling is broadly applied to the determination of VOCs in ambient air, especially after the Method TO-17 supplemented the US EPA Compendium of Methods for the Determination of Toxic Volatile Organic Compounds in Ambient Air [12,31,32]. The development of TO-17 was motivated by interest in the use of a new generation of thermal desorption systems as well as the newest solid adsorbents that are available commercially. Shojania et al. [33] reported on their sampling device, an inside needle capillary adsorption trap, and examined the effects of sample volume in active sampling and exposure time in passive sampling on the analyte adsorption. Passive samplers were originally developed to estimate exposure of individuals to VOCs in the workplace. They were designed as portable and noiseless devices without a power supply, suitable for measurement of indoor air pollution. Although they are very simple and convenient to use compared to the active samplers, passive samplers are only used occasionally for the measurement of VOCs at ppbv or sub-ppbv levels in outdoor and indoor air [34]. There are two main reasons for their low popularity in the ambient air VOCs monitoring programs. One is

their validation, which is required by the validation protocols but is very time consuming and expensive to carry out. The other reason is the high cost of current passive samplers [23,35].

Almost all canister and sorbent sampling applications need a cryogenic preconcentration prior to separation and detection of the compounds. Thus, the cryogenic technique itself has been developed to effectively collect VOCs in air. In this method, air is passed through a loop immersed in liquid nitrogen (or oxygen, or argon) in order to condense the VOCs. The sampling loop can be filled with glass beads in order to improve the trapping efficiency [24]. The main difficulty with cryogenic sampling is the storage of the samples until analysis. So nearly, all applications of cryogenical collection of samples are followed by immediate analysis of the samples, e.g., by (automatically controlled) on-line connections between the cryogenic sample trap and the analytical instrument [36]. In addition, the cryogenic technique has to deal with water management interference, even more so than the sorbent sampling technique. Because cryogenic preconcentration is carried out at very low temperatures (less than $-150^{\circ}C$), water vapor can be trapped quantitatively [23].

Sorbent sampling, canister sampling as well as cryogenic sampling enable the effective determination of VOCs in ambient air. This fact, in itself, indicates that each of them has its field of application. The selection of a sampling technique is primarily governed by the objective of the analysis. When using sorbent sampling, attention must be paid to avoid introduction of artifacts and contamination, e.g. during storage. In this technique, breakthrough can be reduced by the use of multi-bed sorbent tubes. Also, in the canister sampling method, the stability of the sample during storage must be taken

into account, because of possible inner surface interactions. From this view, cryogenic sampling is preferred since it avoids the storage step. However, as far as the determination of VOCs at a remote site is concerned, the difficulty of storing cryogenic samples can be a limitation for applicability of this sampling technique [24].

1.2.2 Sorbents for Air Sampling

A wide range of solid sorbents have been used in the measurement of VOCs in air [23,37,38]. Nevertheless, research on the development of new types of sorbents has been reported. Just as promoting the establishment of Method TO-17, the developments in new adsorbents have greatly enlarged the application of sorbent-based sampling in air analysis. An ideal sorbent needs to have four main properties, i.e. infinite breakthrough volume (BTV) for the compounds to be sampled, complete desorption of the target compounds at moderate temperatures, no generation of artifacts and no retention of water vapor. Moreover, it must be possible to seal the sorbent completely from the atmosphere so that contamination before and after sampling can be excluded [23]. No single available sorbent material meets all of these criteria. There is a tendency to use multiple sorbents, which allows one to focus on a wide range of VOCs [24,37].

In the meantime, new types of sorbents have been researched [37,38]. They include porous carbon - the pyrolysis products of saccharose and cellulose (pyrolysis in the presence of silica gel) [37], activated carbon manufactured from pith with a low ash content, carbon molecular sieves made by dehydrohalogenation of poly(vinylidene chloride), cleaned crosslinked styrene [38]. Simpson et al [39] synthesized and characterized an emerging class of VOCs sorbents: Friedel-Crafts modified polystyrene.

They aimed at identifying replacements for activated carbon in pollution control applications, and to demonstrate the feasibility of using these polymer replacements in VOCs recovery applications. A new graphitized carbon black adsorbent (Carbograph 5) was characterized, and combined with other sorbents to form multi-layer cartridges to quantitatively determine VOCs in air [40]. A novel material, mesoporous silicate MCM-41, was developed and believed to have potential applications in adsorption, catalysis, and nanotechnology [41]. It possesses hexagonally packed arrays of one-dimensional cylindrical pores with large surface area and pore volume, so it was proposed as an alternative adsorbent for VOCs abatement. The organophilicity of MCM-41 was studied and compared with hydrophobic silicalite-1 using adsorption and temperature-programmed desorption methods.

In contrast to an adsorption process, equilibrium sorptive enrichment is used to concentrate VOCs in the air sample prior to analysis. This allows the use of a high-inertness sorption material, such as polydimethylsiloxane (PDMS). PDMS is basically a new type of sorbent since it is based on an absorptive process instead of an adsorption process [10,23]. This polymer has some advantages when compared to the other materials. First, water retention is low. Secondly, its degradation products are usually not compounds that are to be detected in ambient air sampling. Thirdly, it provides an analytical blank free from interference. Furthermore, since PDMS is a widely used polymer in GC, information about sorption equilibrium can be gained from research work done in the field of GC (e.g. Kovats indices as estimates for gas/polymer equilibrium coefficients). The main limitation however in the development of PDMS as a sorbent material is the mass transfer rate of the compounds from the air matrix to the polymer

[23]. The use of new sampling media such as mesoporous carbons and a reversed-phase packing material (C_{18}-Silica) for airborne VOCs sampling was also evaluated against criteria such as compatibility, reusability, and background interference in the GC analysis [10].

In addition, financial considerations are taken into account during the development of adsorbents. This can be achieved by deriving adsorbents from inexpensive raw materials and chemical treatment. These raw materials include saccharose and cellulose [37], activated coals [42], and even natural crab shell [28]. The last one was evaluated as an adsorbent for preconcentrating airborne VOCs collected in a canister. The by-product of fullerenes production, fullerenes-extracted soot, was also applied as adsorbent to collecting VOCs in air [43]. This by-product results from fullerenes extraction from soot generated by graphitized carbon evaporating under arc discharge. Unlike graphite with regular lattice and graphitized carbon produced from carbon blacks, the fullerenes-extracted soot is complex multicomponent mixture, which is abundantly porous and has a large specific area.

1.2.3 Multi-bed Sorbent Trap

Although a number of sorbent materials have shown utility for trapping and thermal desorption of organics [23,37,38], no single material can individually handle the complete range of VOCs encountered in the environment. Thus, a combination of sorbents is necessary. The best approach is to make sorbent tubes containing layers of different materials to attain the desired collection and desorption efficiency. Sequential trapping takes place in these so-called multi-bed sorbents, where the air sample passes

progressively through the weakest sorbent to the strongest. The materials would ideally have the ability to stand up to repeated use and heating without changing their characteristics and should additionally give a low background in the analysis. It is also desirable that they would have a low affinity for water.

The use of multi-bed sorbent traps for VOCs sampling followed by thermal desorption-GC/MS (TD-GC/MS) analysis has been popular since the introduction of the Method TO-17 in 1996 [10]. It has been reported in scientific and commercial literature that combination of carbon sorbents allows the sampling of a large variety of compounds differing in polarity (non-polar/polar compounds) and volatility (C_2-C_{15}) at various concentration levels [23-25,37,40,44]. Supelco Inc. (Supelco Park, PA) produces several combinations of carbon sorbents in multi-bed adsorbent tubes. Many of these tubes have 2 to 4-mm I.D. and are used to refocus the analytes after thermal desorption without the need of cryofocusing.

Since humidity affects the adsorption phenomena and/or the chromatography (GC-MS), selection of the proper adsorbent with a lower affinity for water is very important. Various approaches to selective removal of water from sampled air have been developed, but these are connected with the losses of some components [23,37,40]. Supelco proposed a combination of graphitized carbon blacks (GCBs) with carbon molecular sieves (CMS) for monitoring volatile and semi-volatile compounds as they enable sampling in highly humid conditions, e.g., Carbotrap and Carbosieve S-III [45,46]. There is, however, contradictory information in the literature in this regard, that Carbosieve S-III would lead to enrichment of water [23,24].

Compared to the commonly used adsorbents, such as Tenax, porous polymers and graphitized carbons, carbon molecular sieves (CMS) are the most efficient adsorbents to quantitatively trap the most volatile species due to their high adsorption capacity. Simmonds et al. [44] found that the most efficient adsorbents for trapping hydrohalocarbons were a CMS sold under the trade name of Carboxens (Supelco Inc., Bellafonte, PA). Helmig and Greenberg [47] also concluded that a multi-adsorbent trap containing Carbotrap C, Carbotrap B and Carbosieve S-III gave the best results because of the wide range of compounds that could be trapped without breakthrough. However, Carbosieve S-III retains more water than Tenax [23,24]. The affinity of Carboxen 1000 for water vapor is also well known, and some decrease in capacity for the target vapors was expected [48,49]. Therefore, to achieve the maximum efficiency in VOCs sampling, optimal combinations of multiple sorbents should be chosen by carefully considering their adsorption capacity for both interested analytes and moisture.

In this research, based on the breakthrough data and the effect of humility, Carboxen 564, Carbopack B and Carbotrap C were chosen to construct a multi-bed microtrap. This was done by sequentially packing the adsorbents into a small diameter tubing. Due to its low thermal mass, the microtrap could be heated rapidly to generate a sharp injection of the trapped VOCs into an analytical system. The performance of this multi-bed sorbent was characterized with both large molecules (e.g., toluene) and small molecules (e.g., propane, and methanol).

1.2.4 Solid Phase Microextraction (SPME)

Solid phase microextraction (SPME) is a recent development in sampling and sample preparation for trace analysis. This technology uses a small, polymer-coated fiber to extract analytes directly from an aqueous or gaseous phase. Hence, sampling, extraction and concentration are accomplished in a single step. The adsorbed analytes can be easily desorbed into an analytical instrument via the heated injection port. Thus, this technology is fast, solvent-less, and offers the benefits of minimal sample loss, and maximum sample utilization, since there is no dilution involved. The first SPME device was developed in 1989 and reported in 1990 by Pawliszyn [10,50]. Continued interest in SPME has been fueled by its commercialization by Supelco (Bellefonte, PA) in 1993, and by the choice of almost a dozen different fiber coatings, which allow the analyst to optimize the extraction of various compound classes. The use of SPME has exploded in the last few years. It can be considered a universal extraction method, as it can be used on gases, liquids, and solids (the headspace above the solid is typically sampled). It has been applied to the detection of diesel exhaust, gasoline in fire debris, solvent in water and work space, odors in drinking water, volatile and semi-volatile pollutants in soil, flavor and aroma volatiles in whole fruits [11,50-52].

Air monitoring is a relatively new application of SPME [10,11,51-53]. When the SPME fiber is exposed to the air matrix, the analytes partition between the polymer coating and the sample until equilibrium is reached. The equilibrium time varies from seconds to hours. The amounts of analytes partitioned to the coating are proportional to their initial concentrations in the matrix. As such, SPME is particularly suited for air sampling, where the effects of partitioning on initial analyte air concentration are

negligible. Analysis of SPME fibers usually consists of direct transfer of the SPME fibers to a GC injector. In most cases, after desorption in a GC injector lasting from several seconds to minutes, the SPME fiber is analyte-free, and the device may be immediately deployed for another air sample. The SPME fibers are applicable for long-term and occupational exposure sampling, and also applicable for non-equilibrium sampling and very short sampling times. The flexibility of selection of a wide range of sampling times, which is possible with a single SPME device, e.g., from less than 1 min to days, is not currently achievable with conventional methods [11].

SPME can be easily coupled with GC, and requires no solvent. This makes it an excellent sample preparation technique for field analyses, and is particularly well suited to rapid response applications. There are many publications about this technique. However, some aspects of SPME, including the fundamentals of how analytes interact with the fiber coatings and the stabilities of analytes collected on a fiber, remain to be addressed. In addition, obtaining accurate quantitation with SPME can be challenging. One reason is that factors such as matrix composition, temperature, pH, and extraction times, must be strictly controlled. The other is due to a limited amount of adsorbent that can be coated on the surface of the SPME fiber [10]. A device similar to SPME, called an inside needle capillary adsorption trap (INCAT), was reported to sample VOCs in air actively and passively [33]. This INCAT device had an adsorbing carbon coating on the interior surface of a hollow needle.

The development of an improved SPME method results in a relatively new method – stir bar sorptive extraction (SBSE) [54]. In SBSE, a glass stir bar was coated with poly(dimethylsiloxanes) (PDMS). It possessed up to 500x of loading capacity of a

typical SPME fiber, and was successfully applied for the sampling and quantitative analysis of airborne VOCs and semi-VOCs. More applications of this new SBSE method are expected in the future.

1.3 Developments in Detecting VOCs

Besides the recent developments in sampling, there are more trends in environmental analysis. One is the implementation of faster analysis and more automation (e.g., direct introduction MS, SPME coupled with GC). Another is the move towards miniaturization of instrumentation (e.g., GC with acoustic wave detector, capillary electrochromatography) and field portable instrumentation. The demand for faster time responses has lead to a proliferation in essentially uncoupled detector-only instruments. For example, the uncoupling of mass spectrometry from chromatographic stages using a direct ionization or protonation of analytes in air is gaining in popularity [55,56].

1.3.1 Gas Chromatography (GC)

Given the high complexity and low abundance nature associated with ambient VOCs, the chromatographic methods are preferred for their efficient separation and detection capability over other analytical means. However, conventional GC analysis is slow in separation. Additionally, the involvement of cryogenic sorbent traps for preconcentration has inherent disadvantages. The logistical problems arising from cryogen supply also renders this preconcentration method very undesirable for field analysis [57]. In recent years, the demand for accurate, sensitive, faster and simple techniques for the monitoring of low levels of VOCs in the atmosphere has increased tremendously. Responding to this,

high-speed, high-resolution, automated and field portable GC systems have been developed.

One technique is using dual sampling loop or trap as preconcentrator, coupled with one or dual column to realize continuous, near-real-time analysis [57-61]. This whole system allowed continuous measurement of VOCs without the use of cryogen for preconcentration and oven cooling. It also substantially enhanced the number of compounds that can be separated and detected simultaneously.

Another trend is using simultaneous detection by different detectors, or by comparing retention times from GC columns of different polarity for validation. This technique increases sensitivity because no effluent splitting is required. Meanwhile, sample throughput is much enhanced since several items of information are obtained simultaneously. Thus, misidentification due to overlapping peaks can be drastically reduced [62]. Simultaneously used stationary phases include 100% PDMS (C_1- to C_{10}-VOCs), Al_2O_3/KCl porous layer open tubular (PLOT) columns (C_2- to C_5-VOCs) and a permethylated ß-cyclodextrin column (C_6- to C_{11}-VOCs). The detectors used in these new identification systems can be universal ones such as FID, less-specific ones such as ECD, and specific ones such as mass spectrometry (MS) [24,62]. These detectors can be used sequentially or simultaneously. The reported combinations include ECD/FID, either in series [62] or in parallel [63], photoionization detector/electrolytic conductivity detector (PID/ELCD) in parallel [64], Fourier transform infrared/mass spectrometric detector (FTIR/MSD) in series [65], PID/FID/dry ELCD in series [11], PID/ECD/FID in series and FID/MS in parallel [24].

High-speed gas chromatography (HSGC) has become a more highly developed technique in the past few years [56,59,66]. Its instrumentation utilizing narrow injection pulses has led to separation times for mixtures of VOCs that are 10-60 times faster than those of traditional GC techniques, with little or no loss of resolution. High-speed GC analysis was also achieved with temperature programming and a constant (tuned) junction-point pressure [61]. Moreover, a new detection technique, atomic emission detection (AED), was very recently employed in GC analysis, due to its unique selectivity and sensitivity [67,68].

1.3.2 Mass Spectrometry (MS)

Mass spectrometry (MS) has long been playing a prominent role in environmental monitoring because of its high chemical specificity and exquisite sensitivity; molecular weights and structural information are both available through the appropriate choice of ionization methodology [69]. It has been extensively used in environmental analysis by coupling with GC to provide sensitive and reliable measurements. However, many of its applications are time-consuming and do not offer sufficiently rapid analytical methods for reliable control of emissions. The demand for faster time responses leads to a rapid increase in the development of direct introduction mass spectrometry (DIMS). In DIMS, analytes from a sample are directly introduced into a mass spectrometer using a simple interface with minimal sample preparation and no prior chromatographic separation [56].

The most common inlets for DIMS include capillary restrictors, membranes, atmospheric pressure ionization (API) and atmospheric sampling glow discharge ionization (ASGDI) [70]. The applications, advantages and limitations of these

techniques have been widely reported in literature [55,69-74]. However, it is worthwhile to be mentioned that only very recently, membrane inlet mass spectrometry (MIMS) is widely developed and applied for the analysis of VOCs in air [69-74]. The major disadvantages of MIMS include slower instrument response, temperature-dependent performance, potential cross-contamination (memory effects), and membrane selectivity between polar and nonpolar compounds. Sudden rupture of a membrane may also lead to serious damage of the MS [55,70].

Proton transfer reaction mass spectrometry (PTR-MS) is a very recent development. It allows MS for on-line measurements of trace VOCs with concentration as low as a few pptv. Lindinger et al. [75] reported their PTR-MS system in 1998. The advantage of this PTR-MS method is that ambient VOCs can be monitored simultaneously and on-line down to the 10 pptv range without the need for preconcentration or chromatography. An additional significant feature of the PTR-MS instrument is that it can be operated for extended periods of time, e.g. days, weeks, and even months at a time with little or no interruption except for calibrations [76]. This technique has been applied to on-line analysis of VOCs emitted from trees [77,78], grass [76], cutting and drying crops [79]. Since the PTR-MS is able to measure compounds with a proton affinity higher than water with a high time resolution of 1 s per compound, nearly all VOCs can be detected on-line [78]. This technique has many potential applications in food research, medical and environmental analysis by measuring VOCs emissions from various resources [75,80].

1.3.3 High Performance Liquid Chromatography (HPLC)

HPLC is a powerful, practical, and hence, common separation technique used for analysis of chemical and biochemical mixtures. The success of HPLC is due to the attention given to developing column technology, establishing rigorous separation protocols, and improving detection methods. Several on-line methods have been developed and shown success either by providing selective information, such as *m/z* rations when interfacing HPLC with MS, or by providing structural information when combined with NMR, FTIR, Raman and Fluorescence Spectroscopy [71,81,82]. However, most of these applications are for the analysis of SVOCs in water or bio-matrix.

In air analysis, HPLC is mainly developed with appropriate sampling for the measurement of airborne oxygenated VOCs and SVOCs. With the development of 2,4-dinitrophenylhydrazine (DNPH) cartridge sampling and in-situ derivatization, HPLC has been employed to measure carbonyl compounds in ambient air [83,84], and those emitted from motor vehicles [65], crops [79], and air filters of HVAC systems [85]. This DNPH derivatization-HPLC method is very selective, sensitive, and reliable. However, the use of HPLC can be cumbersome and the detector, usually UV detector, lacks the specificity offered by a mass detector. In view of these requirements and taking advantage of the state-of-the-art bench top GC/MS systems, those oxygenated VOCs and SVOCs have been recently analyzed by using GC/MS with new sampling and sample preparation methods [10].

1.3.4 Sensors

Recent advances in both miniaturization and "micro" versions of traditional analytical techniques drive the development of sensing systems. Typical sensors used in those systems are quartz crystal microbalances (QCM), surface acoustic wave devices (SAW), semiconductor gas sensors and conducting polymers [55,86]. The chemical-selectivity of a sensor-based system is conferred via three approaches [87]. The "traditional" approach uses a single sensor functionalized with a chemically sensitive material selective for the analyte. The second approach is to separate analytes in time, space or the spectral domain. The third approach, using sensor arrays, is the most recently developed technology. One array can be composed of optical fibers, electrochemical sensors, chemiresistors, metal oxides, and/or thermal devices. Designing a sensor array for a particular application should include the evaluation of coatings from many categories: metal films, ceramics, organic, organometallic, and inorganic semiconductors, organometallic compounds and coordination complexes, organic oils and waxes, and a vast collection of organic polymers [87]. Assuming a wide range of thin films is available, there remain two difficult questions: How many sensors should comprise the array, and which films should be selected?

Nakamura et al. [86] developed QCM odor sensors by choosing 24 sensing film materials from GC stationary phases and lipids. These films were classified and evaluated with 41 VOCs and odorants. Although metal oxides based semiconductor gas sensors are commercially available, some researchers manufactured their own sensor arrays with 10 and 15 thin films of tin oxide [88,89]. These arrays were applied to the recognition and quantification of VOCs in air. This kind of semiconductor gas sensors was also combined

with QCM devices, electrochemical sensors and calorimetric sensors [90]. This hybrid modular sensor system was used to quantitatively identify odors and flavors.

Furthermore, the use of mass sensitive devices on the basis of SAW have been demonstrated for the analysis of volatile organic solvents, and for the determination of complex organic vapor mixtures like odors [91]. Ricco, et al. [87] evaluated a number of chemically sensitive interface materials for SAW. Their long-term goal is to assemble of a "library" of chemically sensitive interfaces whose responses to a range of vapors and gases are characterized, allowing selection of the best subset of materials for a particular application scenario. An array of polymer-coated SAW sensors was used with vacuum-outlet GC to perform high-speed analysis of complex indoor VOC mixtures. The entire mixture of 42 VOCs and SVOCs was analyzed in about 400 seconds [61]. As stated by Ricco et al. [87], the next generation of chemical sensor systems is likely to increase discrimination capabilities while maintaining or shirking the number of sensor elements. This can by realized by (1) the use of heterogeneous arrays, (2) measurement of multiple physical parameters, e.g., mass and conductivity, for each chemically sensitive interface, (3) measurement of response kinetics, and (4) measurement of controlled extrinsic perturbation-dependent responses, e.g., temperature or wavelength dependence.

1.3.5 Non-methane Organic Carbon (NMOC) Analyzer

Non-methane organic carbon (NMOC) is a measure of total organic carbon except that from methane. It is a convenient and useful way of expressing total VOCs in terms of parts per million (or billion) of carbon (ppm_c or ppb_c), because methane is nontoxic and non-reactive in the atmospheric photochemistry leading to smog formation. When

speciation of the individual compound is not required, NMOC can be a fast and inexpensive way of measuring VOCs in ambient air, or in an air emission. This measurement also allows different emission sources to be compared in terms of total carbon emissions irrespective of the specific compounds being emitted [92]. The conventional NMOC analyzer, as described in EPA standard method 25, has its inherent disadvantages, such as the interference from high concentrations of moisture and CO2, relatively high detection limits, and the inability to do on-line monitoring [93].

To solve these problems, a microtrap based NMOC system (referred to as C-NMOC) has been developed [94-97]. This instrument combines the microtrap with a sampling valve and a conventional oxidation/reduction NMOC detector. Besides being an on-line concentrator and injector, the microtrap serves as a separator that isolates NMOC from H_2O, CO, CO_2, CH_4 and other background gases. This novel system has been successfully used to evaluate the performance of a laboratory scale catalytic incinerator, and also field tested at an industrial site (a coatings facility in North Carolina) to evaluate its viability as a continuous emission monitor (CEM) [92,98]. In this work, a new combination of multiple sorbents was used to further improve the collection efficiency of small molecules by the C-NMOC analyzer. In addition, novel sampling configurations were developed with the multi-bed microtrap and the C-NMOC analyzer to meet various analytical needs.

1.4 Measurement of VOCs Emitted from Polymers

1.4.1 Origin of VOCs Emissions

Organic emissions can be generated biogenically and anthropogenically. On a global scale, biogenic sources represent a more sizable contribution, accounting for about 80% of the emissions [4]. The most abundant ambient VOCs vary both in concentration and order depending on geography and year. The following VOCs appear on the top list: monoterpenoids, isoprene, propane, toluene, isopentane and ethylene. The first two compounds are naturally emitted by vegetation, and the others are produced mainly by fossil fuel combustion and industrial processes [27,29,99]. In the USA, organic emissions from anthropogenic sources are comparable in magnitude to those from biogenic sources [4,99]. Among anthropogenic sources, industrial processes generate the highest amount of VOC emissions (58%), followed by motor vehicles (37% of VOCs) and consumer solvents (5% of VOCs) [3]. As the plastic processing industry has grown to its present size, its emissions, consisting of volatiles and particulates, constitute 5% of the actual tonnage of resins processed annually in the United States. There has been an increasing interest on the part of government agencies that have regulatory responsibilities. The EPA and the Occupational Safety and Health Administration (OSHA) have been concerned with a number of potential problems related to emissions from the plastics processing industry. Meanwhile, the Food and Drug Administration (FDA) is mostly concerned with the suitability of plastics products for food and drug packaging and consumer usage [100].

A wide range of VOCs are generated during extrusion, injection molding and other polymer processing steps with concomitant potential environmental impacts.

The types and the amounts of VOCs emitted depend upon the material used and the operating parameters. Although most thermoplastics are processed well below their decomposition temperatures, some resins may begin to decompose at the high end of the processing temperatures. In addition, VOCs emissions may occur at fairly low temperatures from volatile additives such as antioxidants, UV stabilizers and low-molecular-weight plasticizers [100].

1.4.2 Conventional Approach: Thermal Analysis

Polymer degradation is ubiquitous in that it can occur at any stage of its lifetime, such as during polymer formation, during recovery and processing, and in end-use period. Degrading polymer molecules undergo a series of reactions. This leads to the formation of monomeric molecules, oligomers, chain fragments, and new compounds [101]. The thermal stability of polymers and features of the degradation processes are most commonly investigated by means of thermo-analytical techniques. These include thermogravimetric analysis (TGA), differential thermal analysis (DTA) and differential scanning calorimetry (DSC).

TGA is a technique in which the *mass* of the sample is monitored against time (or temperature) while the temperature of the sample is programmed in a specified atmosphere. Whereas, in DTA, the *difference in temperature* between the sample and a reference material is monitored, and in DSC, the *difference in heat flow* (power) to a sample (pan) and to a reference (pan) is monitored. Careful distinction should be made between the terms *derivative* and *differential*. Differential techniques involve the measurement of a *difference* in the property between the sample and a reference.

Derivative techniques imply the measurement or calculation of the mathematical first derivative, usually with respect to time. For example, derivative thermogravimetry (DTG) is the measurement of the *rate* of weight loss plotted against temperature [102]. DTG trace is frequently drawn only in order to enhance the steps in the thermogravimetric curve.

Because of its simplicity and the information afforded from a simple thermogram, TGA is widely used in the characterization of polymeric materials. These applications include comparisons of the relative thermal stability, the effect of additives on the thermal stability, moisture and additive contents, studies of degradation kinetics, direct quantitative analysis of various copolymer systems, oxidation stability, and many others. DTA and DSC are routinely used to measure glass transition temperatures, melting points, degree of crystallinity, heats of fusion and/or crystallization, decomposition temperature, and numerous other parameters [103]. The recent developments in these traditional techniques not only advance the applications in polymer characterization, but also in polymer thermal degradation. The most obvious thermal analysis unit to study thermal degradation is TGA. It is extensively used to study thermal decomposition, to determine moisture, volatiles and ash contents. One schematic diagram of TGA is shown in Figure 1.1. It was used for the pyrolysis of polypropylene in municipal solid waste, and the effects of moisture were studied [104]. When the polymer degradation involves cross-linking, it is generally observed as an exothermic process on DSC [105].

However, any single thermal method can not always give sufficient information to tell what is occurring. For example, DTA and DSC curves can not differentiate

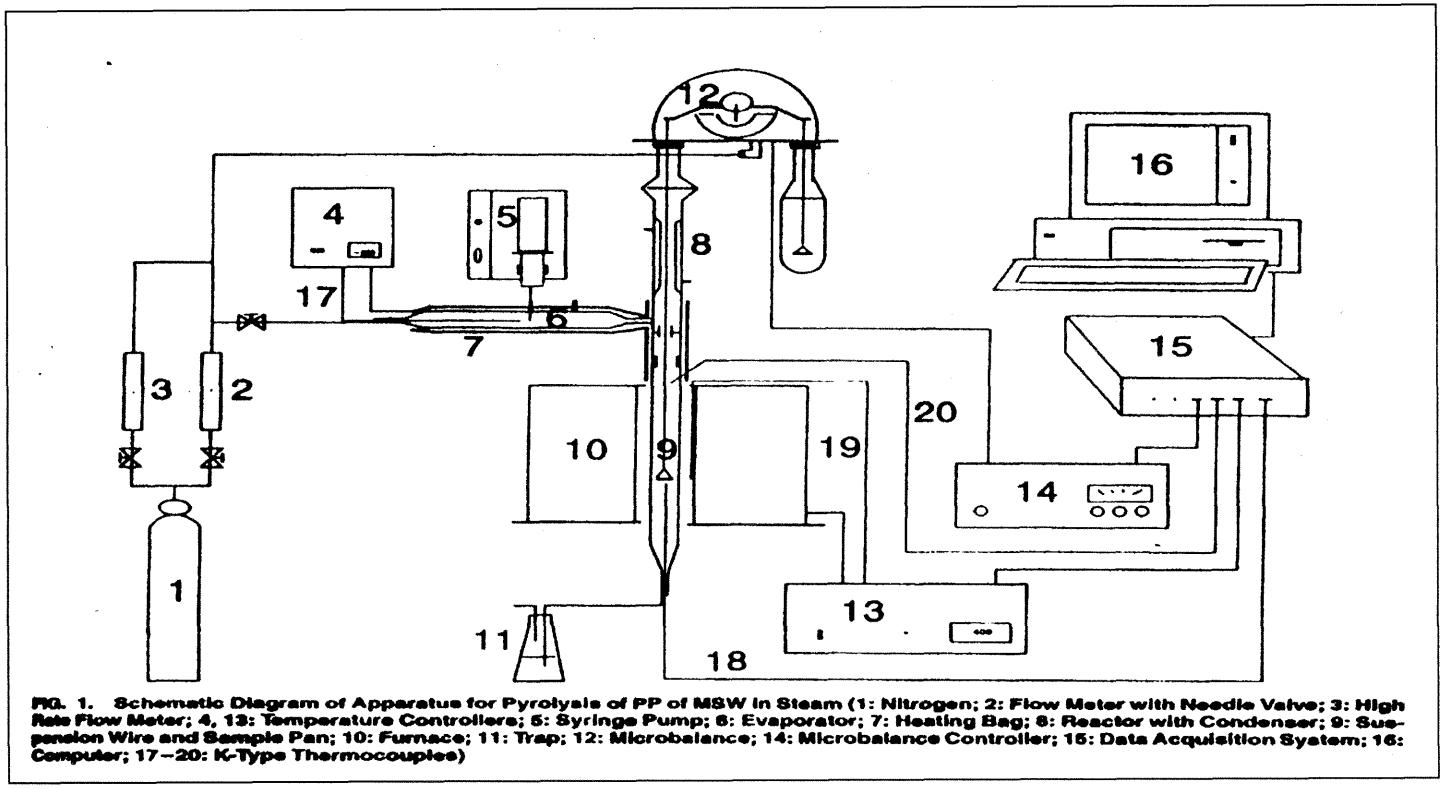

FIG. 1. Schematic Diagram of Apparatus for Pyrolysis of PP of MSW in Steam (1: Nitrogen; 2: Flow Meter with Needle Valve; 3: High Rate Flow Meter; 4, 13: Temperature Controllers; 5: Syringe Pump; 6: Evaporator; 7: Heating Bag; 8: Reactor with Condenser; 9: Suspension Wire and Sample Pan; 10: Furnace; 11: Trap; 12: Microbalance; 14: Microbalance Controller; 15: Data Acquisition System; 16: Computer; 17–20: K-Type Thermocouples)

Figure 1.1 Schematic diagram of TGA used for pyrolysis of PP in MSW [104].

a chemical reaction from a physical change, whereas TGA can not tell whether a mass loss is due to the release of organic volatiles or inorganic volatiles. This restricts its use in addressing the increasing environmental concerns about the potential impacts resulting from harmful VOCs generated during polymer degradation. It is clear that combination of several analytical methods is needed to give a better profile of the changes taking place. Very nearly, every analytical method has been employed as a complementary technique to a thermal method. Gases evolved during polymer degradation have been separated by GC, dissolved and titrated, measured electrochemically and spectroscopically, particularly by IR and by MS [105-107].

1.4.3 Characterization of VOCs Generated from Polymers

In light of the Clean Air Act Amendments (CAAA) of 1990, the reduction of various pollutants released to the atmosphere became mandatory. An established permit program requires processing plants (emission sources) to provide a baseline of their potential emissions. This is aimed at an eventual reduction in emissions [108]. As recognized by the US EPA, emission factors and emission inventories are fundamental tools to achieve this aim. In response to these needs, some studies have been conducted to determine the emission factors of some resins during processing. These resins include polyethylene (PE), polypropylene (PP), acrylonitrile-butadiene-styrene (ABS), ethylene-vinyl acetate (EVA) and ethylene-methyl acrylate (EMA) [100,108-110]. The emitted VOCs were classified and reported as hydrocarbons, aldehydes, ketones and organic acids. The measurement of hydrocarbons involved the use of Summa canister and modified TO-14 method. Aldehydes/ketones were collected with DNPH tube followed by acetonitrile

desorption, then analyzed with HPLC. For organic acids, KOH impregnated filter was used for sampling. Then the filter was desorbed with dilute H_2SO_4, and the analysis was done with ion exclusion chromatography/UV detector [108-110].

There is also growing concern regarding VOCs emitted during the usage of polymer products. A chemical composition analysis was developed and applied to the estimation of VOCs emission rates from hydrocarbon solvent-based polyurethane surface coating materials [111]. The estimation was based on the assumption that the emission rate of individual VOCs was proportional to its molar fraction in the evaporative mixture at the time, its saturated pure vapor pressure and total remaining VOCs in the material. The estimated total VOC emission rates were in good agreement with the results of weight loss experiments.

Pyrolysis-GC is well established as a method for the analysis of polymers. More specifically, pyrolysis-GC/MS has been used to analyze cured polyfunctional epoxy resins, determine the sequence of phenol units and study mechanistic and kinetic aspects of the thermal degradation of phenol-formaldehyde polycondensates [112]. In one study, it was used to identify the major VOCs released during thermal decomposition of a novolac resin (Plasti Flake 1105). Meanwhile, TGA was employed to produce information on the quantity of volatiles and the temperatures at which these volatiles evolved. These data were used to determine the basic operating parameters for the pyrolysis experiments. The objective of this study was to model under laboratory conditions, the production of volatiles, which are typical of metal pouring and casting. Data produced from TGA and pyrolysis-GC/MS were compared to assess the VOCs released during decomposition of the novolac resin. The comparison was performed to

determine the compatibility of the techniques in terms of volatilization [112]. Ross et al. coupled pyrolysis-GC with atomic emission detection (AED) for on-line analysis of VOCs (C_1-C_8), evolved from a range of samples including coal, biomass, waste tyres and plastics [67]. This analysis was performed using a tar trap, coupled to a thick film column. For the analysis of high molecular weight material, pyrolysis-GC/AED was carried out using direct transfer of pyrolysis products onto a thin film column. An off-line method for VOC material was also developed, offering a degree of selectivity and sample enrichment. Due to its unique selectivity and sensitivity to a wide range of elements, AED has been developed as one of the most powerful detectors available for GC. The potential application of pyrolysis-GC/AED system is high in many areas, including fuel analysis, polymer characterization and forensic sciences [67].

Emissions of VOCs from different thermoplastics, flame retarded polymers used in electrotechnical applications, were investigated using a purge and trap procedure. It involved adsorption on Tenax GR, followed by thermal desorption GC/MS analysis. To investigate the emission rate of volatiles from flame retardant polymers during the operation of electronic appliances, test chamber experiments were suggested to be most suitable. They were useful for obtaining an overview on the total emissions, although the sampling time required was long. Results were compared to those for an operating TV set monitored in a test chamber. Substances identified were monomers, volatile additives, or related compounds [113].

Polyethylene (PE), as one of the most common plastics, is widely used in industries involved in the packaging of items. Some of them, such as food and pharmaceuticals, are sensitive to organoleptic contamination. Therefore, the formation of

VOCs in PE is of great concern to these industries. Villberg et al. [114] analyzed the odor and taste problems in high-density PE with GC-MS-SNIFF and GC-FTIR-SNIFF systems. They also determined the off-odor compounds and VOCs in fumes from extrusion coating of low-density PE [115]. Hodgson et al. [116] reviewed the analytical methods for VOCs that originated from PE during its manufacture, processing, storage, and service life. The following methods were discussed: (i) chromatographic techniques and their associated sampling techniques, including the "hot-jar" method and dynamic headspace sampling, (ii) sensory evaluation, GC-olfactory sensing, and artificial olfaction or "electronic nose" technology.

More comprehensive reviews [100,117] presented information related to the types of volatiles emitted during the processing of commodity thermoplastics and reinforced thermosets. They were PE, PP, polystyrene, polyvinyl chloride, and other miscellaneous plastics. The analytical methods used for the VOCs measurement included GC/FID, GC/flame-photometric detector, GC/ECD, head-space GC, GC/MS, pyrolyzer-GC/MS, time-of-flight MS, HPLC, IR, TGA-GC-IR-MS, polarography and colorimetry. Those complex analyses have been made faster and easier by the advances in gas and liquid chromatography. It also attributes to the availability of new detectors and packing materials, combined with computerized data acquisition and statistical analysis methods [100].

With the development of recycling technologies, more and more waste plastics are being re-processed. On what basis should virgin or recycled plastics be chosen as a feed material is an important question. Besides economic and material considerations, environmental impact such as VOCs emissions must be taken into consideration.

Therefore, a simple and fast method is needed to evaluate the potential VOCs emissions during polymer processing. The conventional thermo-analytical techniques, such as TGA, DTA and DSC, can not provide an accurate measure of VOCs. In contrast, the chromatographic and spectroscopic techniques are powerful to characterize VOCs generated from polymers, but they are time consuming. In this research, an analytical system was developed, and a direct flame ionization detector (FID) was used to measure the emissions during non-isothermal polymer degradation. This direct FID measurement was a fast, sensitive and inexpensive method for determining total VOCs. It was also applied to studying the generation kinetics of these VOCs [118].

1.5 On-line, Real-time Monitoring of VOCs

A significant trend in analytical chemistry today is away from the use of laboratory-based methods and instrumentation towards on-line, in-situ methods. The latter provide faster information, are less expensive and often more reliable than conventional techniques [69,119-121]. A top priority in the environmental field is real-time analysis. This can be achieved by moving a laboratory to the field, or by using field-portable instrumentation to perform the measurement directly on site. Moving a laboratory is not an easy option. So the latter option is more desirable, especially since more and more technologies are available for on-site analysis. Seventeen of these technologies are covered in a manual of field methods entitled *Current Protocols in Field Analytical Chemistry* (CPFC, V. Lopez-Avila, Editor-in-Chief) [55]. Those for VOCs analysis include GC, GC/MS, DIMS, microsensor devices, infrared/near infrared (IR/NIR) spectroscopy, reagent chemistry, immunoassays, fiber optic sensors, etc.

GC is generally considered to be slow for continuous, on-line monitoring [59]. However, in the cases when continuous data is required to be reported on an hourly or every few minutes, GC is sufficiently fast. The further development of GC in real, or near real-time monitoring includes application of on-line sampling, injection technologies, and faster column separation.

To combine preconcentration and injection, a sorbent trap is placed in an on-line position with the subsequent GC analysis [23]. One such technique is the combination of microtrap systems with GC [94-97,122-124]. The microtrap is a small dimension tubing packed with one or more adsorbents. Due to its low thermal mass, it can be heated rapidly and allows immediate on-line injection of the trapped VOCs into a GC. These microtrap systems function not only as on-line injectors, but also as separator and concentrator. Membrane has been combined with a microtrap system to enable continuous GC monitoring of air and water [125-128]. Measurements in these studies were taken every 5-10 minutes, necessitated by sampling and separation times. In a field air analysis, SPME has been combined with fast portable GC to reduce the sampling and analysis time to less than 15 minutes [11].

With recent developments, GC analysis has become more and more rapid (high speed), selective (high resolution), automated and field-portable. Therefore, GC is being employed nowadays in continuous on-site monitoring systems. This is achieved by using different techniques. Dual sampling loop or trap, coupled with dual GC columns, realizes near-real-time analysis [11,57-61,66]. Sensitivity, sample throughput and identification of overlapping peaks can be dramatically enhanced by simultaneous use of different types of column stationary phases and different types of detectors [11,62-65,68,129].

Miniaturization of instrumentation drives the development of micro(chip)-GC, and sensors as detectors [55,61,66,129]. This makes GC systems not only more field-portable, but also faster. It was reported that only a few seconds were needed for the analysis of both VOCs and SVOCs by GC/SAW systems [55].

Until 1995, on-line monitoring with an MS was not considered an important technique [69,121]. However, with the demand for faster responses and more automation, direct introduction mass spectrometry (DIMS) has become a popular technique for rapid measurement of VOCs in air, water and soil samples [55,69,70]. Among DIMS, membrane inlet mass spectrometry (MIMS) gains more attention in development and applications. It possesses the apparent merits of being simple, fast, sensitive, and free of matrix effects. So MIMS is well suited for on-line, real-time analysis. It has been applied to the analysis of VOCs and SVOCs in various matrixes [10,23,71-74]. Sorbent trap followed by thermal desorption (ST/TD) has been used as direct sampling interface for MS in continuous emission monitors [130]. With this interface, detection limits of low pptv are possible. Sampling times vary from under one minute to several minutes depending on the detection level required by the application. Meanwhile, this ST/TD-MS system can provide real-time data with a sampling frequency on the order of 1 second. Detection limits have been reported in the low ppbv range. A microtrap was also reported to function as the interface for MS in the on-line monitoring of air emissions [131]. A recent development, proton transfer reaction mass spectroscopy (PTR-MS) allows MS for on-line measurements of trace VOCs with concentration as low as a few pptv [75-80]. This technique has many potential applications.

Optical instruments such as UV, IR, and laser spectroscopy, have been developed to obtain real-time data. Modern instrumentation, e.g., Fourier transform infrared spectroscopy (FT-IR), is capable of generating massive amounts of data which can be stored in low-cost storage devices. With this massive amount of data and many data interpretation tools, one can increase not only the confidence of unknown identification but also data quality. Multi-beam, real-time optical remote sensing has been used to monitor toxic emissions around a petroleum refinery [10]. This remote sensing is usually done by FT-IR, differential optical absorption spectroscopy (DOAS), and tunable diode laser spectroscopy (TDL). Infrared, especially remote FT-IR and open-path FTIR, has been popular for detection of hazardous gas pollutants with up to ppb sensitivity. The advantages of infrared gas monitoring include sensitivity, consistency and specificity. Two commercial, portable IR analyzers were employed to monitor low-level hydrocarbon emissions. With a sampling cycle of approximately 1 min, the IR analyzers were able to produce a near-real-time distribution of the hydrocarbon vapors in the test site emissions [132].

The near real-time analytical information can be used to facilitate chemical hazard assessments and to take mitigative actions during: (a) emergency responses to chemical spills; (b) remedial investigations and feasibility studies of hazardous waste sites; (c) removal operations at hazardous waste sites; (d) special investigative operations such as drum and tank head-space analysis; (e) soil gas analysis and fence line monitoring; (f) point source emission monitoring; and (g) fugitive emission monitoring. Therefore, fieldable instruments, procedures, and sampling methods should have the analytical, operational and value-added characteristics as outlined by Overton et al. [129].

The increasing demand for faster responses has lead to a proliferation in "detector-only" instruments. Besides the above mentioned DIMS techniques, a variety of sensing systems have been developed, as detector-only instruments, to provide on-site, real-time monitoring [55,86-91]. C-NMOC analyzer is a detector-only technique. It can be used under harsher conditions than DIMS and sensors. When speciation of the individual compound is not required, C-NMOC can be a fast and inexpensive way of continuously monitoring VOCs in ambient air, or in an air emission [94,95]. In this research, further improvements of the C-NMOC analyzer were achieved by using a multi-bed microtrap and novel sampling configurations.

CHAPTER 2

RESEARCH OBJECTIVE

The focus of this research is two-fold:

- Develop a fast and sensitive analytical system to study the VOCs emissions generated during polymer processing
- Improve the continuous non-methane organic carbon (C-NMOC) system

The objective of the first project was to study total VOCs emissions generated during thermal degradation of polymers. The potential environmental impact, resulting from these organic emissions, was evaluated for both virgin resins and commingled plastics. The effects of process parameters, i. e., temperature, heating rate and residence time, were studied. The kinetics and characteristics of VOCs emissions were also studied using the developed analytical system under non-isothermal conditions.

In addition, the VOCs emissions from polypropylene (PP) after multiple melt reprocessing via injection molding and extrusion were studied. The variations in emissions were correlated to the changes in chemical structure, and rheological properties. The effects of material type and reprocessing conditions on emissions and structural/rheological changes were also explored. To provide a better understanding of the extent of thermal degradation, a simulation was performed by multiple heating and cooling of a single PP sample under static conditions, and under different gaseous atmospheres.

Continuous non-methane organic carbon (C-NMOC) analysis was considered to be more accurate and on-line for the VOCs emissions during polymer processing. In the

current C-NMOC system, breakthrough of low-molecular-weight compounds is a serious problem, which can be a source of error. In this research, a backflushed multi-bed microtrap was developed to reduce breakthrough of small molecules. Meanwhile, novel sampling configurations were developed to meet various analytical needs. The performance of the improved C-NMOC system was evaluated in terms of the capabilities to adsorb small molecules, desorb large molecules, and to separate NMOC from background gases, etc.

CHAPTER 3

EVOLUTION AND KINETICS OF VOCS GENERATED DURING LOW TEMPERATURE POLYMER DEGRADATION

3.1 Introduction

A wide range of VOCs are generated during extrusion, injection molding and other polymer processing steps with concomitant potential environmental impacts. The types and the amounts of VOCs emitted depend upon the material used and the operating parameters. Although most thermoplastics are processed well below their decomposition temperatures, some resins may begin to decompose at the high end of the processing temperatures. In addition, VOCs emissions may occur at fairly low temperatures from volatile additives such as antioxidants, UV stabilizers and low-molecular-weight plasticizers [100]. Meanwhile, with the increasing cost of landfill disposal, and due to the growing concern about resource utilization, plastic recycling is receiving much attention [133]. Since commingled waste plastics contain many contaminants, the air emissions are expected to be significantly higher during the recycling process. Therefore, the VOCs emission potential of these polymers should be evaluated.

To address such environmental issues, the Society of the Plastics Industry, Inc. conducted a study to measure the emission factors for resins, such as polyethylene (PE) [109], polypropylene (PP) [108], acrylonitrile-butadiene-styrene (ABS) [100], ethylene-vinyl acetate (EVA) and ethylene-methyl acrylate (EMA) [110]. Two recent reviews [100,117] reported the analytical methods, and listed the volatiles emitted from injection molding machines and extruders. Kinetic studies on thermal degradation of virgin polymer resins such as PE, PP, polystyrene (PS), styrene-butadiene rubber (SBR), and polyethylene terephthalate (PET) have been carried out by several research groups

[104,134-141]. The majority of these studies deal with high temperature pyrolysis and the use of thermogravimetric analysis (TGA) as the tool. Little work has been reported on direct measurement of VOCs emissions and the kinetics of their generation from polymers at normal processing temperatures.

The objective of this research was to estimate the thermally generated total VOCs from pure resins and from recycled polymers. An analytical system was developed, and a direct flame ionization detector (FID) was used to measure the emissions during non-isothermal polymer degradation. This direct FID measurement is a simple, fast and inexpensive method for determining total VOCs when the identification of individual components is not required. It is routinely used in industry (EPA Method 25 A) to estimate the total organics in air emissions [142]. Two techniques namely, thermogravimetric analysis (TGA) and differential scanning calorimetry (DSC) are most commonly used in the thermal analysis of polymers. TGA measures the total weight loss, whereas DSC measures heat flux while the polymer is heated [104,134,135,139-141]. Since FID does not respond to H_2O, CO and CO_2, this approach provides a more accurate measure of organic emissions. Another advantage of this system is that the FID has a low detection limit for organics.

Another goal of this project was to study the kinetics of VOCs emissions. Reaction kinetics is normally studied under isothermal conditions. However, during irreversible thermal polymer degradation, the reactions may be initiated even before the sample is heated to the desired temperature [141,143-144]. Therefore, a non-isothermal method was applied in this work to study the polymer degradation kinetics. Another

advantage of this method is that the entire temperature range can be studied in one experimental run.

Kinetic Model for VOCs Evolution from Polymers: Thermal degradation of polymers is usually studied by the change in a measured parameter as a function of time. Frequently, the derivative form of the selected parameter is proportional to the reaction rate. Weight loss (for TGA) and heat flux (for DSC) have been the most commonly studied parameters during polymer degradation. In this study, the rate of VOCs evolution is used as the measuring quantity, and their kinetics is investigated under non-isothermal conditions.

The rate of VOCs evolution with respect to temperature (dV/dT) is given as [143-144]:

- for a first order reaction:

$$dV/dT = (k_o V_o/m) \exp \{ (-E_a/RT) - (k_o R/mE_a)T^2 \exp (-E_a/RT)\} \quad (3.1)$$

- for a reaction with order n:

$$dV/dT = (k_o/m) \exp(-E_a/RT) \{ V_o^{-(n-1)} + (n-1) (k_o R/mE_a) T^2 \exp(-E_a/RT)\}^{-n/(n-1)} \quad (3.2)$$

where, dV/dT = VOCs evolution rate with respect to temperature, T = temperature (K), k_o = frequency factor ($min^{-1}cm^{3\,(1-n)}$), E_a = apparent activation energy (kJ mol^{-1}), V_o = total volume of VOCs released ($cm^3\ g^{-1}$), m = rate of heating (dT/dt) (K min^{-1}), t = time (min), R = gas constant (kcal $mol^{-1}\ K^{-1}$).

Based on the assumptions that there is no back reaction, and the time derivative of the peaks equals zero at the temperature corresponding to the maximum in the evolution profile, Equation 3.2 can be differentiated to obtain a simple equation independent of the reaction order:

$$\ln (T_m^2 / m) = (E_a/RT_m) + \ln (E_a/k_o) \quad (3.3)$$

where T_m is the peak temperature at which the volatile evolution rate reaches a maximum for each peak. Thus, when $\ln (T_m^2 / m)$ is plotted against $1/T_m$, a straight line is obtained. From its slope and intercept, the apparent activation energy (E_a), and the frequency factor (k_o) can be determined.

3.2 Experimental

Materials: Commercial-grade low-density and high-density polyethylene (LDPE, HDPE), PP, PS and PET were used in this study. The recycled polymers used were auto shredder residue (ASR), recycled carpet residue and post-consumer PET. ASR was the refined polymeric fraction (after separation from wood and metal) which was the left-over when all useful materials including large polymer parts and metals had been recovered from an auto shredder. It was obtained from a major auto recycler. It contained approximately 75% vulcanized rubber and miscellaneous polymers along with organic impurities [145]. Carpet residue was obtained from Honeywell Corp. (developmental Q product) as dark-colored brittle flakes, containing 63-65% calcium carbonate, 15-18% PP and 12-15% SBR by weight. It was the depolymerization byproduct of Nylon 6. Carpet residue/LDPE composite was produced in-house by compounding carpet residue with LDPE at a ratio of 80/20 by weight in a twin screw extruder. Typical operating conditions were screw speed of 200 rpm, barrel zone temperature of 150°C, die temperature of 180-190°C, and die pressure of 3.5-7 MPa. Simultaneous devolatilization was performed during this compounding process [146]. Post-consumer PET comprised of recycled

pellets, nominal I.V. (intrinsic viscosity) of 0.7. All virgin and recycled polymers were used after grinding and screening as a –30 +35 mesh fraction.

Analytical System and Procedures: A schematic diagram of the analytical system is shown in Figure 3.1. The reactor was 5" long and 1/4" (OD) stainless steel tubing packed with glass fiber on both ends. About 2.0 mg of the polymer was placed in the reactor in a N_2 flow of 30ml/min. The reactor was heated in a temperature-controlled oven from room temperature to a predetermined final value. For the estimation of maximum VOCs emissions, the sample was heated at a fixed ramp rate of 40°C/min, and was held at the final temperature for over 60 minutes. The kinetic studies were carried out by heating the polymers at different ramp rates of 1°C/min, 5°C/min, 10°C/min, 15°C/min, 20°C/min and 40°C/min. The majority of the previously reported polymer degradation studies were carried out under pyrolysis conditions at high-temperature (typically over 400°C) [104,134-141]. Since the transition and processing temperatures of most common polymers are significantly lower (less than 300°C) [147], this study is focused on the kinetics of VOCs emissions at normal processing temperatures.

The VOCs evolution as a function of time/temperature is referred to as the evolution profile, which can be integrated at different time periods to obtain the cumulative VOCs emissions as a function of time. Quantitation was done with a propane standard (balance, N_2). The standard flow rate was the same as for the reactor gas while the reactor was heated to the same temperature as the polymer samples. Blank runs were performed for both the standard and the polymer samples. The reactor was cleaned as follows. First, the fiber glass and sample residue were removed, and the tubing was heated at 550°C for 2 hours. After cooling, the tubing was blown with compressed air,

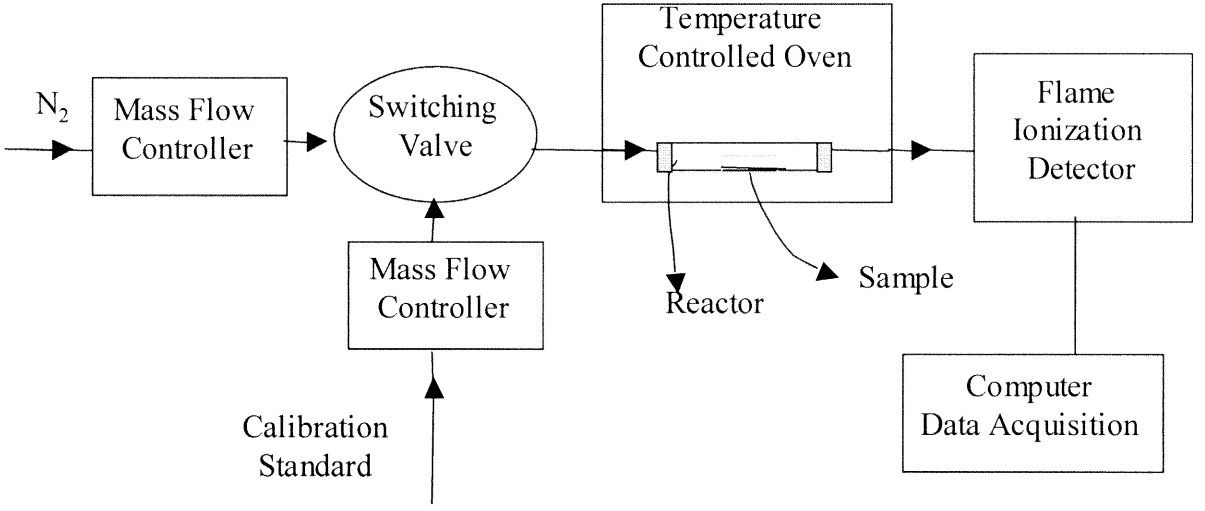

Figure 3.1 Schematic diagram of the analytical system.

then stored in a dry place. Before each run, the system was cleaned by heating the precleaned reactor to a high temperature in a flow of carrier gas, and the blank was monitored by the FID.

3.3 Results and Discussion

3.3.1 VOCs Evolution Profiles and Total VOCs Emissions as a Function of Time

Figure 3.2 shows the evolution profiles and the total VOCs emissions from two mixed waste streams, namely carpet residue and ASR as a function of time. For both streams, the VOCs evolution rates were negligible during the first 3 minutes, when they were heated at 40°C/min from 36°C to 150°C. A temperature of 150°C is close to the extrusion temperature reported for the melt processing of LDPE samples containing these streams [146]. After that, the VOCs evolution rates increased rapidly to their maximum before decreasing slowly as the sample in the reactor was consumed. After a certain point, the VOCs evolution continued at a reduced rate. The initiation of VOCs evolution occurred at a higher temperature for ASR, and it generated significantly more VOCs than the recycled carpet residue.

The curves in Figure 3.2, representing the cumulative VOCs, show that no signal from VOCs was detected at room temperature, or during the first 3 minutes of heating. However, significant emissions were observed at the processing temperature of 150°C. With the extension of heating time, cumulative VOCs increased although their rate decreased. In addition, the ASR generated more VOCs than the recycled carpet residue. Since the carpet residue contained a significant amount of smaller molecular weight products (degraded PP and SBR, during the depolymerization of Nylon 6),

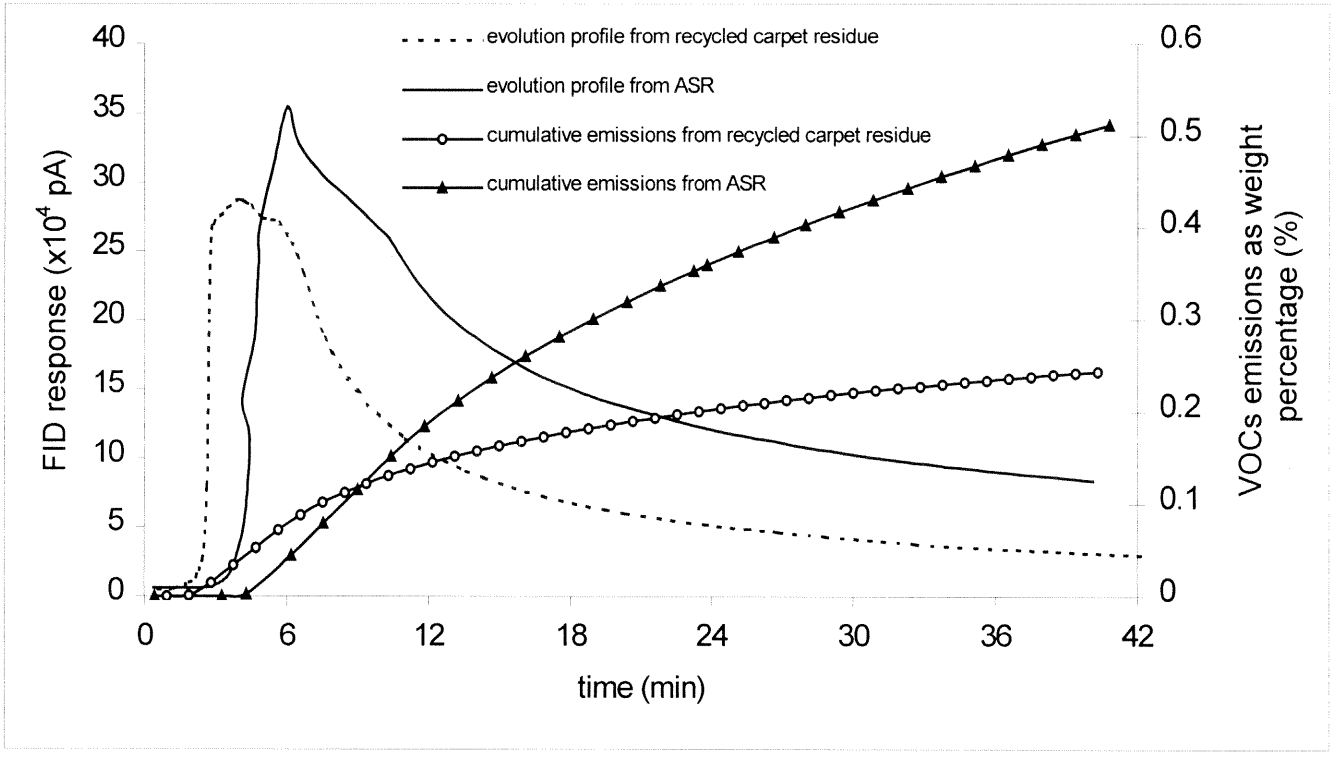

Figure 3.2 VOCs evolution profile, and the cumulative VOCs emissions from recycled carpet residue and ASR at 150°C.

the VOCs evolution was initiated at a lower temperature and increased rapidly within a shorter time period. For instance, within 3 minutes after the temperature reached 150°C, the total VOCs emitted from the recycled carpet residue were about 0.08% by weight, but only 0.04% from ASR. Three minutes may be considered to be characteristic thermal exposure during polymer processing. However, as the thermal exposure of the polymers increased to over 30 min (by far exceeding typical residence times in extruders), the total VOCs emissions from ASR increased to a value as high as 0.5%, while those from the recycled carpet residue were about 0.2%. Some of these emissions could be decomposition products generated during the long heating period.

3.3.2 VOCs Emissions as a Function of Temperature

VOCs emissions as a polymer weight fraction at different temperatures for 60 min are presented in Figure 3.3. It is seen that as the temperature increases beyond 50°C, the maximum emissions increase exponentially from a few ppm to 1% at 200°C for the recycled carpet residue. This demonstrates that the operating temperature has a significant influence on VOCs emissions during polymer processing. The effect was more pronounced for ASR. Although in real-world processing, the emissions are influenced by several other factors [100,108], this experiment may be used to approximate the effect of temperature.

Table 3.1 presents the VOCs generated from different polymers at different temperatures, with an exaggerated thermal exposure of 60 minutes. It is seen that the emissions vary widely. For example, over 0.6% ASR was emitted as VOCs at 150°C, whereas the carpet residue produced half of that. Contaminants such as auto fluids could contribute to the high emissions from ASR. As expected, the VOCs emitted from virgin

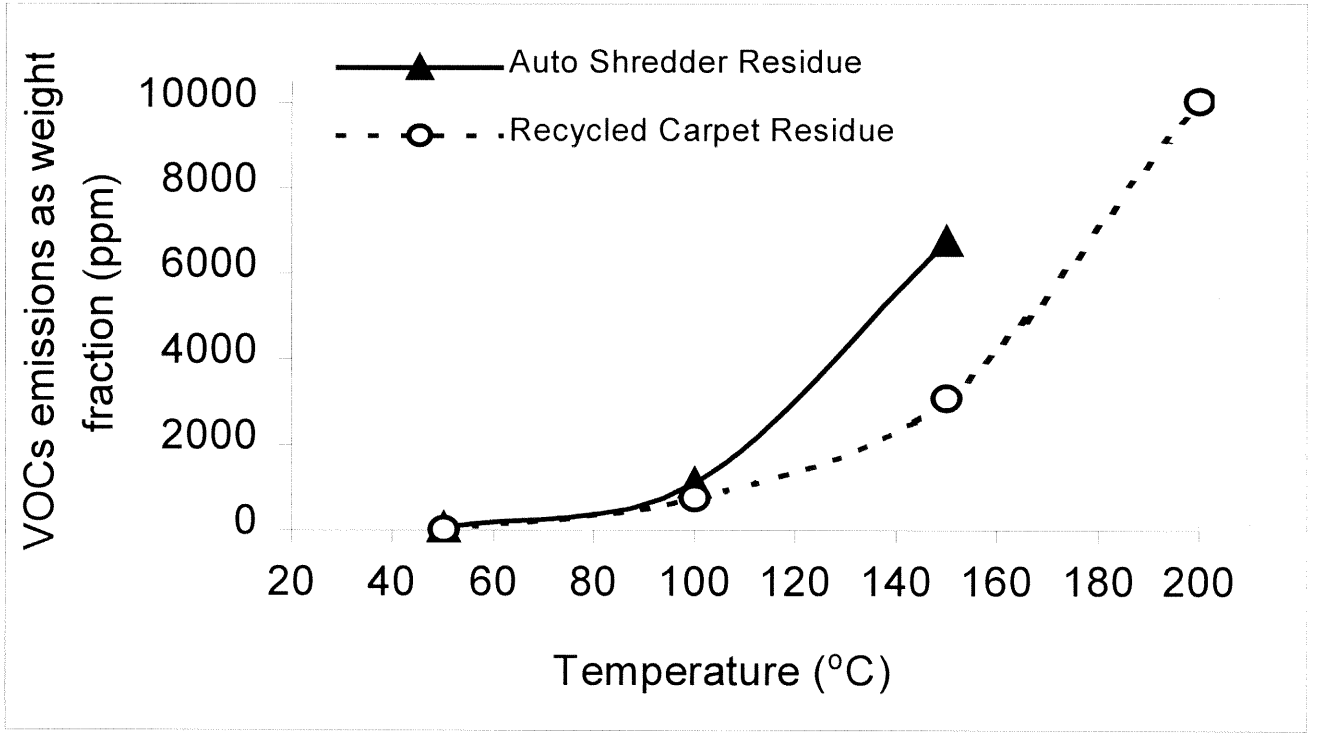

Figure 3.3 VOCs emissions for two recycled streams at different temperatures when held for 60 minutes.

Table 3.1 Comparison of the VOCs emissions thermally generated from different polymers at different temperatures for 60 minutes

Polymer	Temperature (°C)	VOCs emissions as weight percentage (%) or ppm_w *
Auto Shredder Residue (ASR)	50	(63 ± 18) ppm_w *
	100	(0.11 ± 0.01)%
	150	(0.67 ± 0.05)%
Recycled Carpet Residue	50	(8.3 ± 2.2) ppm_w *
	100	(734 ± 96) ppm_w *
	150	(0.32 ± 0.04)%
	200	(1.00 ± 0.23)%
Recycled Carpet Residue /LDPE Composite (80/20)	150	(0.31 ± 0.01)%
LDPE	150	(0.09 ± 0.01)%
PET (virgin resin)	275	(0.51 ± 0.07)%
PET (post-consumer)	275	(0.39 ± 0.16)%

Note: *: 1% = 10^4 ppm_w

low-density polyethylene (LDPE) resin were much lower than those from recycled polymers. The VOCs from LDPE were possibly due to the volatilization of additives as well as degradation of the LDPE itself (the melt temperature of LDPE is around 110°C).

Although the results from the recycled carpet residue and its LDPE composite (80% carpet residue/ 20% LDPE) were not that different, they were not comparable since the composite had experienced an additional thermal exposure during its production. Similarly, the results from pure PET and the post-consumer PET were not directly comparable because the sources of the recycled PET and the virgin resin were not the same. Therefore, each polymer needs to be evaluated individually for its potential environmental impact, and the results may not be extrapolated to other polymers unless source, composition and thermal history are known.

3.3.3 Effects of Heating Rate on Evolution Profile and Cumulative VOCs Emissions

Figures 3.4(a) and 3.4(b) are the VOCs evolution profiles from the recycled carpet residue/LDPE composite (80/20) as a function of time and temperature respectively, when the samples were heated from 36°C to 200°C at ramp rates of 5°C/min, 10°C/min, 20°C/min and 40°C/min. In each run, the sample was kept at 36°C for 10 minutes to reach a stable initial temperature. Thus, in Figures 3.4(a) and 3.4(b), initiation of heating was at 10 minutes. With increasing ramp rate, the VOCs evolution rate in Figure 3.4(a) reached its maximum (the peak temperature is referred as to T_m) in a shorter time period. The absolute value of this maximum evolution rate also increased and moved to a higher temperature with increasing ramp rate (as shown in Figure 3.4(b)). However, since the time required to reach the given temperature (200°C) is shorter at higher heating rate, smaller amounts of VOCs were emitted from the polymer when this temperature was

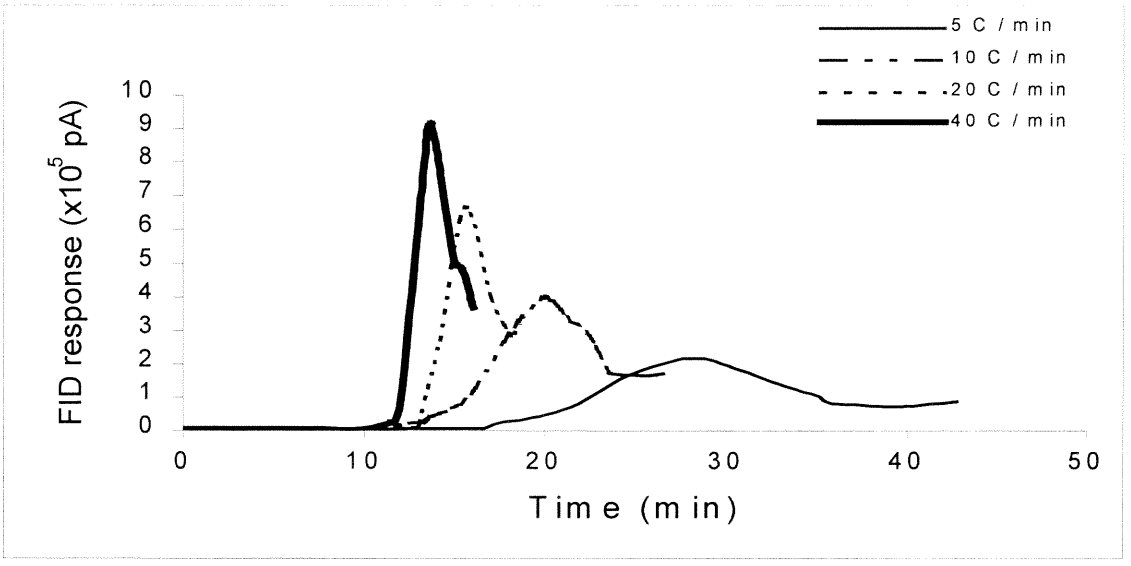

Figure 3.4(a) Effect of temperature ramp rate on the VOCs evolution profiles for the recycled carpet residue / LDPE composite (80/20) as a function of time.

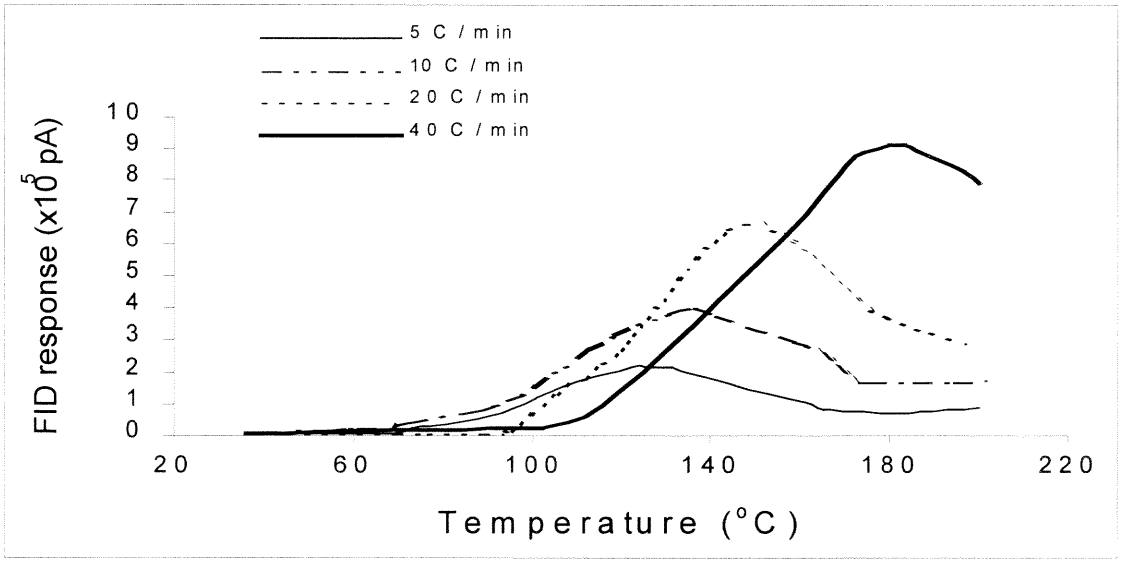

Figure 3.4(b) Effect of temperature ramp rate on T_m for the recycled carpet residue/LDPE composite (80/20).

reached. This can be seen from the integration of the VOCs evolution profiles in Figure 3.4(a), which shows that higher the ramp rate, the lower is the integrated area (i.e., lower VOCs emissions).

The effects of temperature ramp rate were more obvious on the VOCs evolution profiles from the virgin PET, as shown in Figures 3.5(a) and (b). As the same as above, the samples were heated at ramp rate of 5°C/min, 10°C/min, 15°C/min and 20°C/min. It can be seen that all the profiles had three distinguishable peaks, representing three degradation stages. With the increase of ramp rate, the profiles in Figure 3.5(a) moved to the left (shorter time period) and became narrower. For the first and third degradation stages, the integrated area of the corresponding peaks decreased with increasing the ramp rate, whereas, the second degradation stage became more obvious, and the corresponding peak area increased with heating rate. However, the second and the third stages were very close and dependent on the heating rate. By considering them together, it can be found that the total integrated area of these two stages decreased with increasing heating rate, as the first stage did.

This observation was also obtained from the other studied polymers. It is consistent with data from literature [104], where the thermal degradation of PP was studied with TGA. The results showed lower residual mass fractions at lower heating rates. Data from virgin LDPE, recycled carpet residue and its LDPE composite showed similar trends. As shown in column A of Table 3.2, while the samples were heated from 36°C to 200°C, three to four times more VOCs were generated at 1°C/min than at 40°C/min. However, after the polymers were held at 200°C for an additional 10 minutes, the cumulative VOCs emitted at different heating rates were the same for each polymer

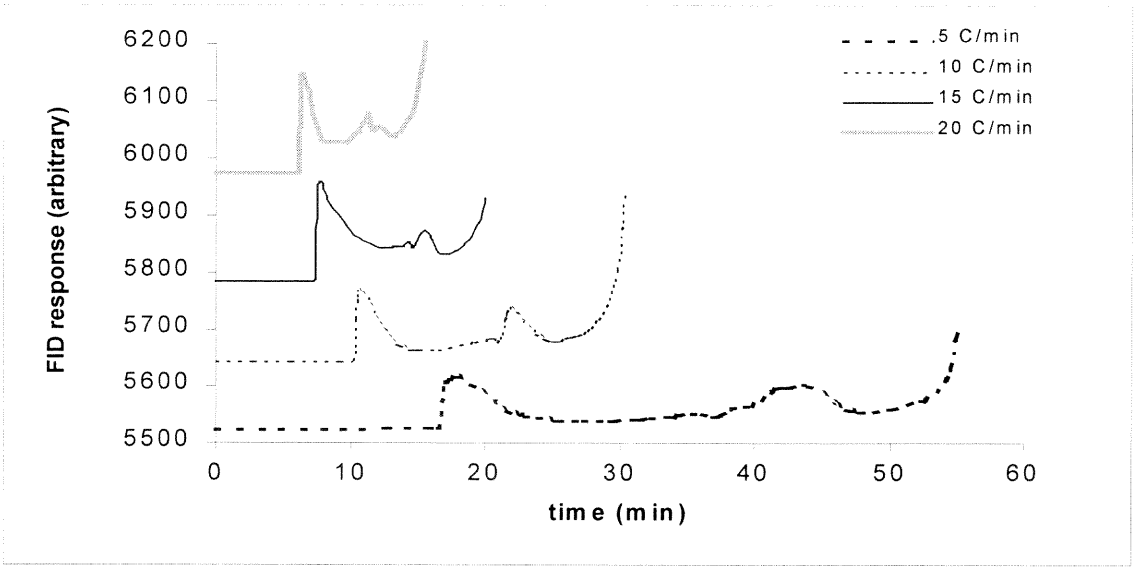

Figure 3.5(a) Effect of temperature ramp rate on the VOCs evolution profiles for the virgin PET (The initiation of heating was at 0 minute).

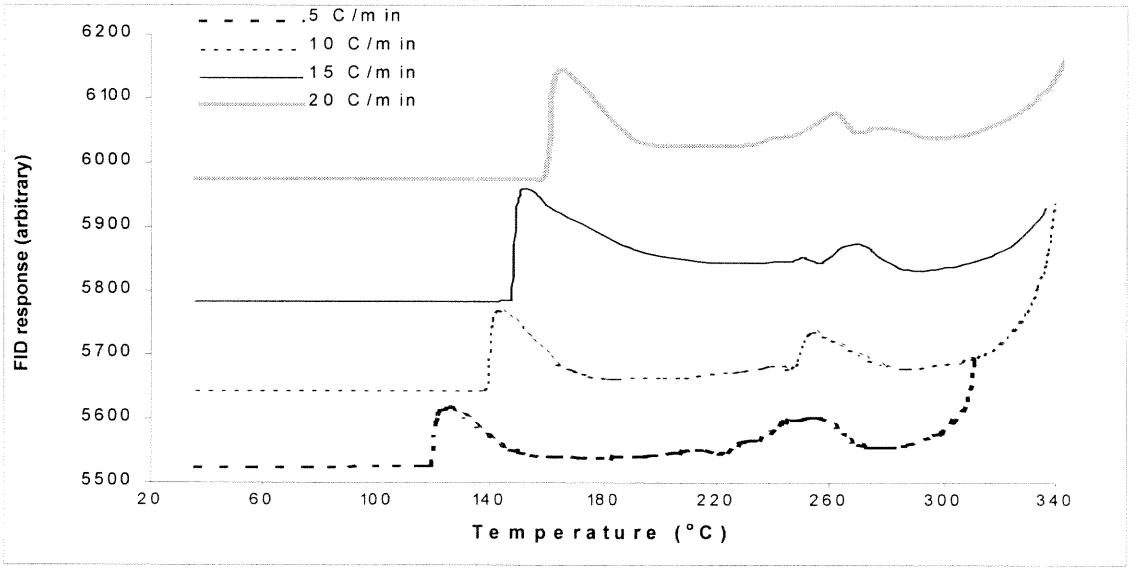

Figure 3.5(b) Effect of temperature ramp rate on T_m for the virgin PET.

Table 3.2 Effects of temperature ramp rate on the cumulative VOCs emissions generated from different polymers (heated from 36°C to 200°C)

Heating rate (m, °C/min)	VOCs emissions as weight percentage (%)					
	Recycled carpet residue		Recycled carpet residue / LDPE composite (80/20)		LDPE	
	A	B	A	B	A	B
1	0.75	0.84	0.65	0.69	0.14	0.16
5	0.38	0.57	0.51	0.64	0.09	0.13
10	0.32	0.60	0.43	0.61	0.05	0.11
20	0.18	0.54	0.29	0.48	0.05	0.11
40	0.17	0.63	0.24	0.68	0.03	0.12

Note: Column A – samples heated from 36°C to 200°C at different heating rates
Column B - samples held at 200°C for additional 10 minutes

(column B, Table 3.2). Since the typical thermal exposure period of polymers during processing is less than 3 minutes, the results here indicate that VOCs emissions would decrease, if the polymers are heated rapidly to their desired processing temperature, and the processing time is shortened. In addition, the data showed that under similar conditions, the amounts of VOCs emitted from the carpet residue, and its LDPE composite were close to each other, but much higher than those from the virgin LDPE resin.

3.3.4 Kinetics of VOCs Emissions

LDPE, PP, Carpet Residue and its 80/20 LDPE Composite

The VOCs evolution profiles in Figures 3.6(a) and (b) refer to four different polymers at the ramp rate of 10°C/min. The virgin LDPE and PP produced smoother profiles and lower VOCs emissions compared to the relatively complex recycled polymers (or their composite). The carpet residue and its 80/20 LDPE composite generated similar VOCs evolution profiles. However, compared to the recycled carpet, the VOCs emissions from its composite were higher in the low temperature range, but decreased around the processing temperature of 180-200°C. This may be due to the additional thermal exposure of the composite during its production at 180°C, as the longer thermal exposure causes more degradation. However, exposure to higher temperatures did not enhance VOCs evolution from the composite. On the contrary, the compounding of carpet residue with virgin LDPE resulted in lower VOCs emissions.

The VOCs evolution profiles also show that at temperatures below 200°C, there were two degradation stages for the recycled carpet residue and its LDPE composite, whereas there was only one for LDPE and PP. Each stage showed a peak temperature T_m

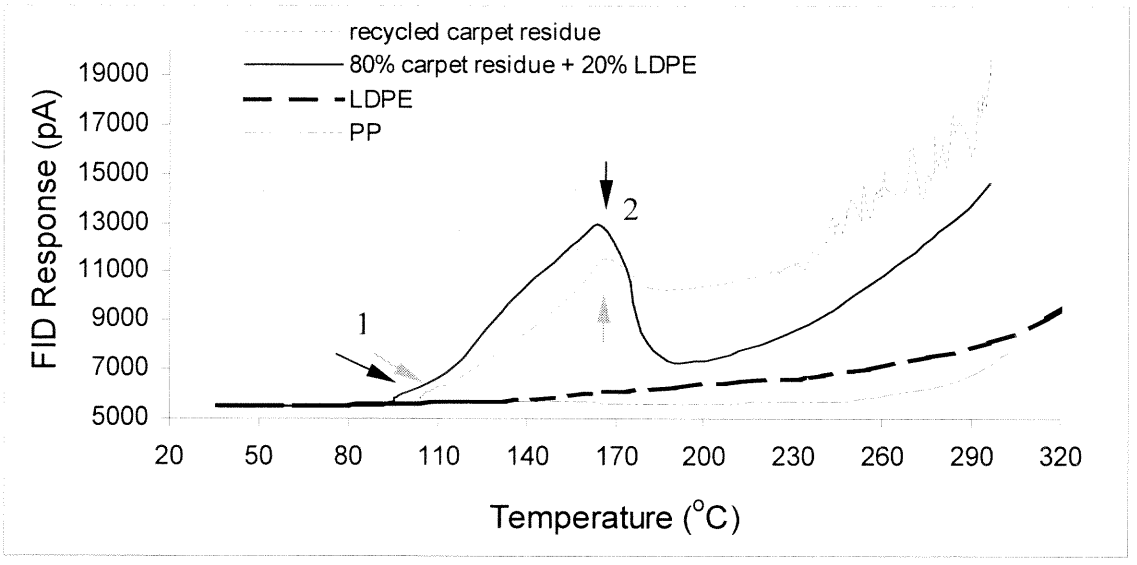

Figure 3.6(a) VOCs evolution profiles of PP, LDPE, recycled carpet residue and its LDPE composite (80/20) at the ramp rate of 10°C/min (arrows indicate T_m).

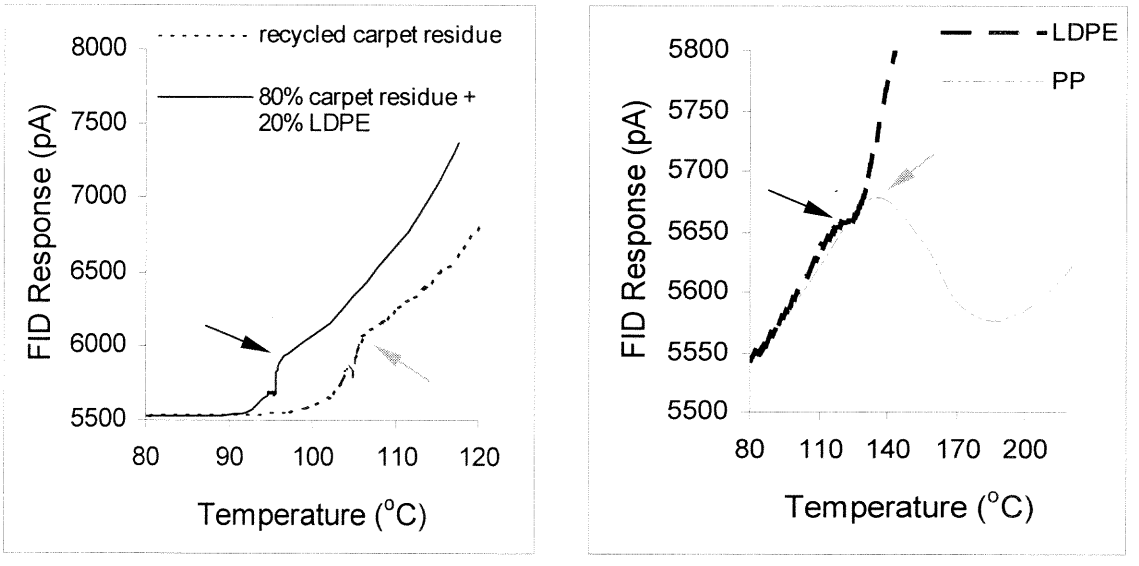

Figure 3.6(b) Magnified profiles in Figure 3.6(a) to show T_m (indicated with arrows) from the first degradation stage in lower temperature range or in lower scale of FID response.

at which the VOCs evolution rate reached a maximum. For the recycled carpet residue and its LDPE composite, the first stage overlapped with the second resulting in "a shoulder". The VOCs evolution from the composite was initiated at a lower temperature than the 100% carpet residue. T_{m1} for the first maximum was also lower for the composite, but T_{m2} for the second maximum was close to that from the recycled carpet residue. As mentioned earlier, the additional thermal exposure of the composite caused VOCs emissions to occur at a lower temperature, but this effect was less pronounced when the actual processing temperature was approached. In the studied temperature range, PP produced a degradation peak while the LDPE profile showed only a shoulder at a relatively low T_m (as shown in Figure 3.6(b)).

As shown in Figures 3.4(b) and 3.6(a), the second degradation stage was between 110°C and 200°C for the recycled carpet residue/LDPE composite (80/20). The evolution profile in Figure 3.4(b) shifted to the right as the heating rate increased; T_m of the second stage also shifted to the right (higher temperature). This right-shifting of T_m was applied to study the kinetics of the VOCs emissions. Table 3.3 lists the T_m for four different polymers at different ramp rates. For each degradation stage, T_m shifted to a higher temperature when the heating rate was increased. For the recycled carpet residue, T_m values for the two stages were higher than those of its LDPE composite. The maximum corresponding to the first stage degradation of PP occurred at a relatively higher temperature than LDPE. This may be due to the higher melting point of PP, as emissions from additives and polymer are facilitated by melting the polymer. Other factors such as the interactions between additives, polymer and contaminants may also contribute to the difference in T_m.

Table 3.3 T_m of the VOCs evolution profiles at different temperature ramp rate for different polymers

Heating rate (m, °C/min)	Peak temperature (T_m, °C)						
	Recycled carpet residue		Recycled carpet residue / LDPE composite (80/20)		LDPE	PP	
	1st stage degradation	2nd stage degradation	1st stage degradation	2nd stage degradation	1st stage degradation	1st stage degradation	High temperature degradation (> 400°C)
2							432
3							434
5	90	162	85	128	117	124	445
10	106	169	96	137	125	135	
15	124	174	106		130	149	
20	129	186	116	146	138	156	
40				180			

As per equation 3.3, ln (T_m^2 / m) was plotted against $1/T_m$, and straight lines were obtained as shown in Figure 3.7. From the slope and intercept of these lines, the activation energy (E_a) and the frequency factor (k_o) were calculated, and are listed in Table 3.4. As mentioned before, this work focused on processing temperatures < 300°C, and the kinetic parameters were computed in that range. Most published kinetic data are at temperatures higher than 400°C; only PP was studied at high temperatures so that the results of the present study could be compared to those from the literature.

Due to the nature of polydispersity, the kinetics of polymer degradation is quite complicated. The mechanisms are influenced by several factors, such as the initial molecular weight, stereoregularity, the presence of additives (stabilizers, plasticizers, antioxidants, etc.) and residuals (monomers, catalysts, solvents and moisture), and experimental conditions such as temperature range, and the atmosphere in which the reaction is carried out (nitrogen, oxygen, vacuum or moisture) [104,134-141,148]. Moreover, data acquisition is affected by the particular analytical method (different instruments and kinetic models, isothermal or dynamic condition). Therefore, the literature data on the kinetics of thermal and/or oxidative degradation of PP vary widely [104,134-136,149,150]. For example, during high temperature (>400°C) pyrolysis of PP, the activation energy was reported to be in the range of 171-327 kJ/mol, while the frequency factor was between $7.2\text{x}10^{11}$–$1.4\text{x}10^{24}$ (min^{-1}) (Table 3.4) [134-136]. The pyrolysis in the presence of H_2O gave a lower E_a (145 kJ/mol) and k_o ($1.0\text{x}10^{10}$ min^{-1}) [104]. In this study, for PP, E_a was 258 kJ/mol, while k_o was $1.6\text{x}10^{16}$ (min^{-1}). These results are in good agreement with those from literature data. E_a and k_o are greater in the higher temperature range than those in the lower temperature range. At high temperature,

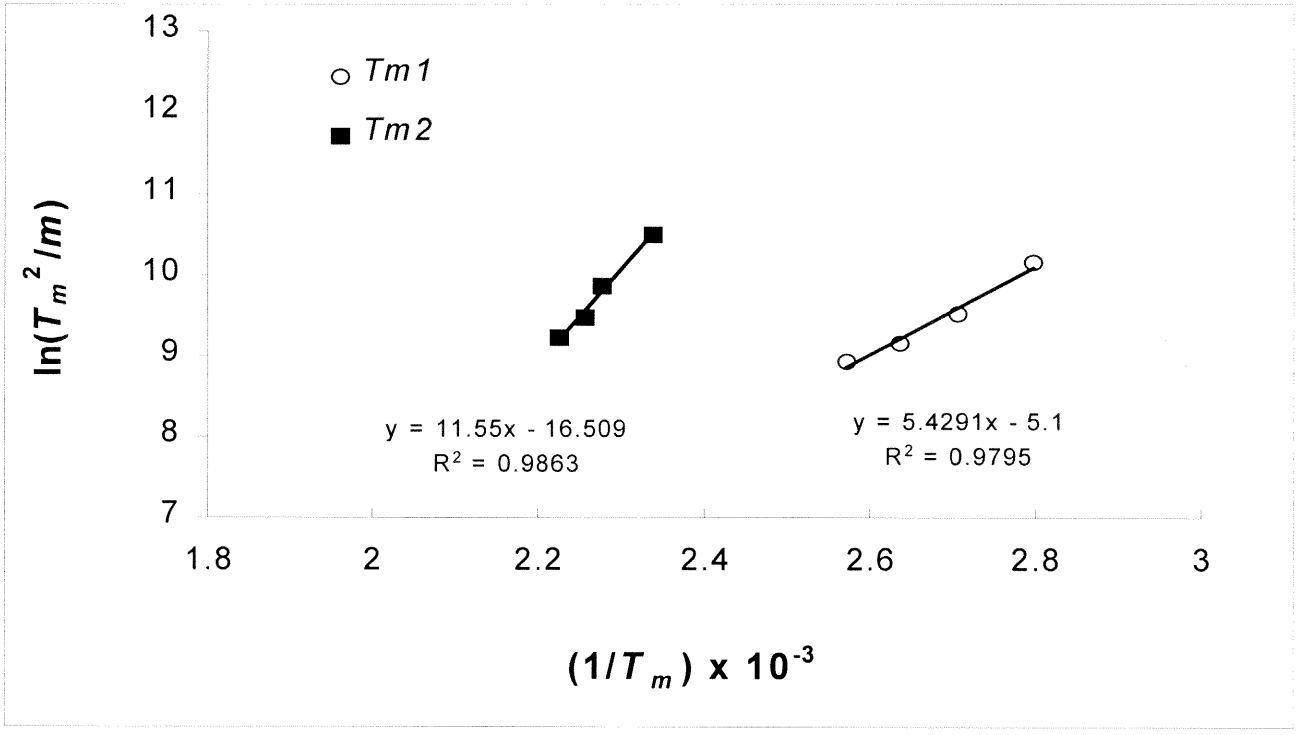

Figure 3.7 ln (T_m^2 / m) vs. $1/T_m$ from recycled carpet residue / LDPE composite (80/20).

Table 3.4 Comparison of the kinetic parameters in this work with those in literature (temperature range(°C), E_a (kJ/mol) and k_o (min^{-1}))

Polymer	Present work			Literature data	
	1st stage degradation	2nd stage degradation	high temperature degradation	high temperature range	low temperature range
PP	121-156 °C 52 kJ/mol 1.1×10^4 min^{-1}		430 - 450 °C 258 kJ/mol 1.6×10^{16} min^{-1}	Westerhout (1997) [134] T=370 - 440 °C E_a=171-285 kJ/mol $k_o = 7.2 \times 10^{11} \sim 2.4 \times 10^{20}$	Gambiroza (1992) [149] T=100 - 600 °C E_a=83-128 kJ/mol
				Wu (1998) [104] (in H_2O) T=227 - 527 °C E_a=145 kJ/mol $k_o = 1.0 \times 10^{10}$	Verdu (1997) [150] T= 80 - 150 °C E_a=90-120 kJ/mol
				Chan (1997) [135] T= 400 – 580 °C E_a =327 kJ/mol $k_o = (0.04 - 1.43) \times 10^{24}$	T= 45 – 400 °C E_a= 98 kJ/mol $k_o = (0.69 - 2.07) \times 10^6$
				Bockhorn (1999) [136] T= 410 – 460 °C E_a =220 kJ/mol $k_o = 1.1 \times 10^{15}$	T= 20 – 410 °C E_a =223 kJ/mol $k_o = 7.9 \times 10^{15}$
LDPE	118-138 °C 84 kJ/mol 5.1×10^8 min^{-1}			Westerhout (1997) [134] T= 246 - 520 °C E_a =163-330 kJ/mol $k_o = 7.2 \times 10^{10} \sim 4.3 \times 10^{23}$	Sezgi (1998) [137] E_a =146 kJ/mol $k_o = 6.6 \times 10^9$
				Bockhorn (1999) [136] T= 430 - 480 °C E_a =268 kJ/mol $k_o = 6.0 \times 10^{17}$	

Table 3.4 Comparison of the kinetic parameters in this work with those in literature (temperature range(°C), E_a (kJ/mol) and k_o (min^{-1})) (Continued)

Polymer	Present work			Literature data
	1st stage degradation	2nd stage degradation	high temperature degradation	
Recycled carpet residue (15-18% PP and 12-15% SBR)	90 – 129 °C 34 kJ/mol 97.4 min^{-1}	162-187 °C 89 kJ/mol $1.2x10^8$ min^{-1}		For styrene-butadiene rubber (SBR): Lin and Chang (1996) [139] T: 177-377°C 377-477°C 427-587°C E_a: 52 kJ/mol 151 kJ/mol 169 kJ/mol k_o: $2.3x10^3$ $1.5x10^{10}$ $3.5x10^{10}$ Chen (1997) [140] T: 250-289°C(in N_2) 430-485°C(in O_2) 485-565°C(in O_2) E_a: 211 kJ/mol 153-176 kJ/mol 132-169 kJ/mol k_o: $1.3x10^{14}$ $5.8x10^8$ $8.3x10^{13}$ OH (1999) [141] E_a=55 – 344 kJ/mol
Recycled carpet residue / LDPE composite (80/20)	84 - 116 °C 45 kJ/mol $7.4x10^3$ min^{-1}	154 –176°C 96 kJ/mol $1.4x10^9$ min^{-1}		Not available

more energy is required for the random scission, which results in polymer decomposition throughout the polymer matrix. Whereas, at low temperature, less energy is needed to break the weak links among residuals, low molecular fragments and their degradation products, from which the emissions mainly originate. Therefore, as expected, the overall activation energy is higher for the high-temperature decomposition.

The values of the kinetic parameters were quite low for the recycled polymers. Since the recycled polymers usually contain some low molecular weight contaminants, more VOCs are generated at low temperatures. Furthermore, the low parameters from the first and second degradation stages of the recycled polymers corresponded very well with the data from virgin resins (in Table 3.4), i.e. PP, LDPE in this study, and SBR in literature [139-141]. The decrease in the values of these parameters is attributed to aging, long thermal exposure, interactions between polymer components and presence of contaminants in the recycled polymers. Interestingly, the kinetic parameters for the recycled carpet residue were relatively lower than those from its LDPE composite. This may have resulted from the additional stabilization of PP (15-18% of the recycled carpet residue) by compounding with LDPE [151], as the thermally labile tertiary alkyl radicals of PP are diluted by the LDPE domains.

ASR, HDPE, PS, PET and Post-consumer PET

Figures 3.8(a), (b) and (c) represent the VOCs evolution profiles from the five polymers at the heating rate of 10^{o}C/min. It can be seen that the recycled ASR gave out the highest VOCs evolution rate and the highest cumulative emissions (based on the integrated area under the profile). Contaminants such as auto fluids, could contribute to this high

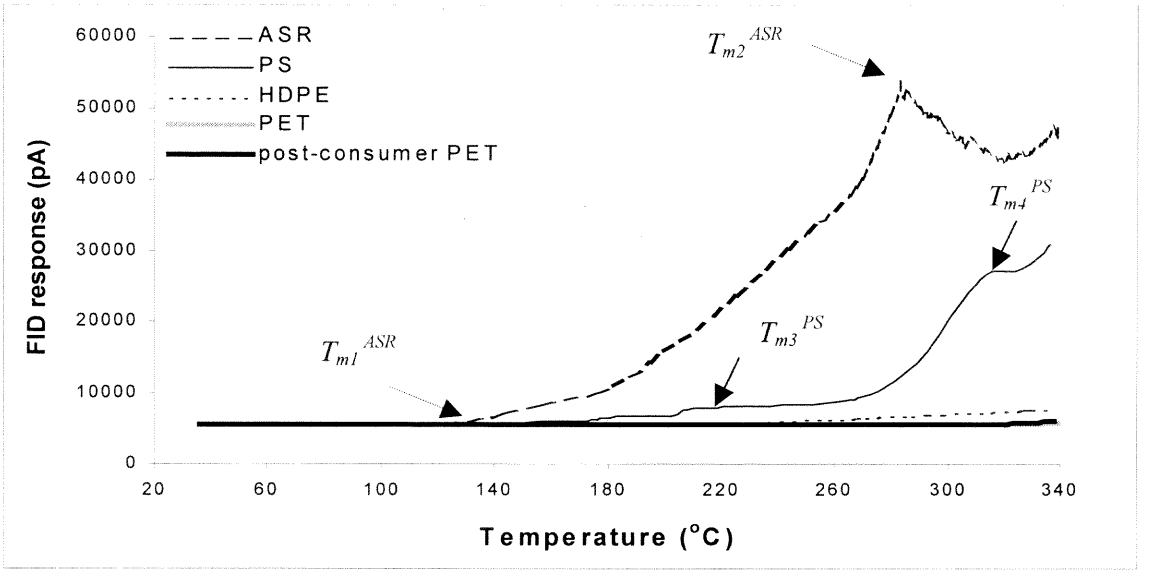

Figure 3.8(a) VOCs evolution profiles as a function of temperature at the ramp rate of 10°C/min.

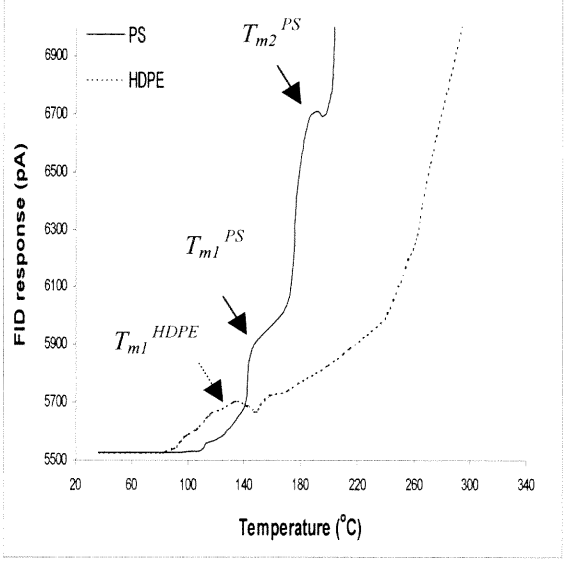

(b)

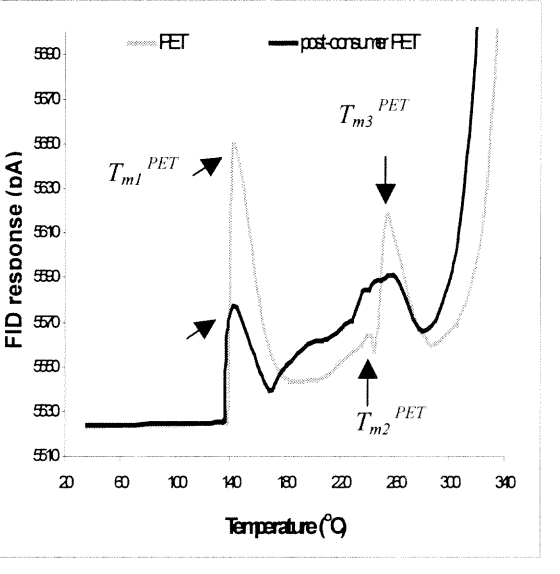

(c)

Figure 3.8(b) and (c) Magnified profiles in Figure 3.8(a) to show T_m in lower scale of FID response.

emissions from ASR. Its profile also showed two distinct degradation stages in the temperature range of around 130°C and 280°C. The virgin resin PS was ranked the second in terms of VOCs evolution rate and cumulative amount. But its profile demonstrated a more complex degradation mechanism with at least four stages (Figures 3.8(a) and (b)). For HDPE, the onset temperature of VOCs evolution was the lowest (around 85°C). This was possibly due to the lowest melt temperature of HDPE. After this onset point, complex interactions took place throughout the HDPE matrix, which resulted in a non-smooth profile and only gave a relatively obvious peak around 135°C (Figure 3.8(b)).

Interestingly, the post-consumer PET as well as the virgin PET gave out the lowest VOCs evolution rate and cumulative emissions. Their profiles (as shown in Figure 3.8(c)) were very similar to each other. Whereas, the virgin PET indicated three distinguishable degradation stages; for the recycled PET, except the first stage, other stages were quite complicated and showed more "shoulders". In addition, in some temperature ranges, the evolution rate from the post-consumer PET was even lower than that from the virgin PET. Below the processing temperature (290°C), the cumulative emissions from the recycled PET seemed fewer than those from the virgin PET. This agreed very well with the previous static experimental results. However, exactly after the processing temperature (290°C), the VOCs evolution rate from the post-consumer PET increased rapidly, which could be resulted from the presence of contaminants, aging and longer thermal exposure of the recycled resins.

Similar to the results from the previous four polymers, the right-shifting of peak temperatures (T_m) was also observed from these five polymers, e.g., virgin PET as shown

in Figures 3.5 (a) and (b). The activation energy and the frequency factor were also calculated, based on this right-shifting of T_m. For the virgin PET, there were three degradation stages. The calculated kinetic parameters were 36 kJ/mol, 63.7 min^{-1} at 122-182°C (the first stage); 58 kJ/mol, $1.7x10^3$ min^{-1} at 214-265°C (the second stage); and 67 kJ/mol, $1.2x10^4$ min^{-1} at 231-278°C (the third stage). In literature, there are reports about the existence of three or four stages in the high-temperature decomposition or burning process of PET [152]. For each stage, the reported apparent E_a based on TGA or DSC varies widely from tens kJ/mol (or even a few kJ/mol for the last stage) to over 290 kJ/mol. This wide variation is due to the difference in the chosen kinetic model, the isothermal or dynamic condition, the heating rate, degree of conversion, the presence of catalysts or additives, different atmosphere (N_2, air or vacuum), etc. In the low temperature range of 270°C to 370°C, the reported E_a of PET degradation is between 94-287 kJ/mol in N_2, 72-249 kJ/mol in air and 159 kJ/mol under vacuum. Compared with these widely scattering literature data, the results here corresponded very well with the experimental conditions (at even lower temperature, 122-278°C).

The PS showed four degradation stages in the studied temperature range. The kinetic parameters from the fourth stage (106 kJ/mol, $6.3x10^6$ min^{-1} at 311-345°C) were in very close agreement with Jellinek's data (103 kJ/mol at 250-340°C) [153]. Amelin et al. [154] noted that there were two stages for the thermal degradation of PS, and attributed the relatively low E_a of 84-146kJ/mol in the first stage to weak bonds. While in this work, the values of E_a for the first three stages were between 46-88 kJ/mol at a lower temperature range (103-245°C), resulting from the weakest bonds in the polymer matrix.

Similarly, the E_a was agreeably low from the low-temperature HDPE degradation (56 kJ/mol at 122-154°C).

For the recycled polymers, ASR had a very low E_a from the first degradation stage (29 kJ/mol at 111-172°C) due to the weak links among the miscellaneous polymer and organic impurities. Whereas, the E_a was higher (62 kJ/mol) from the second stage which occurred at a much higher temperature range (260-317°C). As noted before, the post-consumer PET showed a more complicated degradation profile, so only the E_a from the first stage was estimated to be 21 kJ/mol. It is much lower than the corresponding value from the virgin PET.

3.4 Summary

The evolution profile, the cumulative amounts, and the kinetics of thermally generated VOCs emissions from virgin and recycled polymers were estimated. The data illustrated that processing parameters, such as temperature, heating rate and residence time, strongly influenced the evolution profile and the cumulative VOCs emissions. More VOCs were generated from recycled waste streams than from virgin polymers. The kinetic studies showed that below the processing temperature (<200°C), virgin PP and LDPE had one degradation stage, while the recycled carpet residue and its LDPE composite had two. The other five polymers had more complicated degradation processes. The kinetic parameters were in good agreement with those from the literature.

CHAPTER 4

VOLATILE EMISSIONS AND STRUCTURAL/RHEOLOGICAL CHANGES DURING MULTIPLE MELT PROCESSING OF POLYPROPYLENE

4.1 Introduction

Polypropylene (PP) is widely used in commodity as well as engineering applications, in unfilled and reinforced versions. With increasing costs of landfill space and with the growing interest in waste minimization, a variety of techniques for recycling /reusing waste PP as a single resin or in combination with other plastics are being developed [133,155]. La Mantia and Capizzi [155] reported the recycling of compatibilized and uncompatibilized nylon/PP blends. Wyser, et al. [156] studied recycled multilayer PP/PET/SiOx films. Other combinations, such as PP/acrylonitrile-butadiene-styrene (ABS) and PP/polyethylene [157], long glass fiber reinforced polypropylene [158], and PP from lead/acid batteries [159], have also been recycled and/or investigated. A number of technical issues must be resolved if recycled plastics are to be used with any degree of confidence in new or demanding applications. Usually, cleaning and separation need to be done for post-consumer plastic wastes, which are expensive. However, recent studies show that these plastic wastes may not need to be cleaned before recycling as they retain their properties despite the impurities in the material [160]. This would provide favorable economic considerations for recycling. Compatibilization is crucial in composites of recycled polymer matrix [157,161], while re-stabilization is the only chance to stop or to slow the degradation and then the deterioration of the mechanical properties of recycled polymers [162]. Radiation treatment and electron beam surface modifications also found their way in reinforcing and recycling of polymers [161,163].

Selection of recyclable feedstock and recycling method should be based on the mechanical and rheological properties of the polymer, and on the environmental impacts of the process. Given the large quantities of PP used in a variety of applications, melt reprocessing by extrusion or injection molding appears to be the methods of choice. With respect to recycling by reprocessing, environmental problems related to emissions have been of concern to the Environmental Protection Agency (EPA) and the Occupational Safety and Health Administration (OSHA). Emissions generated during processing can be as high as 5% of the annual tonnage of resins processed in the U.S., [100]. Among the different species generated during reprocessing, volatile organic compounds (VOCs) have received the most scrutiny. They originate from devolatilization and degradation of additives (plasticizers, stabilizers, antioxidants) and resins. Many of these VOCs are hazardous air pollutants that are also involved in photochemical reactions to form smog and ground-level ozone. Therefore, the Clean Air Act Amendments (CAAA) of 1990 regulate these VOCs, and the Title V of this Act established a permit program for their eventual reduction [108].

Reprocessing of scrap plastics may generate a significantly higher amount of VOCs emissions than virgin resins because they have had long thermal and mechanical exposure in oxidizing environments. Types and amounts of these emissions depend upon the material and the operating parameters. Degradation mechanisms are complicated and depend on the processing atmosphere. A general mechanism of thermal degradation of unstabilized PP adapted from Refs [164] and [165] is shown in Figure 4.1. Polymer molecules (RH), through thermal energy, mechanical stress and promoted by catalyst residues, produce free radicals (R•) via hydrogen abstraction occurring mostly at the

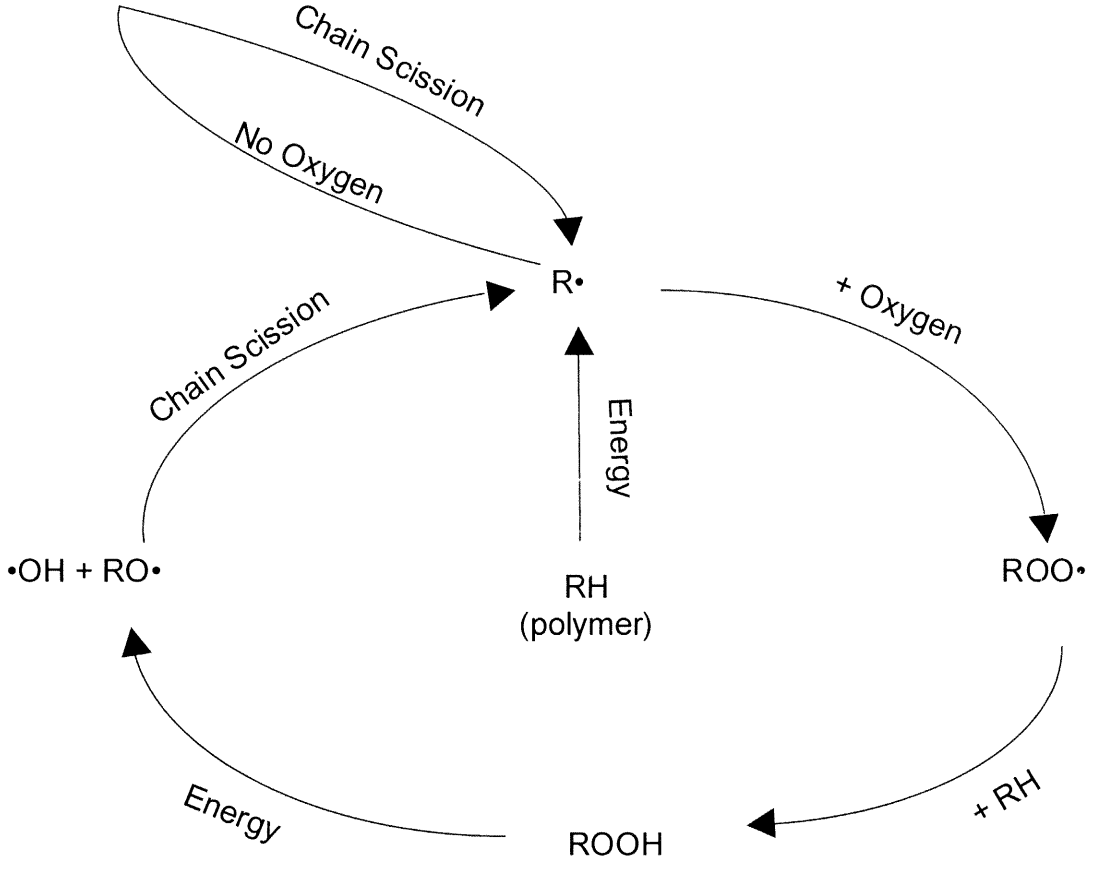

Figure 4.1 Schematic of thermal/oxidative degradation of polyolefine.

labile tertiary carbon atom. Usually, oxygen is trapped between powder particles or pellets during the feeding step in extruders or injection molders, and this begins the autooxidation cycle. The macroradicals react with the trapped oxygen to form peroxy radicals (ROO•), which interact with polymer molecules to generate hydroperoxides (ROOH) and more macroradicals (R•). The unstable hydroperoxides (ROOH) easily decompose into hydroxyl (•OH) and propoxyl (RO•) radicals. The hydroxyl radicals (•OH) may abstract hydrogen from the polymer molecules to form water and more free radicals (R•). Whereas, the propoxyl radicals (RO•) further decompose through chain scission to generate smaller molecules containing carbonyl groups and new free radicals with lower molecular weight. Termination may occur by deactivation of the free radicals, which can take place at any part of the cycle in the presence of primary stabilizers acting as "radical scavengers", or secondary stabilizers known as "hydroperoxide decomposers". In the absence of oxygen, the free radicals [165] undergo chain scission to produce smaller molecules containing unsaturated (C=C) and smaller macroradicals. As either of the above cycles continues, the cascading degradation generates more and more free radicals. The polymer molecules are consumed and decomposed into smaller free radicals and small molecules. The VOC emissions are associated with these small molecules.

A variety of species have been identified under laboratory conditions or in the vicinity of actual extrusion equipment. Depending on the PP grade, they include a series of low molecular weight aldehydes, ketones, alcohols and carboxylic acids (mostly aliphatic), lower olefins, cyclic ethers, esters, water and carbon monoxide. For PP, the onset of the CO evolution has been reported to occur at about 200°C [117].

The above thermooxidative degradation processes have resulted in structural changes with concomitant effects on properties. [133,166-168]. Consequently, the recycling of polymers is very difficult because the properties of the resulting secondary material are quite poor. In order to solve this problem, stabilization /re-stabilization plays an important role and gains much attention [162,169,170]. In literature, the degradation of stabilized and unstabilized PP grades was extensively studied during their multiple melt reprocessing. These studies mainly focused on chain scission, and the corresponding changes in molecular weight, rheology, chemical structure, microstructure (morphology, gas transportation properties) and mechanical properties [100,133,164-174]. However, the effects of multiple melt reprocessing on VOCs evolution and its relationship to structural changes of polyolefines have not been reported. This research examines the total VOCs emissions from unstabilized and stabilized PPs processed several times by injection molding and twin-screw extrusion, respectively. It focused particularly on the effect of stabilizer and type of processing conditions on the evolution of volatiles and the concomitant structural changes. In addition, the changes in chemical structure as a result of the reactive degradation were analyzed with Fourier Transform Infrared (FTIR) spectrometer. They were correlated with melt viscosity and molecular weight changes.

VOCs measurements were carried out with an analytical system based on non-isothermal heating of the polymers followed by direct emission analysis with a flame ionization detector (FID). Since FID does not respond to H_2O, CO and CO_2, this method provided an accurate measure of the VOCs emitted from polymers, which could be related to the environmental impacts of repeated polymer recycling. Another advantage of this system is its low detection limit and high sensitivity compared to traditional

thermal analysis [118]. The total VOCs emissions from unstabilized PP that was injection molded several times were compared with those from a multiple heating/cooling simulation of a single PP sample in the presence and in the absence of oxygen. This was to study the degradation in the absence of shear, and to differentiate between the emissions of predissolved VOCs and those generated by thermal degradation during measurement.

4.2 Experimental

Materials/Processing: A commercial polypropylene grade (Profax 6501, Montell, USA) in powder form was injection molded up to 10 cycles in a Toyo Ti-90G injection molder equipped with a standard mold for ASTM mechanical properties. The polypropylene was assumed to be minimally stabilized without antioxidants and process stabilizers, and was referred below as U-PP. Experimental molding conditions included barrel temperature profile from 240 to 220°C, nozzle temperature of 240°C and mold temperature of 25°C. Packing pressure and cooling cycle depended upon the cycle number. The first cycle was carried out with the virgin powder polymer, and the remaining 9 cycles with granules produced by grinding ASTM specimens (–20 mesh) obtained in the subsequent injection molding steps. Thus, for the injection molding part of this research, cycle number corresponds to the respective process pass.

A commercial PP homopolymer in pellet form (H306, OPP Petroquimica SA, Brazil) was reprocessed up to five times in a ZSK-30 W&P twin screw extruder, equipped with a K-tron feeder and two 3 mm rod dies [166]. The PP was considered as a stabilized grade and was referred below as S-PP. Two screw configurations (as shown in

Figure 4.2) were used: a mild one consisting of only conveying elements (CON) and a more aggressive one consisting of conveying plus 45^0 kneading blocks (KB). Extrusion conditions were barrel temperature profile as 215-230-240-250-240-235 ^oC, feed rate of 5kg/hr and screw speed of 100 rpm with an open vent. The water-cooled extrudate was pelletized and reprocessed [166]. The as received pellets, which were previously extruded by the manufacturer, corresponded to the U-PP after the first reprocessing cycle. Thus the n-cycle of the S-PP corresponded to the (n+1) cycle of the U-PP.

Total VOCs Measurement: The analytical system used for VOCs measurement is shown in Figure 3.1 and described in Section 3.2. About 2.5 mg of ground PP sample from the selected processing cycle was placed in the reactor. After the system reached a steady state in a 30ml/min flow of N_2, the reactor was heated in a temperature-controlled oven from 36^oC to 180^oC (approximately 15^oC above the melting temperature of PP), at a ramp rate of 40^oC/min. To estimate the maximum possible VOCs emissions, the sample was kept at the final temperature for three additional minutes. The VOCs emissions were measured with the FID as an evolution profile, whose area could be determined by integrating different time segments. This area was proportional to the total VOCs emitted from the polymer. The FID was calibrated with certified propane standard gas.

The multiple processing of PP was simulated by placing 5-6 mg of virgin U-PP in the reactor in Figure 3.1 and by subjecting it through repeated heating and cooling. After the system reached a steady state in a flow of N_2, the reactor was heated from 36^oC to the predetermined final temperature at a fixed ramp rate (40-50^oC/min). After holding at the final temperature for a certain period of time, the reactor tubing was quenched by dipping in icy water to cool it quickly. When the system reached the initial steady state,

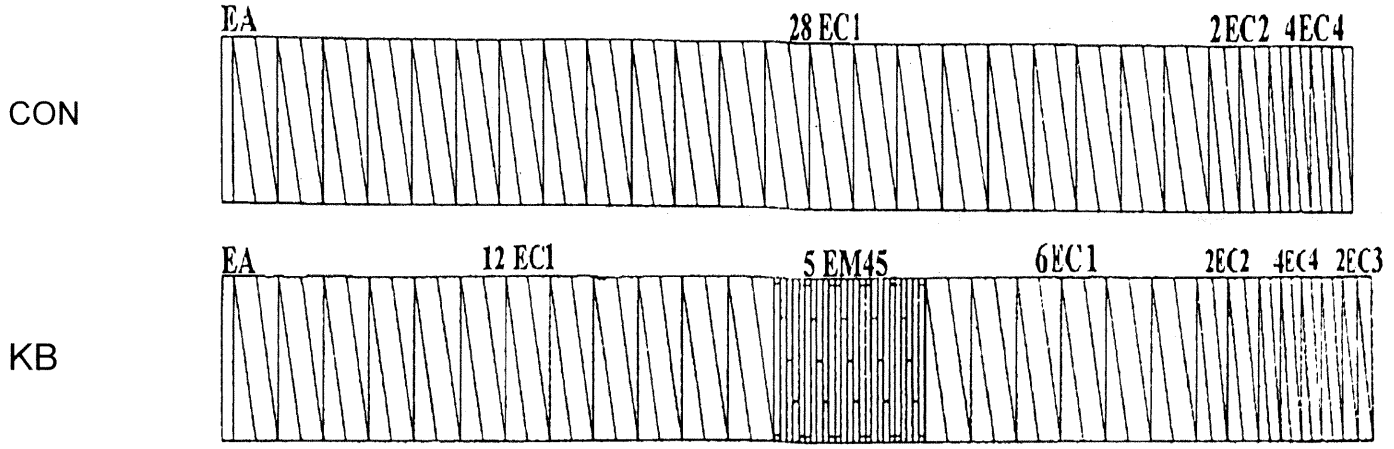

Figure 4.2 Screw configurations used for stabilized PP [166].

the sample was heated up to the same temperature under the same conditions as before. It was again cooled with icy water, and the cycle was repeated several times on the same sample. Besides nitrogen, air was also used as carrier gas to study the effect of oxygen on polymer degradation.

For the injection molding part of this study, cycle numbers correspond to the respective process pass. Thus, all results on the unprocessed U-PP powder are related to cycle 0; the results from the U-PP granules after one injection molding pass are referred to as cycle 1, after two passes as cycle 2, and so on. However, in the simulation part, the first heating cycle corresponds to cycle 0 of the multiple molding process since the unprocessed PP powder was used. The second heating cycle corresponds to cycle 1, and so on.

Differential Scanning Calorimetry (DSC): Experiments with a Perkin-Elmer Differential Scanning Calorimeter DSC-7 were conducted to determine the oxidative induction time (OIT) of the as received U-PP powder and ground S-PP pellets, which was related to their degree of stabilization. The multiple heating process of a single U-PP sample under extreme degradative conditions in a 100% oxygen atmosphere was also simulated in DSC. For the OIT measurements, about 4-7 mg PP powder was weighed accurately to 0.001 mg with a microbalance, and then placed into the sample pan of the DSC without the lid. The sample was first heated under nitrogen from 36 ^{o}C to 180 ^{o}C at a rate of 72 ^{o}C /min, and kept at this temperature for an additional 0.5 minutes. Then the system was switched to oxygen, and the data were collected under isothermal conditions. The time for the onset of oxidative degradation, and the accompanying heat flow were monitored.

Multiple heating/cooling experiments under pure oxygen were conducted on U-PP powder placed in an open sample pan under conditions similar to those used in the molding simulation carried out in air with direct FID measurements (heating from 36 to 180°C at a ramp rate of 40°C/min, holding for 3 minutes followed by cooling to 36°C at 200°C/min). Once the system cooled to 36°C, the sample pan was taken out and weighed accurately to 0.001 mg. It was then placed back, and the cycle was repeated 10 times. For each cycle, the heat flow curves were recorded, and the weight change of the sample was measured with the microbalance.

FTIR Analysis: Polypropylene films from each injection molding cycle and selected extrusion cycles were prepared by compression molding at 210°C under a force of 2200 kg. The thickness of the films ranged from 100 to 125 μm. A Perkin-Elmer Spectrum One FT-IR Spectrometer was used to obtain the IR spectra of the films in the range of 4000-400 cm^{-1}. The resolution was 4 cm^{-1} and 25 scans were averaged.

Melt Flow Index (MFI)/Molecular Weight: MFI, expressed in g/10 min, was measured in a Tinius Olsen Extrusion Plastometer under conditions that were standard for PP (2.16 kg, 230°C). Ground U-PP samples from each injection molding cycle was used. Additional antioxidant (Irganox 1010) was used to prevent further polymer degradation in the Plastometer barrel. Molecular weight changes of the S-PP were measured by size exclusion chromatography (Waters GPC 150 CV in 1,2,4-trichlorobenzene at 140°C in the presence of antioxidant [166].

4.3 Results and Discussion

4.3.1 Effects of Melt Reprocessing on VOCs Emissions from U-PP

4.3.1.1 Multiple Injection Molding

Processing Characteristics / Rheology

Injection molded samples became progressively darker and more brittle as cycle number increased, an indication of thermooxidative degradation. Average tensile elongation at break decreased from 73% for the material from the first cycle to about 20% for the material from the 10^{th} cycle. Increased brittleness made regrinding easier for the samples obtained from the fifth cycle onwards. These results were as expected because a very short OIT value of about 0.96 minutes was observed. This indicated the absence of stabilizers. In comparison, OIT value of the S-PP grade was about 8.2 minutes.

To facilitate easy removal of samples from the mold, the typical cooling time of 15 seconds employed for material from cycle 1 was increased in the subsequent cycles. The maximum applied hydraulic pressure decreased exponentially with increasing processing cycle from about 5220 kPa for the first cycle to 2950 kPa for the 10^{th} cycle. Similarly, the total energy consumption measured by the attached transducers indicated a gradual decrease with increasing cycle number. All these observations indicated reduced melt viscosity, lower molecular weight and a tendency towards further degradation. This is seen in Figure 4.3, where Melt Flow Index (MFI) is shown to increase rapidly with increasing cycle number.

VOCs Emissions from Molded Samples

Figure 4.4 shows the thermally generated VOCs emissions from U-PP samples, i.e., the virgin resin (0), 1^{st}, 3^{rd}, 4^{th}, 6^{th}, 8^{th} and 10^{th} processing cycles. The two sets of data based

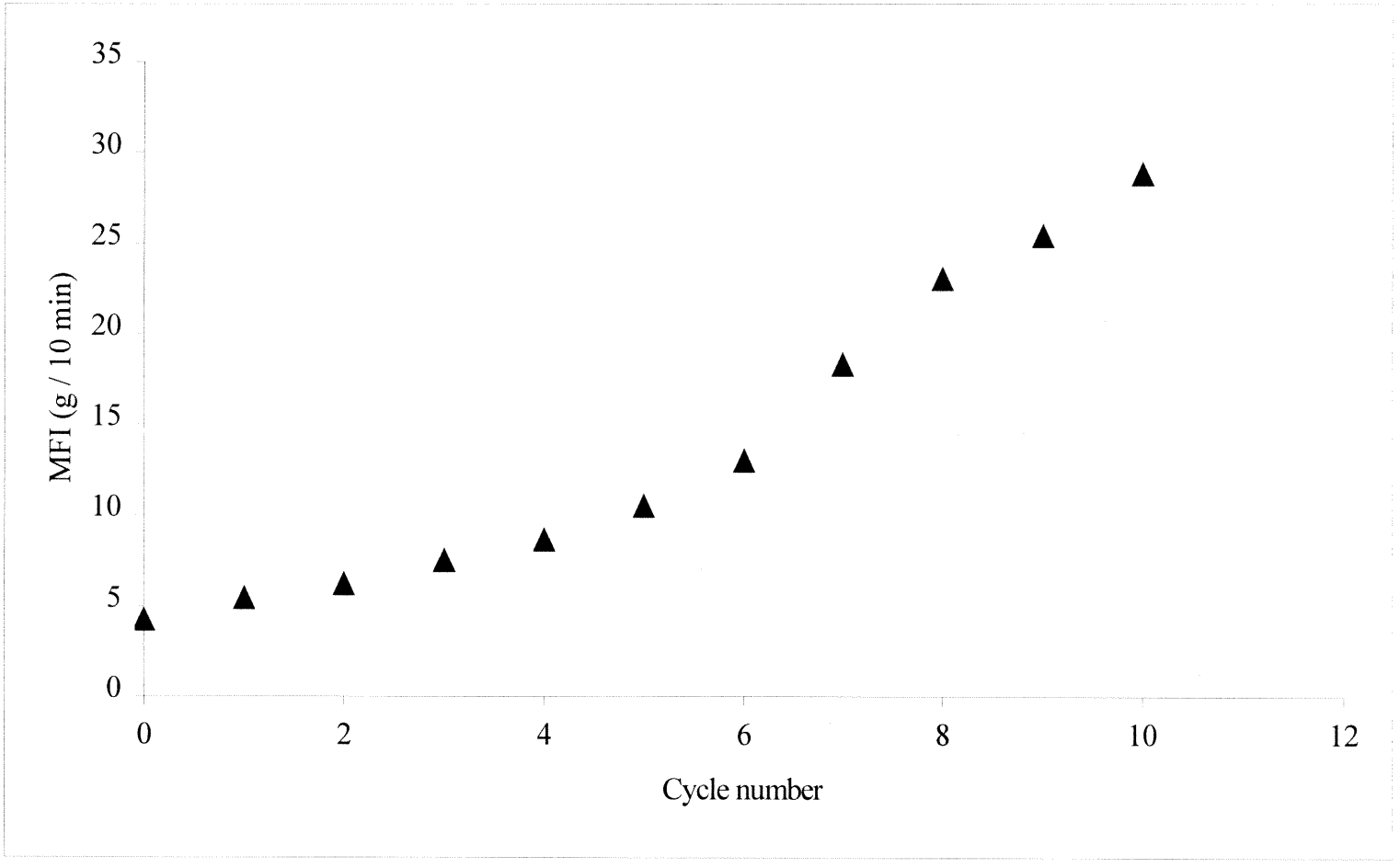

Figure 4.3 Melt Flow Index (MFI) of U-PP after multiple injection molding.

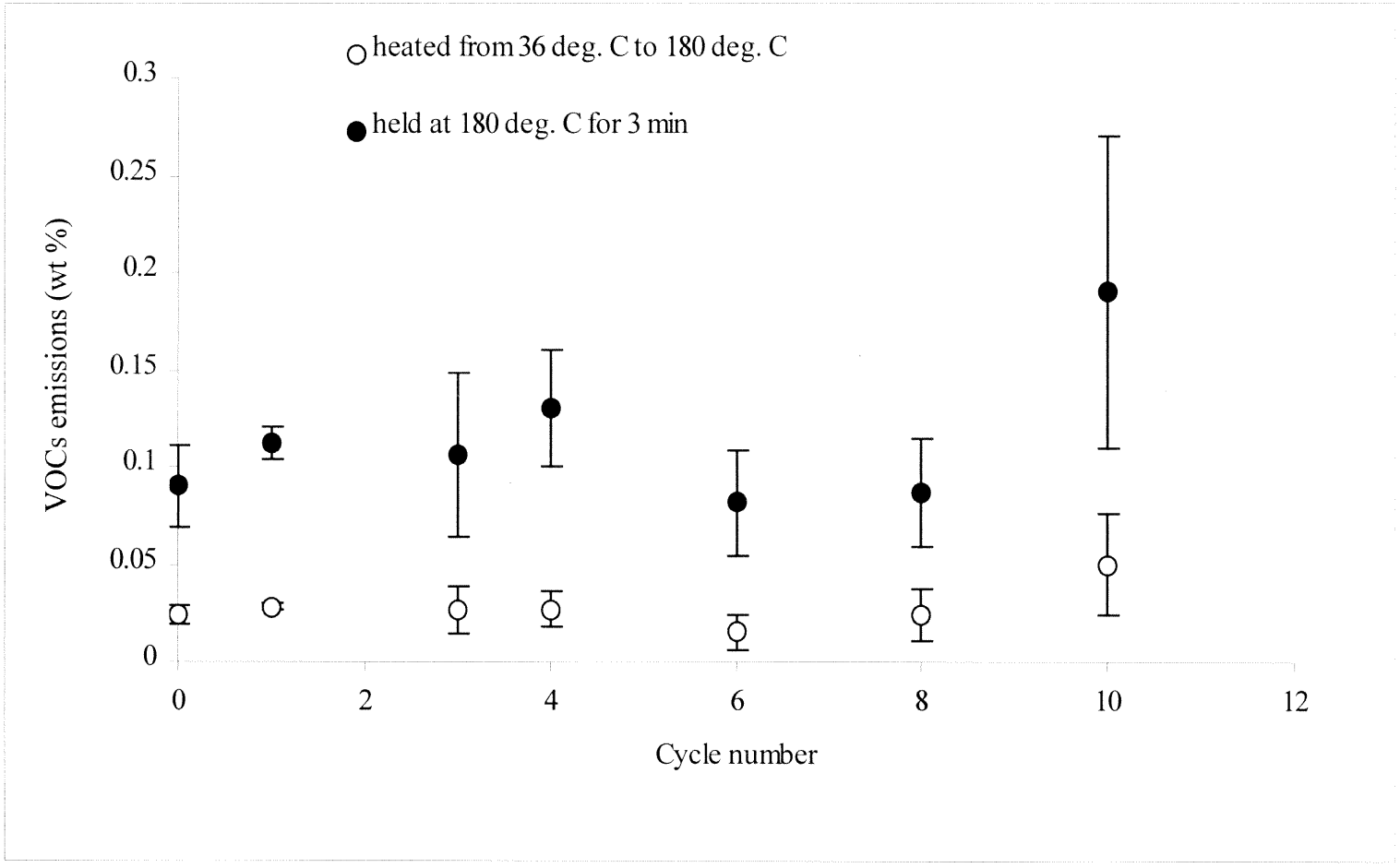

Figure 4.4 Effect of multiple injection molding on the VOCs emissions generated from U-PP when heated from 36°C to 180°C at 40°C/min in nitrogen, and held at 180°C for three additional minutes.

on 3 to 6 replicates represent the emissions obtained when the sample was heated from 36°C to 180°C at a rate of 40°C/min, and then held at 180°C for three additional minutes. For both sets of data (within the range of standard deviation), the average value of total emissions did not vary significantly from cycle to cycle. Standard deviations appeared to increase after the first two cycles, (0 and 1), with the highest values for the 10^{th} cycle. This may be attributed to equipment contamination that occurred during the intervals between the multiple reprocessing and grinding steps. The trends shown in Figure 4.4 are as expected, since the data obtained here correspond to the maximum VOCs generated at those particular experimental conditions. These values may not be equal to the VOCs generated during each processing cycle. VOCs may have been completely vented out during molding, or partly retained in the molded specimens. In addition, the heating times in the reactor (in the absence of shear) are different from the residence times in the injection molder (under shear). For example, it took 3.6 min to heat the sample from 36°C to 180°C at 40°C/min, whereas in real injection molding, the heating rate was higher, the heating time was shorter and the processing temperature was higher (240°C).

The data in Figure 4.4 represent the maximum possible VOCs independent of the cycle number. By contrast, Figure 4.5 presents the cumulative VOCs emissions as a function of processing cycle based on the subtotal of all the previous cycles. This shows a linear increase of the maximum VOCs with increasing number of cycles. The data can be also plotted as cumulative VOCs emissions versus total heating time (Figure 4.6). In this plot, heating time represents the total time in the oven in the absence of shear (under a nitrogen atmosphere) plus an estimated three minutes residence time in the injection molder for each pass (in the presence of entrapped oxygen). Open circles correspond

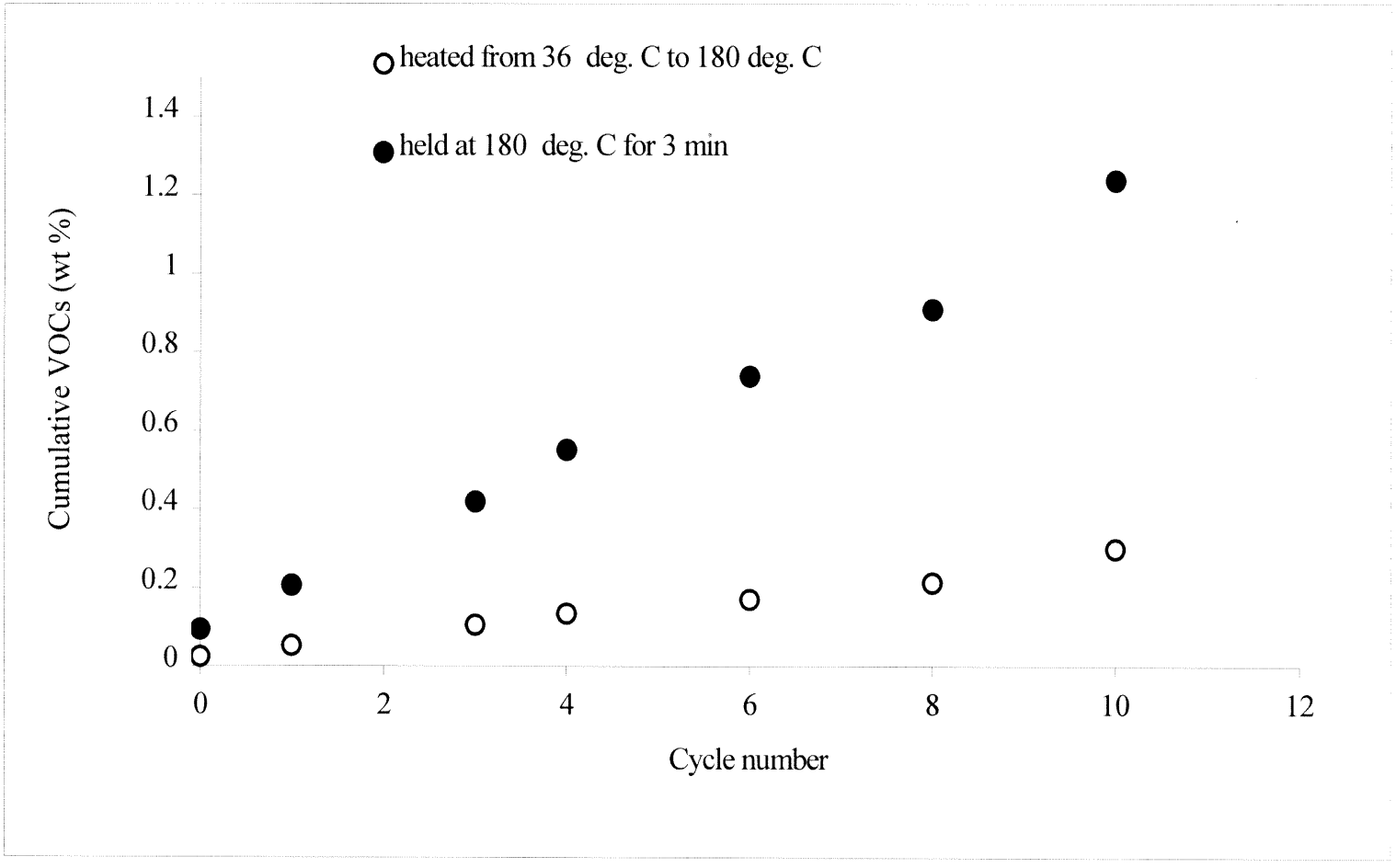

Figure 4.5 Cumulative VOCs emissions from U-PP as a function of processing cycles.

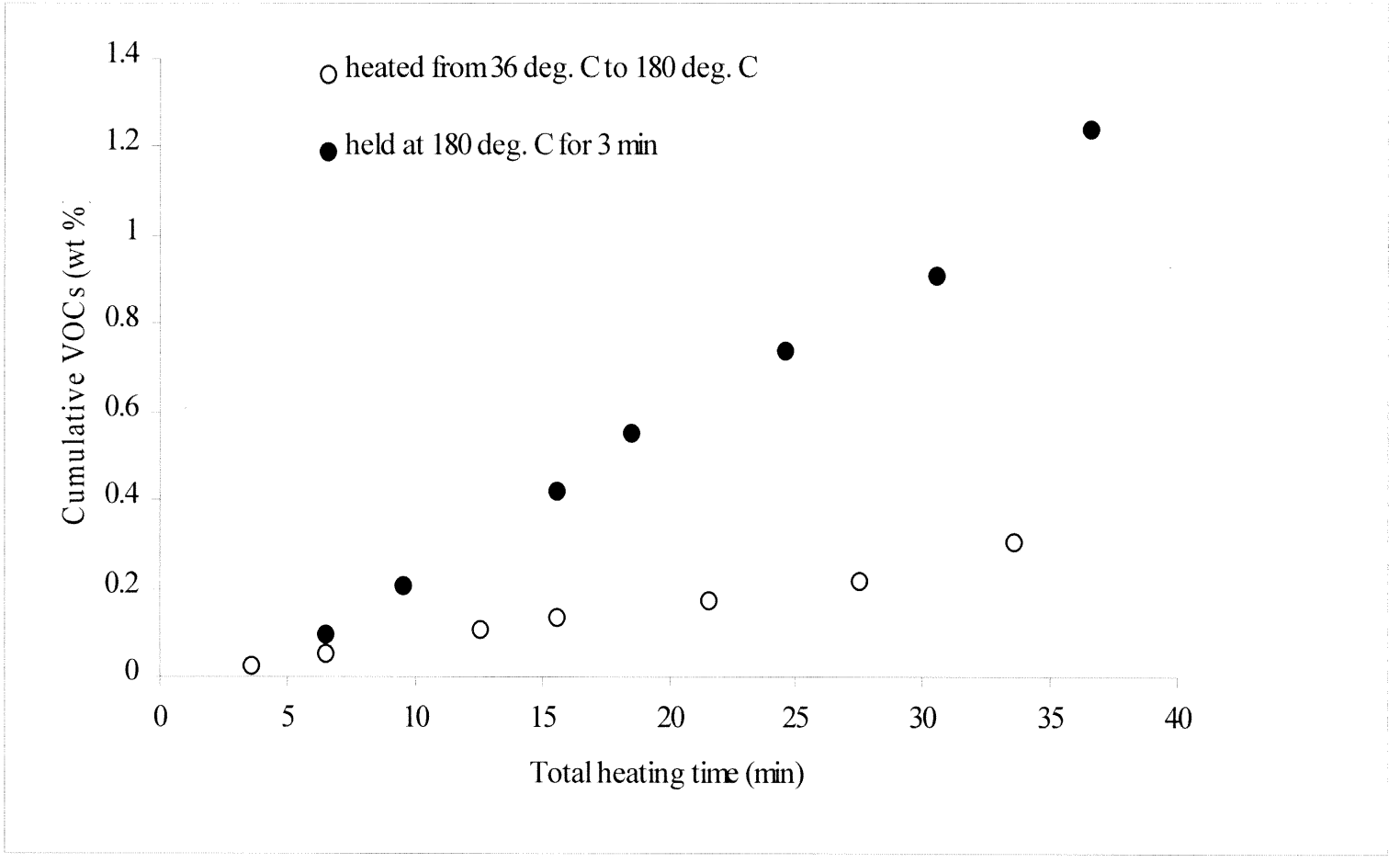

Figure 4.6 Cumulative VOCs emissions of injection molded U-PP samples as a function of total heating time.

sequentially to 0,1,3,4,6,8 and 10 passes, and reflect heating time to 180°C plus the residence time in injection molder. Percentage of total time spent in a pure nitrogen atmosphere, which would favor only thermal degradation, decreases from 100% for cycle 0, to 11% for the 10th pass. Black circles corresponding to the same number of passes are shifted to the right to take into account the additional three minutes in the oven at 180°C. As before, percentage of time spent in the injection molder atmosphere which would favor thermooxidative degradation increased from 0% for cycle 0, to 82% for the 10th pass. As expected, the cumulative maximum VOCs also increased linearly with the total heating time. This trend was similar to increasing the cycle number (Figure 4.5).

4.3.1.2 Simulation by Multiple Heating and Cooling. As shown in Figure 4.4, the total VOCs emissions did not vary as a function of injection molding cycles. The melt processing is assumed to be carried out in the presence of entrapped air that would favor thermooxidative degradation. Subsequent measurements of VOCs emissions in a nitrogen atmosphere would involve mostly thermal degradation plus the release of dissolved/entrapped volatiles. To provide a better understanding of the extent of thermal degradation under different atmospheres, a single U-PP powder sample was repeatedly heated and cooled for several cycles and emissions were monitored.

It should be noted that there are certain inherent differences in the reprocessing and simulation studies presented here. During the multiple processing, milligram level subsamples were taken from a kilogram level starting U-PP. However, the simulation was done using a single milligram level U-PP sample. Also, the U-PP was under shear during molding, something it did not experience in the oven. The molten U-PP in the barrel of

the injection molding machine served as a solvent for the evolving VOCs. This resulted in some of the degraded organics that could not be vented out during the molding cycle to be readsorbed in the sample. When processed U-PP was heated in the reactor in Figure 3.1, the readsorbed organics were reemitted. However, during the simulation experiments, there was no scope of VOCs readsorption, and the FID reading was a true measure of emissions.

Total VOCs in Nitrogen - Comparison with Injection Molded Samples

Data obtained with the FID using nitrogen as a carrier gas under three different heating conditions are shown in Figure 4.7. Only for cycle 0, the long heating time at 180°C of condition A had a more significant effect on the VOCs. When the heating cycle number increased, the results from all three conditions showed not only lower VOCs, but also little difference between the three conditions. The data suggest that if the U-PP was to experience only thermal degradation, multiple reprocessing in the injection molder and more severe reprocessing conditions (e.g., longer heating time, and higher temperature) would not generate more VOCs.

The weight percent VOCs emitted in Figure 4.7 are lower than those in Figure 4.4, where the injection molded samples encountered more severe thermal, mechanical and oxidative degradation. Partial dissolution of volatiles in the U-PP being processed, and external contamination also affected VOCs. Such conditions would contribute to the generation of more emissions from each cycle (around 0.1 % by wt.) under a heating protocol similar to that of A. This possibly resulted in the same amounts of maximum emissions among cycles (as observed in Figure 4.4). Thus, the cumulative VOCs from

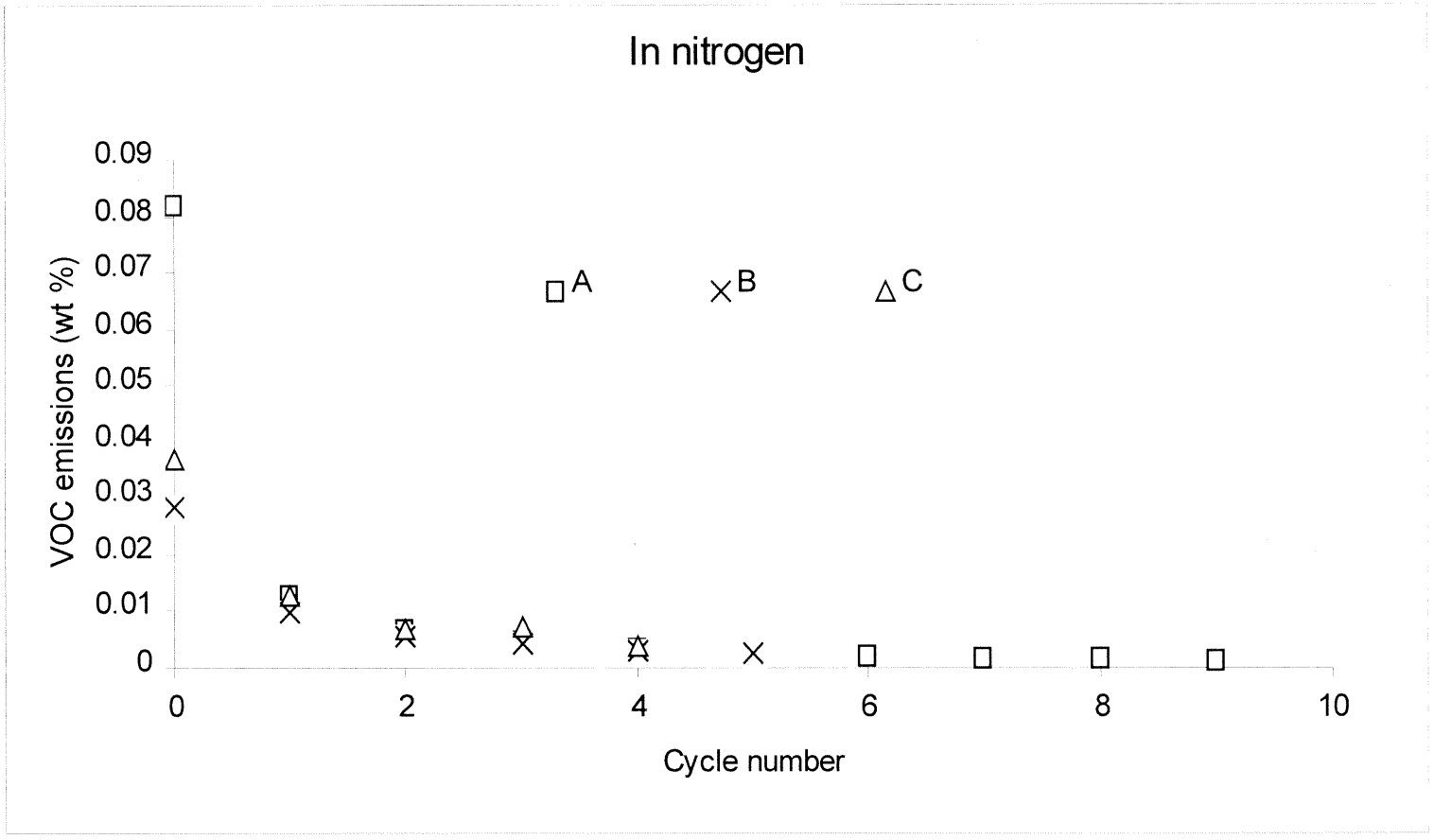

Figure 4.7 VOCs emissions from each cycle during simulation by multiple heating/cooling of a single U-PP sample in nitrogen (FID measurement).

Heating profiles: A. 8.6 min (3.6 min from 36°C to 180°C, then 5 additional min at 180°C)
B. 3 min (2.5 min from 50°C to 180°C, then 0.5 additional min at 180°C)
C. 3 min (from 50°C to 204°C)

injection molded samples ought to increase faster than those from the simulated multiple heating/cooling in nitrogen. This is clearly demonstrated by the difference in the slopes of the two lines in Figure 4.8, (solid circle data from Figure 4.6 and open square data from Figure 4.7), where cumulative VOCs are plotted against the total heating time.

Total Volatiles in Oxidative Environment - Comparison with Injection Molded Samples

To better simulate degradation in the presence of air (exaggerated injection molding conditions, still in the absence of shear), data were obtained with air as the carrier gas and the FID as the detector. As shown in Figure 4.9, the amount of VOCs decreased from 0.043% in cycle 0 to 0.008% in cycle 1, increasing rapidly thereafter and reaching a plateau after about cycle 7. DSC data under pure oxygen are also shown in Figure 4.9, where percentage of total volatiles (including organics and inorganics) was calculated from weight changes during multiple heating/cooling. The combined data clearly showed that there was an oxidative induction period during cycles 0-2 prior to rapid degradation. This was seen as the weight increase accompanying oxidative reactions in DSC experiments corresponding to reducing VOCs in FID measurements. The data also showed that VOCs in the FID measurements, or weight loss in the DSC experiments reached their maximum after a certain number of reprocessing cycles. This explained why the maximum amount of VOCs did not change among cycles in Figure 4.4. Additionally, as shown in Figure 4.10, the DSC heat flow vs. temperature heating curves under oxygen clearly showed a reduction in overall crystallinity, and a decrease in the maximum melting temperature as a result of degradation.

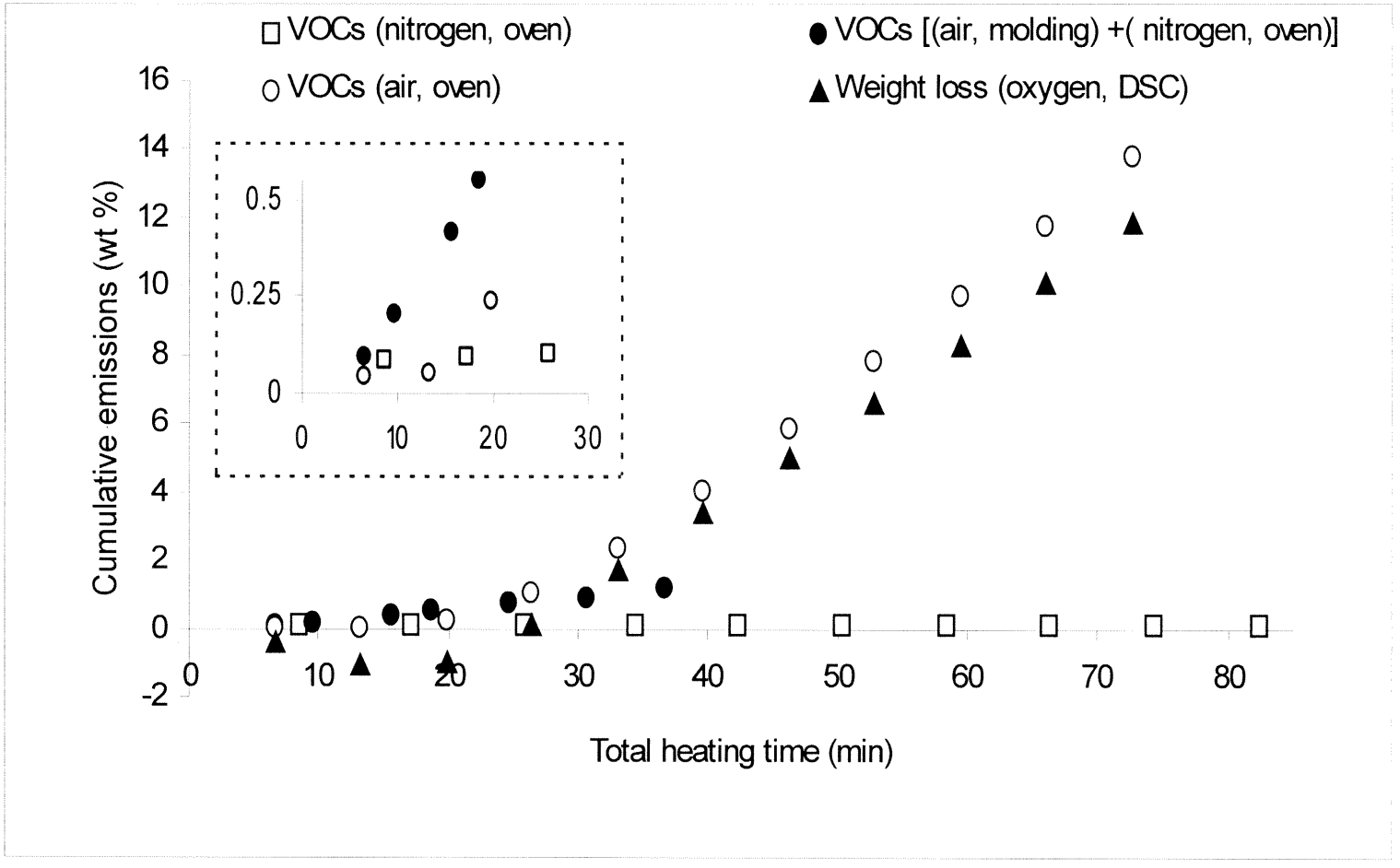

Figure 4.8 Comparison of the cumulative emissions (VOCs for FID or weight loss for DSC) at different conditions as a function of total heating time.
Note: The negative values indicate weight increase instead of generation of volatiles.
The box shows the exploded view of the first ten data points.

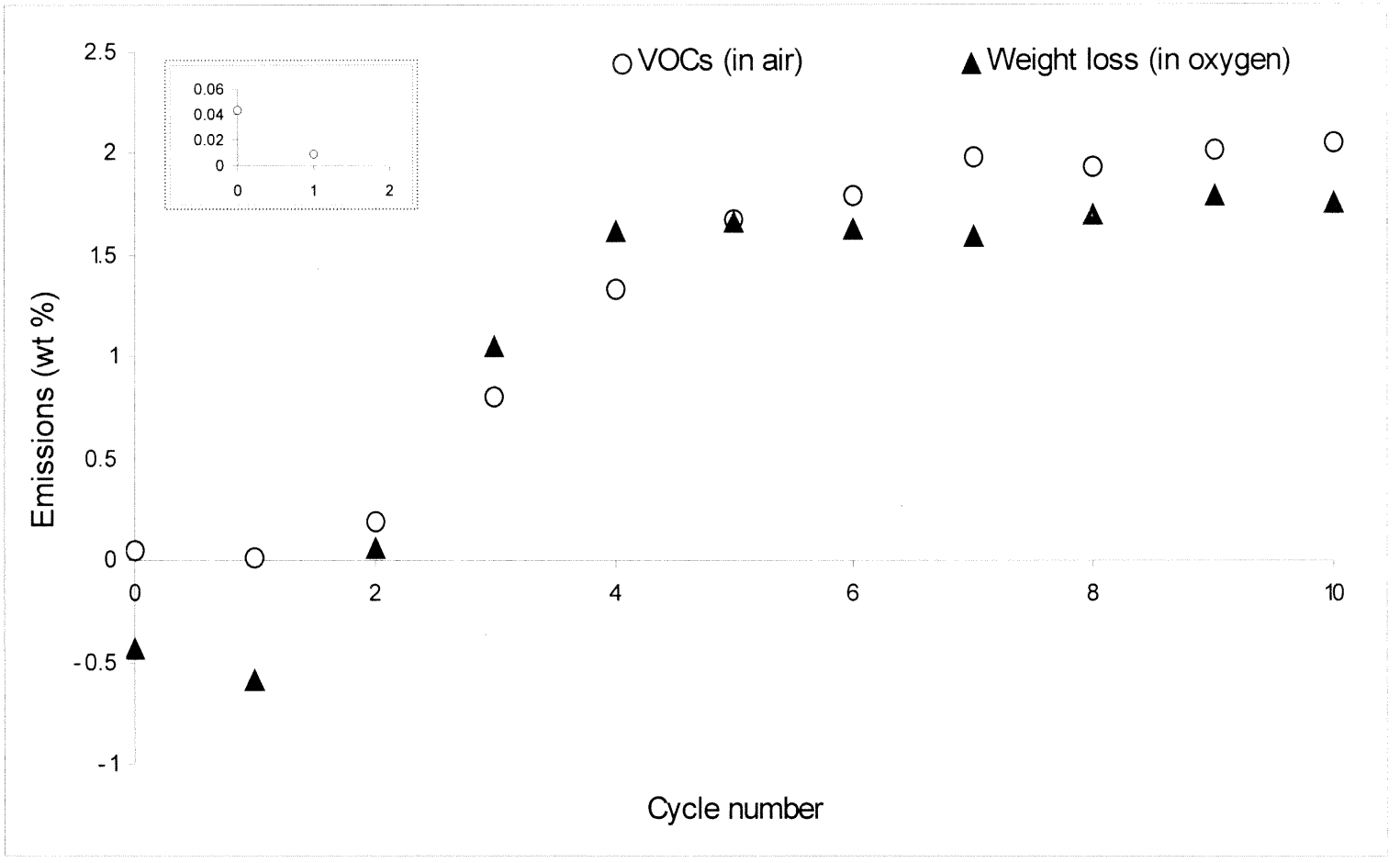

Figure 4.9 Emissions from each cycle of multiple heating/cooling of a single U-PP sample in air (VOCs, FID detector) and oxygen (weight loss, DSC).
For each cycle, total heating time was 6.6 min (3.6 min from 36°C to 180°C, then 3 additional min at 180°C).
Note: The negative values indicate weight increase instead of generation of volatiles.
The box shows the exploded view of the first two data points in air.

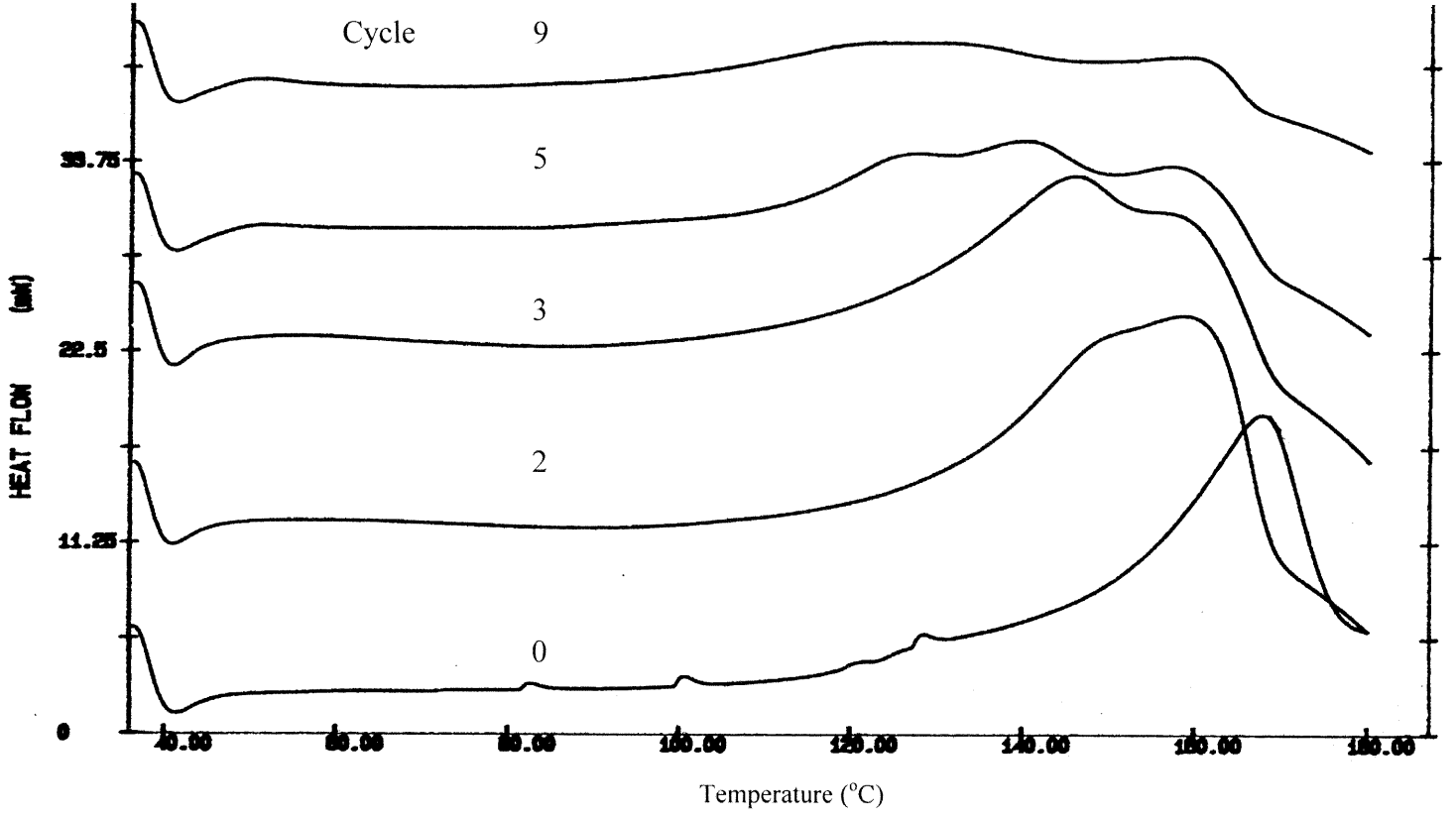

Figure 4.10 DSC heating curves (heat flow vs. temperature) from U-PP after multiple heating/cooling under oxygen.

The cumulative VOCs as a function of heating time from the FID measurements and the cumulative weight loss from the DSC experiments are compared in Figure 4.8. In summary, multiple heating in nitrogen did not increase the cumulative VOCs noticeably, whereas multiple heating in air or oxygen required a certain amount of time before oxidative degradation began, after which the cumulative VOCs or weight loss increased linearly with time at a higher rate (note the difference in slopes). By contrast, during injection molding followed by oven heating in nitrogen, VOCs increased linearly from the first pass (cycle 0). In addition, the slopes of these lines increased as follows: simulation in nitrogen < real reprocessing + oven heating in nitrogen < simulation in air or oxygen.

4.3.2 Effects of Material Type and Reprocessing Conditions

4.3.2.1 Effects of Stabilizer and Reprocessing Conditions on VOCs Emissions. The data in Figures 4.11 and 4.12 includes averages of 3-6 replicates and standard deviation. They represent the emissions obtained from U-PP samples processed up to 10 times and S-PP samples processed up to 5 times. The samples were heated from 36°C to 180°C at the rate of 40°C/min (Figure 4.11), and held at 180°C for three additional minutes under nitrogen (Figure 4.12). It is clear that the length of heating time strongly influences the amount of total VOCs. As shown in Figure 4.12, when the samples were held at 180°C (approximately 15 degrees above the melting temperature of the PP) for three additional minutes, the VOC emissions increased more than three times.

As observed from U-PP and explained in the previous section, the average value of total emissions from S-PP did not vary significantly among cycles, either. The large

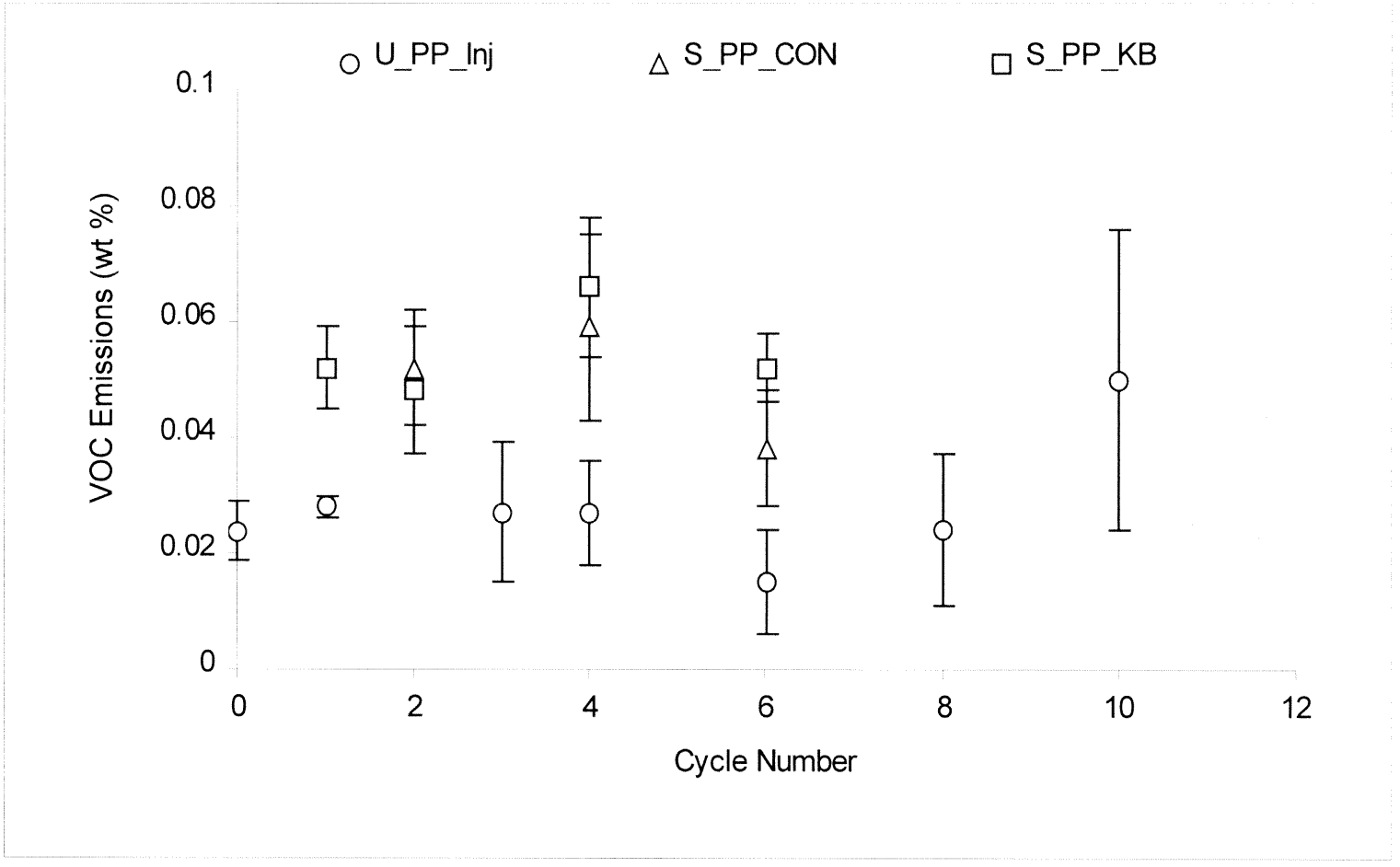

Figure 4.11 VOC emissions generated from multiple processed PP when heated from 36°C to 180°C at 40°C/min.

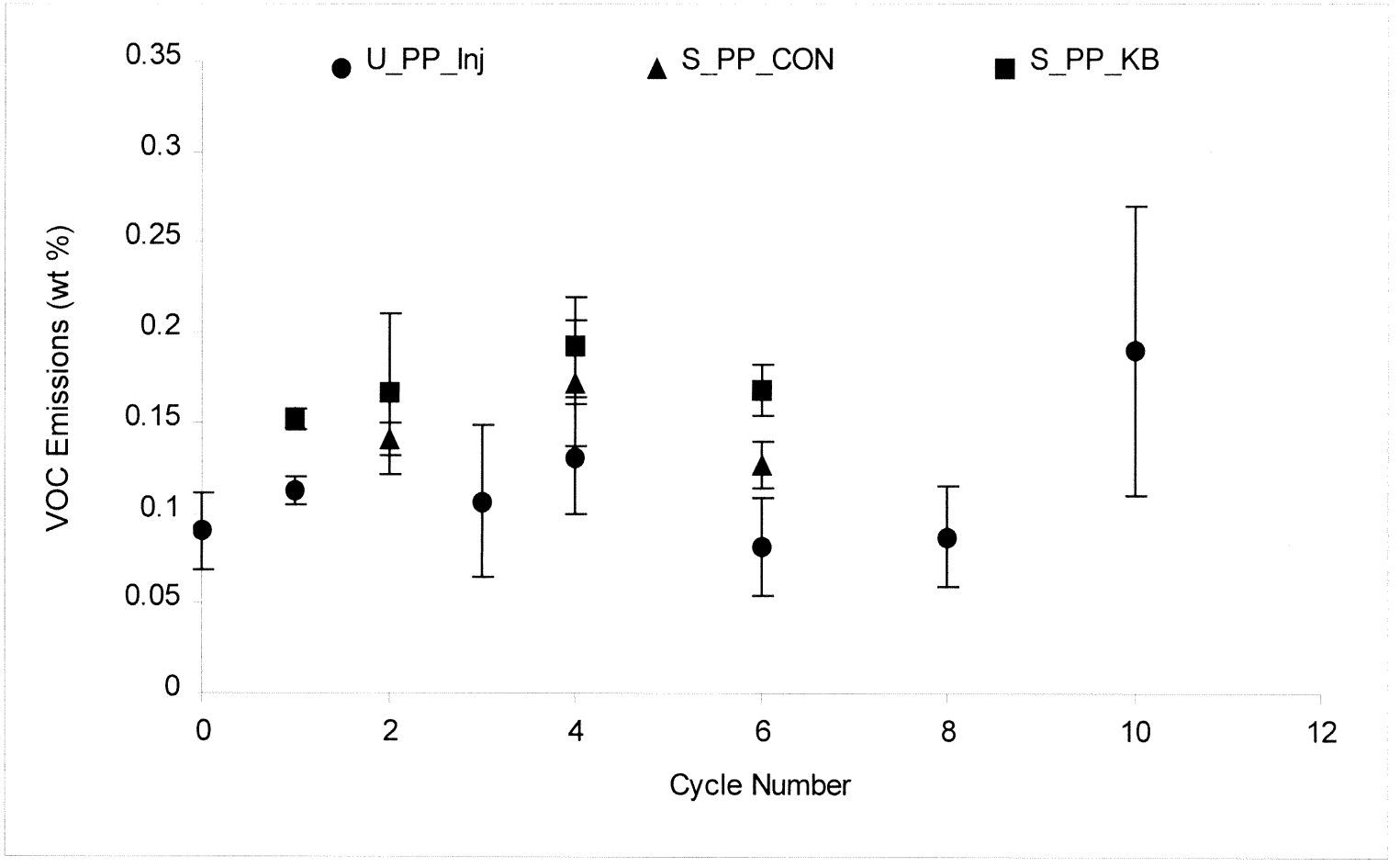

Figure 4.12 VOC emissions generated from multiple processed PP when heated from 36°C to 180°C at 40°C/min and held at 180°C for additional 3 min.

standard deviations do not allow differentiation between the two screw configurations in the S-PP data.

Experimental oxidative induction times of the PPs confirmed that the 6501 resin powder (U-PP) is virtually unstabilized (OIT about 1 min). Whereas, the H306 resin pellets (S-PP) is much less susceptible to thermooxidative degradation (OIT about 8 minutes), presumably as a result of the stabilizers presence. Thus, it is of interest to note the higher values of the VOCs emissions of the extruder reprocessed stabilized material versus those of the injection molded unstabilized grade, particularly in Figure 4.11. The additional heating in Figure 4.12 appears to promote some data overlapping. However, it is clear that the expected effects of the stabilizers were overcome by the effects of reprocessing method (Injection molding vs. extrusion, grinding vs. pelletizing) and the accompanying differences. These differences included shear level (higher in extrusion), processes conditions, possibility of venting/wash out of antioxidants during extrusion/pelletizing, etc.

4.3.2.2 Correlation between VOCs Emissions and MFI/M_W. Figures 4.13 and 4.14 present the melt flow index (MFI) of U-PP, and the weight average molecular weight (M_w) of S-PP respectively as a function of processing cycle. They also include the cumulative VOCs emissions based on the subtotal of all the previous cycles. As the data in Figures 4.11 and 4.12 represent the possible maximum amount of VOCs independent of the cycle number, The data points in Figures 4.13 and 4.14 stand for the cumulative maximum VOCs. They show an increasing tendency with increasing cycle number. This trend of cumulative maximum VOCs versus cycle number is clearly related to a similar

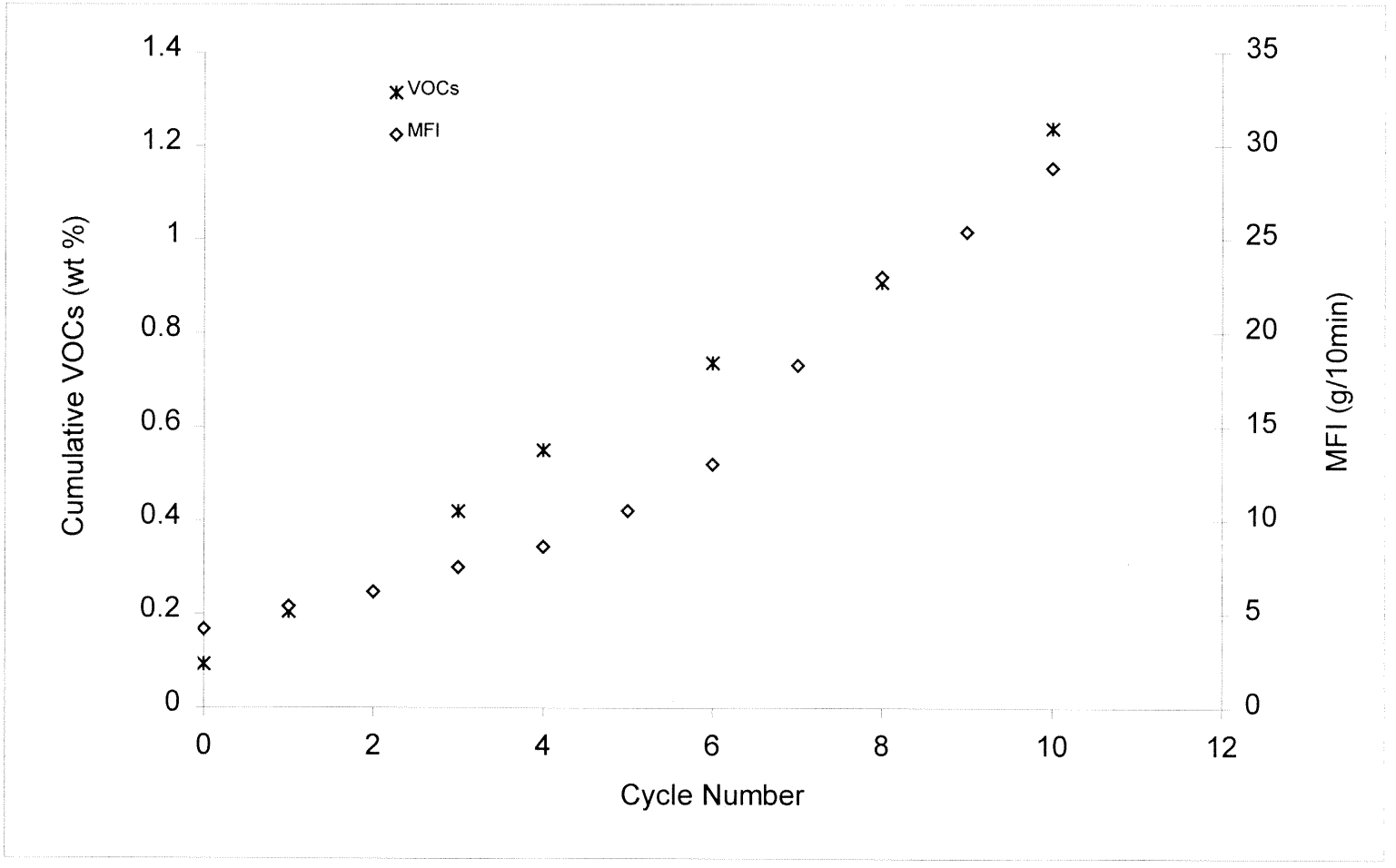

Figure 4.13 Cumulative VOC emissions (when heated from 36°C to 180°C and held at 180°C for 3 min), and melt flow index (MFI) of U-PP after multiple injection molding.

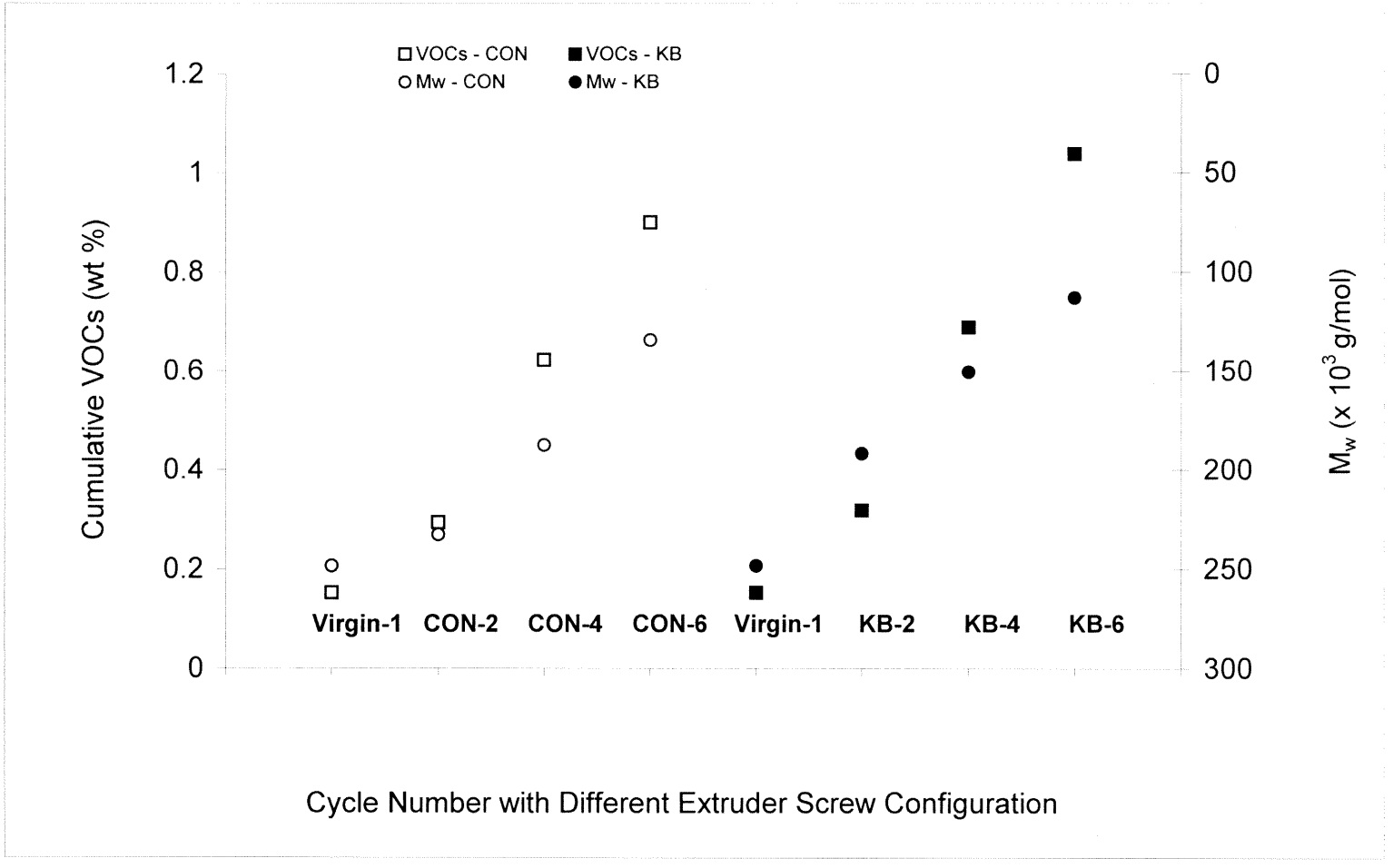

Figure 4.14 Cumulative VOC emissions (when heated from 36°C to 180°C and held at 180°C for 3 min), and weight average molecule weight (M_w) of S-PP after multiple extrusion.
Note: M_w data were adopted from Ref. 166.

trend of increasing MFI with cycle number as shown in Figure 4.13, and decreasing M_w with cycle number as shown in Figure 4.14.

With increasing number of cycles, the increase in MFI of the U-PP indicated a decrease in melt viscosity, a corresponding reduction in molecular weight and a tendency towards further degradation. Figure 4.13 shows that both cumulative VOCs, and the extent of degradation increased linearly up to the 6th cycle, and more rapidly thereafter. These increases after the 7^{th} cycle may be attributed to several factors including higher probability of contamination of molding and grinding equipment, and adjustments in molding conditions required to accommodate materials with increasingly lower melt viscosity. For the S-PP, after multiple extrusions as shown in Figure 4.14, the increasing tendency of the cumulative VOCs vs. cycle number corresponded very well to the decreasing tendency of molecular weight change. Material reprocessed under more severe shear (KB) appeared to produce more volatiles with concomitant fast reduction of M_W as cycle number increased. Thus it appears that decreasing M_w results in higher fraction of small molecules, which generate more VOCs.

4.3.2.3 Determination of Structural Changes by FTIR Analysis

FTIR Spectroscopy

Figure 4.15 shows the FTIR spectra (wavenumber 2000-1500 cm^{-1}) of films obtained from reprocessed U-PP. With increasing cycle number, the absorption increased between 1800 and 1675 cm^{-1}, which is the region where carbonyl group (>C=O) has a strong absorption band. The appearance of carbonyl group indicated that oxidative thermal degradation took place during multiple injection molding. However, the oxidative process

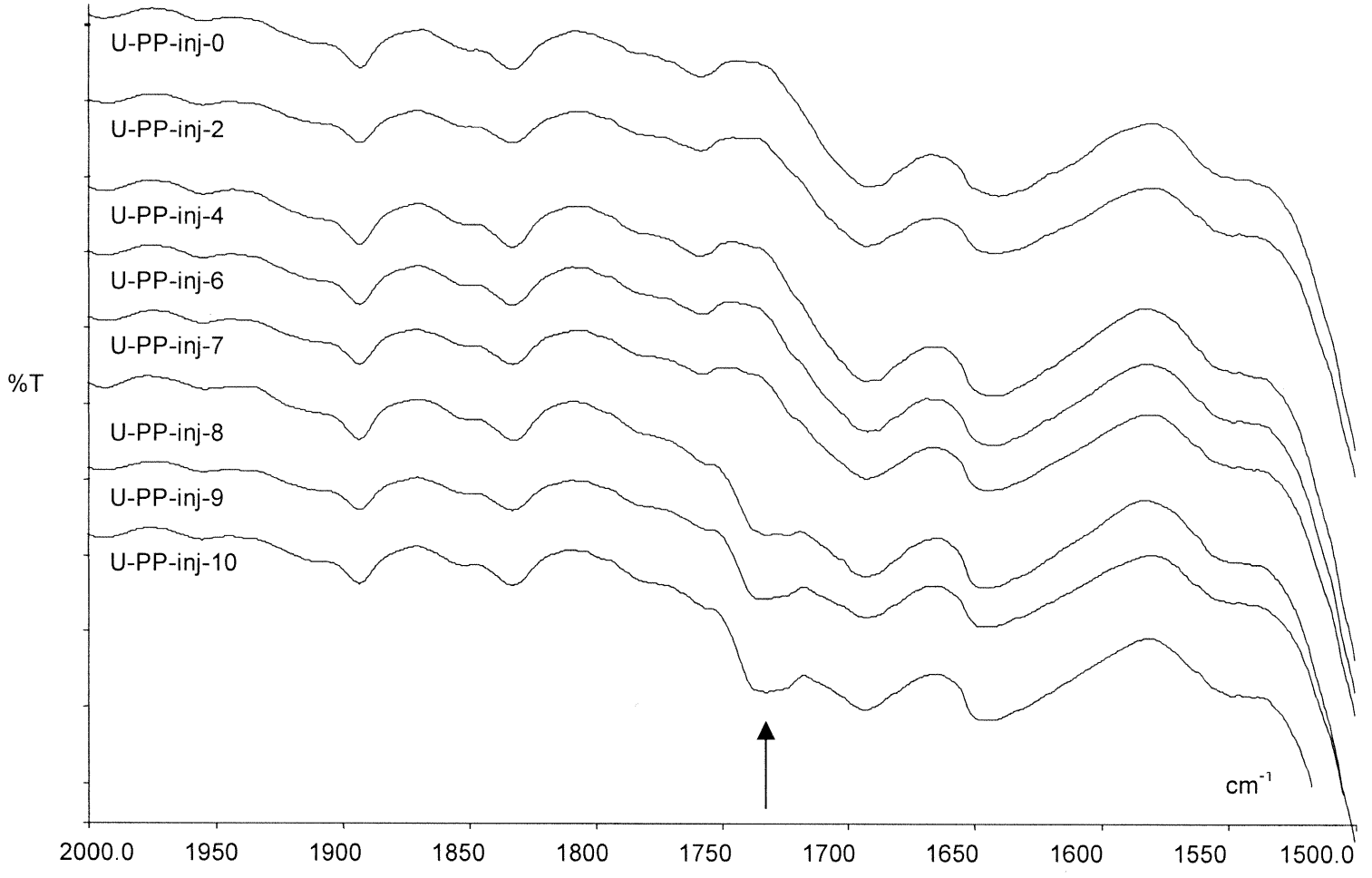

Figure 4.15 Comparison of the FTIR spectra of U-PP after different injection molding cycles.

became more prominent after the 7th cycle, and a large increase in the carbonyl absorption was seen at the 8^{th} cycle. This is evident in Figure 4.17, where the spectra were processed using the one from 0 cycle as the background to eliminate the effect of film thickness (sample concentration). The pronounced increase in carbonyl concentration indicated enhanced oxidation, and this correlated with the rapid increase in the VOCs emission and the MFI after the 7^{th} cycle. This sudden increase also agreed with the observations from simulations in air and oxygen that significant degradation occurred only after a certain number of cycles.

The FTIR spectra of films obtained from S-PP after different extrusion cycles were subtracted by the spectrum of the film of as received pellets. The differences are included in Figure 4.16. It is shown that for the CON samples (cycles 2,4,6), the concentrations of carbonyl groups in their representative region (1675-1800 cm^{-1}) were lower than those in the corresponding KB samples. This means the more aggressive configuration (KB45) did cause higher extent of thermal/oxidative degradation. It is also shown that with increasing cycle number, both screw configurations promoted more degradation corresponding to a proportional increase in the carbonyl group concentrations. These observations are in relatively good agreement with the cycle number versus absolute VOCs, cumulative VOCs, and M_w of Figures 4.11, 4.12 and 4.14. With respect to degradation, it appears that the second extrusion cycle with the KB45 configuration was equivalent to the fourth cycle with the CON configuration, and the fourth cycle with KB45 was equivalent to the sixth cycle with CON. It is of interest to note that the multiple reprocessing resulted in an increasing concentration of

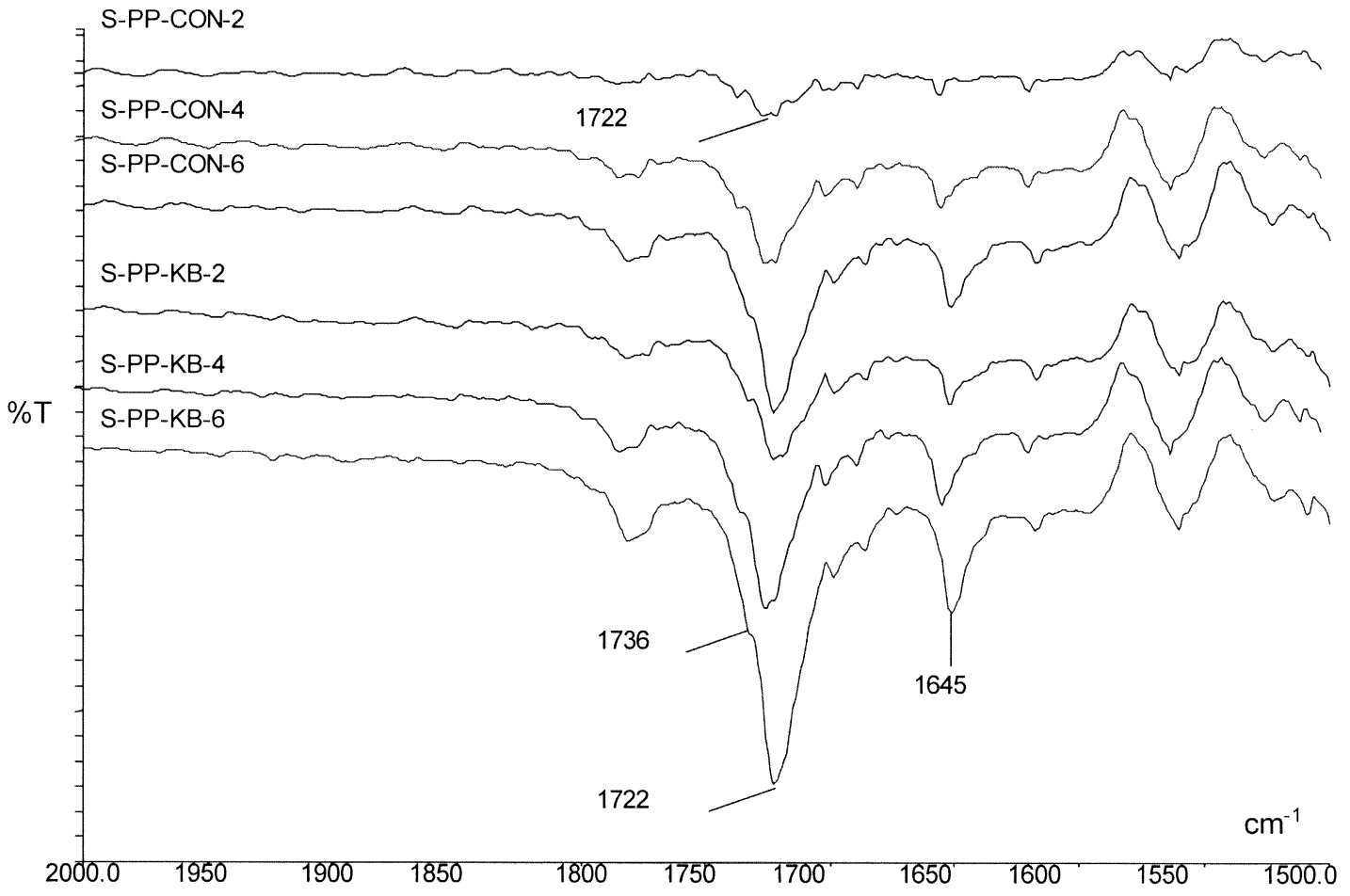

Figure 4.16 Comparison of the carbonyl group of S-PP after different extrusion cycles with two extruder screw configurations (spectrum of as received PP pellets subtracted).

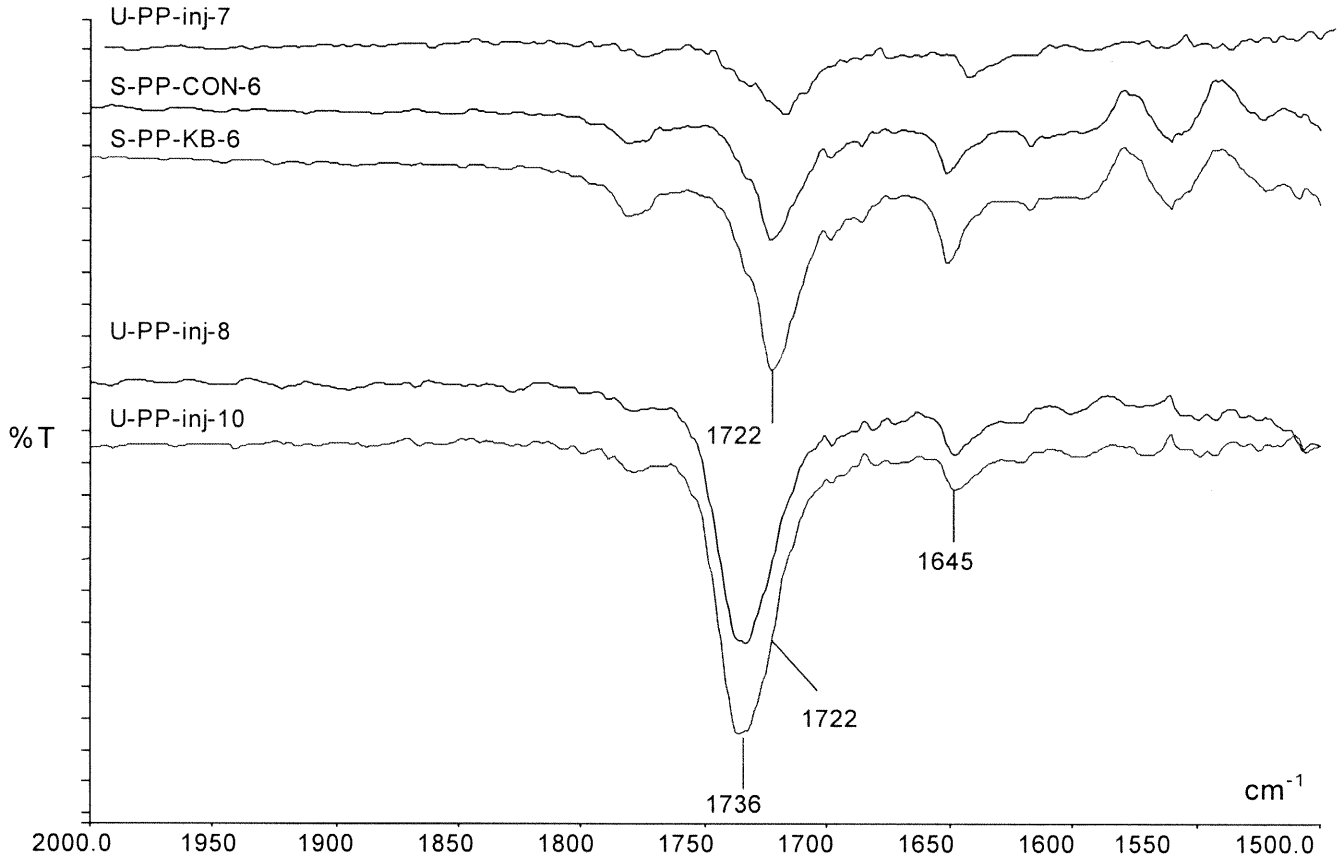

Figure 4.17 Comparison of the carbonyl group of U-PP and S-PP after different processing cycles (spectra of as received PPs subtracted).

unsaturation. This was shown by the increasing absorbance of the peak at 1645 cm^{-1}, which corresponded to C=C double bonds [167].

Comparison of the carbonyl group concentration of U-PP and S-PP was performed. After subtracting the spectra of the "as received" pellets or powder, the normalized spectra at different processing cycles are shown in Figure 4.17. For U-PP, the carbonyl absorption after the 7^{th} cycle increased significantly. Moreover, the location of the dominant carbonyl group absorption shifted to a higher wavenumber. Till the 8^{th} cycle, the carbonyl group showed a relatively strong absorption at 1722 cm^{-1}, after that the absorption at 1736 cm^{-1} increased rapidly. The absorption bands at 1725-1715 cm^{-1} were assigned to aldehyde and ketone, and those at 1745-1735 cm^{-1} were due to the ester group [167]. It appeared that further oxidative degradation occurred after the 8^{th} cycle accompanied by the formation of the new functional groups. This probably affected the measured MFI and VOCs emissions. In addition, the concentration of unsaturated bands increased gradually as shown from the increasing intensity of the C=C peak at 1645 cm^{-1}. By contrast, for S-PP, the carbonyl group at 1722 cm^{-1} (aldehyde and ketone) was still the dominant group with the ester group appearing as a weak shoulder in all spectra of Figure 4.16 and Figure 4.17. Figure 4.16 also shows that the double bonds at 1645 cm^{-1} appeared as early as at cycle 2 (CON-2 and KB-2). The concentration increased with cycle number, and was more pronounced with the KB45 screw configuration.

Carbonyl Index and Unsaturation Index

A carbonyl index (CI) can be defined as the ratio of the peak area of the absorption in the carbonyl region (1800-1675 cm^{-1}) to the area under a reference band. The former area

stands for the total carbonyl concentration. CI can also be calculated as the ratio of the peak height of the individual ketone (1725-1715 cm^{-1}) band or ester (1735-1745 cm^{-1}) band, and the peak height of a reference band. They are referred to as CI_area and CI_height, respectively. Similarly, an unsaturation index can be defined as the ratio of the area or height of the 1650-1645 cm^{-1} peak over that of a reference peak, and referred to as UnsI_area or UnsI_height, respectively. In the literature, different bands were chosen as internal standards (reference) for PP to account for differences in the thickness of the samples. For example, the 974-970 cm^{-1} band which is indicative of a methyl rocking vibration [175-177], the 1470 cm^{-1} band (δCH_3) [178], and the 2730-2720 cm^{-1} band corresponding to stretching vibrations of the aliphatic CH and CH_3 groups [166,179]. In this study, the 2722 cm^{-1} band was used as reference to normalize the absorption of carbonyl and carbon-carbon unsaturation bands. They were represented by the typical peaks at 1722 cm^{-1} (aldehydes and ketones) and 1645 cm^{-1} (C=C), respectively.

The absolute values of the indices were obtained as the average of three replicate samples. The relative standard deviations (RSD%) of the triplicates were less than 10% for CI and less than 3% for UnsI. This demonstrated very good precision during sample preparation, measurement and calculation. Interestingly, for each corresponding cycle up to cycle 6, the absolute value of CI from U-PP was lower than that from S-PP under both configurations, while the opposite was observed in the case of UnsI. This indicated that up to cycle 6, S-PP samples contained higher concentration of carbonyl groups with lower amount of carbon-carbon double bonds. However, after cycle 6, the situation became complicated because in U-PP, the carbonyl groups increased rapidly while the amount of C=C bonds changed little.

In order to compare the increasing tendency of the indices between U-PP and S-PP, relative indices were calculated by subtracting the values of the as received virgin resins. The results were shown as a function of cycle number in Figures 4.18 - 4.21. It is interesting to note that the indices expressed in ratio of area were almost twice of that in peak height, i.e., Figure 4.18 vs. Figure 4.19, Figure 4.20 vs. Figure 4.21. However, the trends in the change of the indices with increasing cycle number were correspondingly consistent.

As shown in Figures 4.18 and 4.19, the CI from U-PP increased very slowly in the first 7 molding cycles, followed by a sharp increase in the 8^{th} cycle. This excellently corresponded to the observations from the FTIR spectra, the MFI and VOCs data. By contrast, the S-PP had a higher and more linear increase within the six extrusion cycles. The higher shear level from KB 45 also made a significant difference from CON.

Compared to CI, the increase in UnsI was much smaller for both S-PP and U-PP. However, the similar linear increase and similar effects of shear level were observed from S-PP (Figures 4.20 and 4.21). For U-PP, the unsaturation indices did not change noticeably among cycles, as observed from their absolute values. However, Hinsken et al [167] reported a remarkable increase in the absorption of C=C double bonds (even higher than carbonyl groups) during multiple extrusion of unstabilized PP. It appeared that it was the processing method (extrusion), not the presence of stabilizers, that promoted the generation of more C=C bonds. According to the reactions in Figure 4.1 and Ref. [167], the formation of C=C bonds during extrusion can be explained by the breakdown of peroxy radicals. Since oxygen deficient conditions exist in an extruder, disproportionation reactions of alkyl radicals contribute to the total yield of C=C bonds.

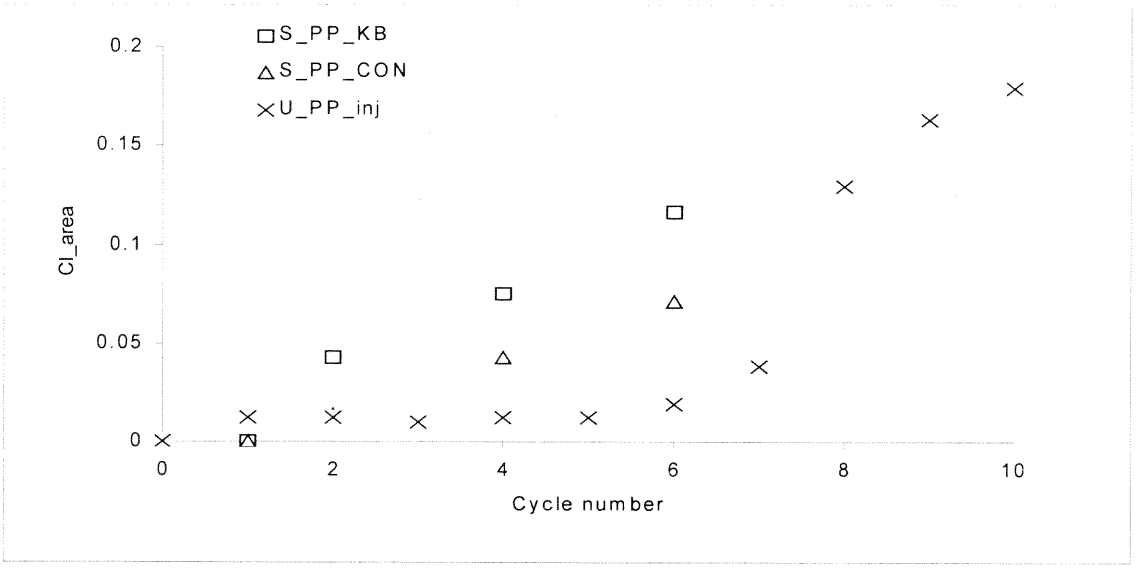

Figure 4.18 Carbonyl indices as total area (CI_area) obtained from U-PP and S-PP after multiple reprocessing.

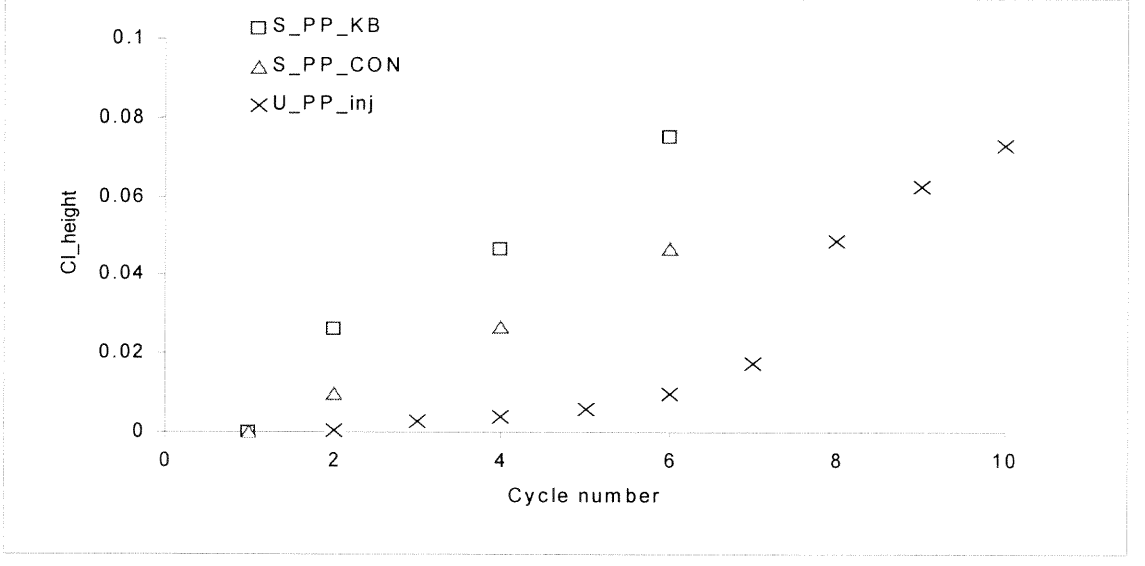

Figure 4.19 Carbonyl indices as height at 1722 cm^{-1} (CI_height) obtained from U-PP and S-PP after multiple reprocessing.

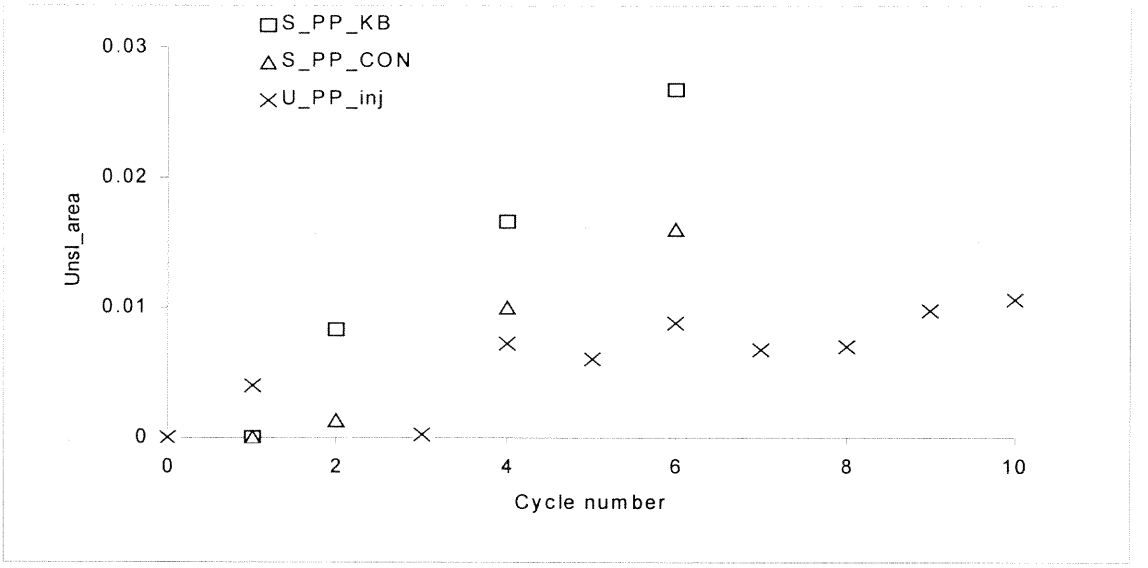

Figure 4.20 Comparison of the unsaturation indices as area (UnsI_area) between U-PP and S-PP as a function of cycle number.

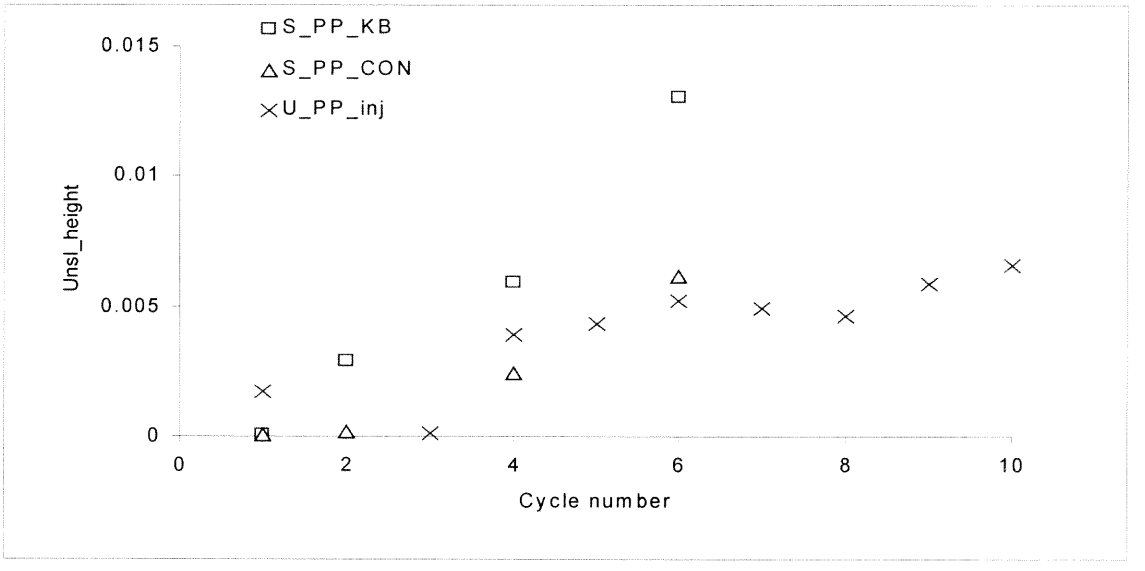

Figure 4.21 Comparison of the unsaturation indices as height (UnsI_height) between U-PP and S-PP as a function of cycle number.

Additionally, the increase in UnsI from the S-PP under CON configuration was within the similar range as the U-PP. This also indicated that processing conditions played an important role in the formation of C=C bonds. These observations were in consistence with those in VOCs variations from S-PP and U-PP, i.e., the effects of reprocessing method and the accompanying difference overcame the expected effects of the stabilizers.

4.4 Summary

Unstabilized and stabilized PP homopolymers were evaluated for total VOCs emissions generated during multiple melt reprocessing by injection molding and extrusion. Results show that the maximum amount of total VOCs from each cycle (up to six cycles for the extruded S-PP and up to ten for the injection molded U-PP) did not change significantly, while the cumulative VOCs increased with increasing processing cycle for both materials. Simulation of multiple heating/cooling of single U-PP samples in nitrogen, and in air/oxygen atmospheres provided limits for mildest and most severe processing conditions in the absence of shear induced mechanical degradation. The results indicate that the actual reprocessing conditions generated emissions whose levels, and rate of generation were closer to the mild thermooxidative process rather than pure thermal degradation.

A good correlation between cumulative VOCs increases and Melt Flow Index (MFI) increase for the U-PP and M_W decrease for the S-PP were obtained. Reprocessing was accompanied by thermooxidative degradation in all cases. FTIR data considering increases in carbonyl content and degree of unsaturation suggest that, at equivalent cycle numbers, degradation appeared to be more severe for the extruded material, in spite of the

longer OIT of the as received pellets. The onset of such structural changes was shown to depend on cycle number and reprocessing method. This was also consistent with the observations from the VOCs measurement, i.e., the effects of processing conditions overcame the expected ones of stabilizers.

CHAPTER 5

IMPROVEMENT OF CONTINUOUS NONMETHANE ORGANIC CARBON (C-NMOC) SYSTEM TO MEASURE SMALL ORGANIC MOLECULES

5.1 Introduction

Nonmethane organic carbon (NMOC) is a measure of total organic carbon except that from methane. It is a convenient and useful way of expressing total VOCs in terms of parts per million (or billion) of carbon (ppm_c or ppb_c), because methane is nontoxic and non-reactive in the atmospheric photochemistry leading to smog formation. When speciation of the individual compound is not required, NMOC can be a fast and inexpensive way of measuring VOCs in ambient air, or in an air emission. This measurement also allows different emission sources to be compared in terms of total carbon emissions irrespective of the specific compounds being emitted [92].

NMOC is a more accurate measure of total VOCs, compared to the direct FID measurement presented in the previous Chapters. One reason is that the direct FID has different response factors for different compounds. Consequently possible inaccuracies exist in the measurement of a mixture of different compounds. Another limitation is that FID also responds to methane, which is neither toxic nor is it involved in tropospheric ozone formation [93]. So the measurement of VOCs in a high methane background may not truly reflect the environmental impact of the emission source. In contrast, the variable response factors associated with FID are eliminated in the NMOC measurements. Moreover, methane is not counted to the total organic carbon. Therefore, NMOC measurement is a more reliable technique for the measurement of VOCs [92,93]. It can be used for on-line monitoring of VOCs during polymer processing.

A conventional NMOC analyzer is described in EPA method 25 [93]. Here, gas samples are collected through a heated filter and a condensate trap (chilled by dry ice) by means of an evacuated sample tank. After completion of sampling, the NMOC is determined by combining the analytical results from the condensate trap and the sample tank. A portion of the air sample is injected into a GC column, the NMOC in the sample is separated from permanent gases such as CO, CO_2, and CH_4. The NMOC is measured using an FID in-line with two catalytic reactors. First, the organics are catalytically oxidized to CO_2, then reduced to CH_4 for measurement by an FID. This method provides a response proportional to the total carbon. The conventional method is composed of field sampling followed by laboratory analysis. A challenge here is that when sample contains high concentrations of CO_2 and H_2O, the resolution in the GC column degrades and quantitation is difficult. Also, CO_2 gas bubbles are trapped inside the ice formed in the chilled condensate trap during air sampling. It is more difficult to purge out the CO_2 prior to recovery of the condensed NMOC. Another major problem is that the detection limits are high, as there is no preconcentration, and the injection volume is small to obtain good column resolution [94,95]. Furthermore, this conventional method is not designed for continuous on-line monitoring.

5.1.1 Continuous NMOC (C-NMOC) Analyzer

Continuous, on-line monitoring can eliminate, or minimize the errors due to sample handling and transportation. It also provides real-time information as there is no delay between sampling and analysis. Therefore, the major component for an on-line analyzer is the sampling and injection device.

On-line injection devices based on microtrap technology have been developed for continuous monitoring of VOCs [96,97,122]. The microtrap is a small diameter tubing packed with one or more sorbents. As a gas sample continuously passes through the microtrap, the organics are selectively trapped by the adsorbent while permanent gases pass through. The trapped organics are injected into the analytical system by thermal desorption. Since the thermal mass of microtrap is very small, this thermal desorption is very rapid and serves as an injection for GC separation, or MS analysis.

The development of instrumentation for continuous NMOC monitoring has been reported [94,95]. This instrument, referred to as the C-NMOC analyzer, combines the microtrap with a sampling valve and a conventional oxidation/reduction NMOC detector. Besides being an on-line concentrator and injector, the microtrap serves as a separator that isolates NMOC from H_2O, CO, CO_2, CH_4 and other background gases. This novel system has been successfully used to evaluate the performance of a laboratory scale catalytic incinerator, and also field tested at an industrial site (a coatings facility in North Carolina) to evaluate its viability as a continuous emission monitor (CEM) [92,98]. The field test was a collaborative effort between US EPA, Mid-west Research Institute, and Research Triangle Institute.

5.1.2 Microtrap Sampling and Injection Systems

The microtrap is the key part of the C-NMOC analyzer and other continuous monitoring techniques developed in this research group [92,94-98,122,125,131]. The microtrap can be designed with different adsorbents, and can be combined with other sampling techniques, such as valve and membrane. The goal is to obtain high sensitivity,

selectivity, complete separation, and to eliminate interferences. However, due to the small dimension of the microtrap, breakthrough of analytes should be carefully dealt with.

5.1.2.1 Adsorbent. Adsorption was first observed by C. W. Scheele in 1773 for gases, and subsequently for solutions by Lowitz in 1785 [180]. Since the 1960s, characterization of adsorbents has been greatly improved due to the use of gas-solid chromatography (GSC) as a tool. This improvement promoted the application of solid sorbents in the field of environmental monitoring, specifically in airborne contaminant sampling for industrial workplace and ambient air. Meanwhile, considerable attention was given to the development of sorbents with physical and chemical properties that enable them to be used in both GSC and sample enrichment [181].

Classification of Adsorbents

The typical sorbents for sample enrichment are: activated silica gels, porous polymers, and carbonaceous sorbents. Kiselev [182] first categorized the adsorbents into three types (Table 5.1). Type I adsorbents are those that interact non-specifically with the four groups of adsorbates (groups A, B, C, D), while Type II and III adsorbents interact both non-specifically (i.e., London forces, van der Waals forces) and specifically (i.e., strong dipole-dipole interactions) (Table 5.2) [37,183]. However, only Type I adsorbents interact non-specifically with all groups of adsorbates. Examples of the four groups of adsorbates are: group A – n-alkanes; group B – aromatic hydrocarbons, chlorinated

Table 5.1 Classification of adsorbents

Type	Adsorbent	Surface
Type I	Graphitized carbon black	Graphitic carbon (no ions or active groups)
Type II	Activated silica gel	Oxides of silica gel (localized positive charges)
Type III	Activated charcoal	Oxides of amorphous carbon (localized negative charges)
	Porous polymers	Organic "plastics" (weak – strong Type III)
	Carbon molecular sieves	Amorphous carbon (weak Type III, can approach Type I)

Table 5.2 Classification of adsorbates

Group	Molecules	Adsorbents	
		Type I	Type II and III
A	- Spherically symmetrical shells - σ-bonds	Nonspecific interaction	Nonspecific + specific interaction
B	- Electron density concentrated on bonds/links - π-bonds		
C	- (+) charge on peripheral links		
D	- Concentrated electron densities - (+) charge on peripheral links		

hydrocarbons; group C – organometallic compounds; and group D – primary alcohols, organic acids, organic bases.

Nowadays, sampling and preparation involves not only enrichment of the analytes, but also isolation of the analytes from the matrix and removal of interfering compounds. Besides a broad spectrum of sorbents, materials with selective sorption properties (e.g., tailored sorbents) are also being utilized to a large extent. Some carbonaceous sorbents belong to the group of tailored sorbents, which allow optimal solution to specific problems. The main advantage of carbon sorbents is their high chemical inertness and thermal stability. In contrast to sorbents with a SiO_2 matrix (silica gel, porous glass), their use is not limited by pH, and compared to organic polymer sorbents, they withstand much higher temperatures. Sorbents with a carbon matrix may also serve as carriers for various functional groups.

Carbonaceous sorbents

Various kinds of carbon sorbent are available and are already used in air sampling and analysis. They can be divided into four types: activated carbon, carbon molecular sieves (CMS), graphitized carbon black (GCB), and porous graphitic carbon (PGC). They differ in their physico-chemical characteristics, such as pore size and shape, particle size, surface area, functionality of surface and chemical inertness. Consequently, the kinetics and thermodynamics of sorption process are different, and so are properties such as breakthrough volumes, and adsorption isotherms [37,183]. The properties of carbon sorbents can be related to the source of starting material, procedure chosen for

preparation of the product, and conditions under which the adsorbent is used. Table 5.3 lists some of these factors.

Matisova, et al. [37] discussed both advantages and disadvantages of these carbon sorbents, and their use in trace analysis of organic pollutants. The recently developed, thermally modified carbon blacks, carbon molecular sieves and porous carbons, are superior in performance over traditional activated charcoal and porous polymers (e.g., Tenax). The application of the novel adsorbents has minimized the problems of contamination from artifact formation. Hence, they are suitable for the sampling of VOCs and preconcentration/isolation of semi-volatile organics. Betz et al. extensively studied the characterization of carbon-based adsorbents, and utilized them in air sampling [183-186].

Choice of the proper sorbent

The choice of carbon sorbents depends upon the application, as well as the techniques used. The choice is made by considering the nature and concentration of the chemicals to be sampled, the external conditions (temperature and humidity), and the type of sampling and analytical equipment available [38,187]. One must consider a wide range of physical and chemical properties of both the adsorbent and the analytes. In order to get the best adsorption/desorption efficiencies for the analytes, adsorbents are selected based on their collection efficiency, and desorption efficiency, i.e., the ability to quickly release the trapped compounds. The general physico-chemical characteristics taken into account for the evaluation of sorbents are functionality, particle size/shape, surface area, pore size, and chemical inertness [37]. Dewulf and Langenhove [24] summarized four criteria for

Table 5.3 Comparison of the carbonaceous adsorbents

Type	Starting material	Producing process	Surface structure
Activated carbon	Biomass materials, fossilized plant, synthetic polymers	A two-step process of carbonization and then activation by partial gasification	Highly porous, complex surface structure containing a wide range of functional groups
Carbon molecular sieves (CMS)	Suitable polymeric materials (e.g. polyvinylchloride) or petroleum pitch materials	Controlled pyrolysis at temperatures usually above 400°C	Highly porous structure with almost uniform micropores, very small crystallites crosslinked to yield a disordered cavity-aperture structure
Graphitized carbon black (GCB)	Ordinary carbon blacks	Heating to about 3000°C in an inert gas atmosphere	Homogeneous surface without micropores, free of functional groups
Porous graphitic carbon (PGC)	Suitable silica gel or another porous template with a phenol-formaldehyde resin mixture, phenol hexamine mixture, or saccharose, etc.	After polymerization, heating in an inert atmosphere to about 1000°C. Then removing the template by alkali to give PGC. Finally, firing in an inert atmosphere at 2000-2800°C to produce some degree of graphitization	Homogeneous hydrophobic surface; surface chemistry is determined by the final heat treatment, and any subsequent chemical treatment.

the choice of sorbent. First, breakthrough of the analytes has to be avoided. Second, the sorbent itself may not produce any artifacts. The sorbents must be kept free of contamination before and after sampling. Finally, the retention of water on the sorbent material has to be low, so that negative interferences in GC/MS analysis, and the blockage of cryogenic traps may be avoided.

5.1.2.2 Breakthrough of Microtrap. The three most significant parameters of a sorbent trap are sample capacity, desorption efficiency, and storage stability [20,38,188]. Sample capacity is often given in terms of the breakthrough of a constant concentration through the sorbent bed. As stated above, the breakthrough of analytes is the first criterion for choosing a sorbent.

Definition

Normally, breakthrough is defined as the volume in liters required for the outlet concentration to reach 5 percent of the (constant) concentration being sampled (5% V_b), and this has been shown to be effectively independent of the flow rate in the region of normal use. A more practical definition might be the recovery of 5 percent of total sample from the back-up section, but these definitions are not interchangeable [20,38,188]. Lu and Zellers [189] set a higher ratio of outlet to inlet concentration. They defined breakthrough volume (BTV) as the sample volume required for the vapor concentration downstream from their preconcentrator to reach 10% of inlet concentration (i.e., C_o/C_x = 10).

Breakthrough volume (BTV) has also been approximated as the retention volume (V_R) [EPA Method TO-1, and References 190-192] and specific retention volume (V_g^t) [183,184,190]. So, BTV can also be defined as the calculated volume of carrier gas per gram of adsorbent which causes the analyte molecules to migrate from the front of the adsorbent bed to the back of the adsorbent bed [183,190].

Determination of breakthrough

Breakthrough volume (BTV) characterizes the adsorption capacity of an adsorbent towards a given compound. It depends on numerous factors, such as the temperature, the concentration of the compound being studied, the chemical composition of the gaseous mixture, the relative humidity, the flow-rate and linear velocity of the carrier gas, the dimensions of the trap, and a number parameters relating to the adsorbent such as mass, granulometry, pore diameter and specific surface area, repeated re-use and thermal pretreatment. However, it appears that the adsorption temperature and the concentration of the adsorbed compound are the main parameters affecting the BTV value [193]. The relationships between these two parameters and BTV are used to determine the BTV value [44,194,192,193].

Since adsorption is an exothermic phenomenon, the effect of temperature on BTV can be expressed by the Van't Hoff-type equation:

$$\frac{d[\log(BTV)]}{d(\frac{1}{T})} = -\frac{\Delta H_{ad}}{2.303R} \tag{5.1}$$

where ΔH_{ad} is the adsorption enthalpy, R is the gas constant, and T is the absolute temperature. Considering ΔH_{ad} as a constant, Eq. (5.1) can be expressed as

$$\log(BTV) = -\frac{\Delta H_{ad}}{2.303RT} + K \qquad \text{or} \qquad \log(BTV) = a + \frac{b}{T} \tag{5.2}$$

So, BTV can be experimentally determined by injection of analytes onto the adsorbent bed at temperatures higher than the trapping temperature. Linear regression analysis was then used to calculate BTV values at different (subambient) temperatures [44,184,192]. This method requires a large extrapolation to obtain BTV at ambient and subambient temperatures.

The variation of BTV as a function of analyte concentration is consistent with the expression of an adsorbent isotherm satisfying Freundlich's equation [193]:

$$\text{Log (BTV)} = \log a + b \log C \tag{5.3}$$

where C is the analyte concentration. The BTV can be determined by passing the analyte through a sorbent bed. By varying the analyte concentration and the trapping time, it is possible to pass different volumes of gas and different amounts of analyte through the bed. The trapped analyte is subsequently desorbed and analyzed. The masses of the adsorbed analyte are plotted against sample volumes. Then the BTV is defined as the sampled volume corresponding to the end of the linear domain. The extreme value of the linear domain is evaluated by calculation of the intersection between linear and non-linear domains. The linear calibration equation $y = \alpha x$ is calculated by the least-squares method. Data in the non-linear domain are fitted by a power law, $y = cx^d$. The parameters c and d are obtained by the least-squares method. Such a mathematical method to determine the BTV was preferred to the statistical method developed by Liteanu et al [194].

Many other equations, proposed and fit to equilibrium adsorption isotherm data, can also be used to fit breakthrough data. Four of the simplest ones, containing only two adjustable curve fit parameters, are as follows [195]:

The Freundlich isotherm equation:

$$W_e = aC_o^{1/n} \tag{5.4}$$

The Langmuir adsorption isotherm equation:

$$W_e = \frac{W_{max} K_H C_o}{1 + K_H C_o} \tag{5.5}$$

The Dubinin/Radushkevich (D/R) isotherm equation:

$$\ln W_v = \ln W_{vsat} - (\frac{KR^2T^2}{\beta^2})[\ln(\frac{P}{P_{sat}})]^2 \tag{5.6}$$

The Hacskaylo/LeVan (H/L) isotherm equation:

$$\ln P = A' + \ln\theta - \frac{B' + b'(1-\theta)}{C' + T} \tag{5.7}$$

where W_e = adsorption capacity (g/g_c)

C_o = inlet concentration (g/cm^3)

a, n = two adjustable curve fit parameters

W_{max} = the upper limit to capacity at very high vapor concentrations

K_H = Henry's law constant

W_v =volume capacity = W_e/ρ_L (ρ_L = density of condensed liquid in micropores)

W_{vsat} = volume capacity at saturation vapor pressure, P_{sat}

T = absolute temperature

P/P_{sat} = relative vapor pressure = C_o/C_{sat}

R = ideal gas constant ($P = C_oRT$)

K = carbon structural constant

β = affinity (similarity) coefficient

A', B' C' = Antoine constants

θ = fraction of saturation capacity = W_e/W_{sat}

P = equilibrium pressure = C_oRT)

b' = constant of linear variation of heat of adsorption with loading

Eq. (5.4) and (5.5) show a relationship between adsorption capacity (related to BTV) and concentration, whereas Eq. (5.6) and (5.7) indicate the correlation of BTV with the vapor pressure of an analyte. Both relationships have been applied to the determination of BTV data [44,193,195-197].

As most commonly used in predicting service life of an air-purifying respirator (APR) [195-197], breakthrough time (t_b) is also frequently applied to characterize the performance of an adsorbent. The most simple equation is derived from the Freundlich isotherm:

$$t_b = a\, C^b \tag{5.8}$$

where C = concentration (ppm), a = constant for a given set of conditions, and b = constant (<1).

Another common equation for determining t_b is from the modified Wheeler model, which is derived from a mass balance between vapor entering, retained within, and exiting the bed [189,195].

$$t_b = \frac{\rho_b W_e}{C_o}\left[\tau - \frac{1}{k_v}\ln\left(\frac{C_o}{C_x}\right)\right] \tag{5.9}$$

where ρ_b = adsorbent bed density (g/cm^3)

$\tau = W_b/(\rho_b Q)$, bed residence time (min)

Q = volumetric flow rate (cm^3/min)

W_b = bed mass (g)

K_v = kinetic rate constant (min^{-1})

C_0, C_x = inlet, out concentration (g/cm^3)

The variables W_e and k_v vary directly with C_o and can be determined by a number of different approaches.

Although t_b determinations are important, such as in air-purifying respirators (APR) and preconcentrator development [189,195-198], the adsorbent performance parameter of more general interest is the BTV. Via the modified Wheeler equation, it can be expressed as follows:

$$BTV = \frac{W_e W_b}{C_o}[1 - \frac{1}{k_v \tau}\ln(\frac{C_o}{C_x})] \qquad (5.10)$$

This equation relates several important design and performance parameters to the vapor breakthrough volume of an adsorbent bed under a continuous vapor challenge [189]. The term W_eW_b/C_o represents the volume of air containing vapor at C_o that would be required to reach thermodynamic equilibrium, V_t. Since the adsorption efficiency, $1-\ln(C_o/C_x)/k_v\tau$, is generally ≤ 1, BTV is $\leq V_t$. The quantity $\ln(C_o/C_x)/k_v\tau$ represents the fractional unused bed capacity. The decrease in BTV as C_o increases is partially offset by an increase in W_e with C_o. But since W_e typically exhibits a Langmuir, or similar, dependence on concentration, this compensation effect diminishes with increasing C_o.

Obviously, increasing the mass of adsorbent, or decreasing the flow rate maximizes the BTV. However, increasing the adsorbent mass increases the pressure drop

across the bed and may also increase the desorption bandwidth due to heat transfer limitations, increased dead volume, and residual adsorptive interactions of desorbing vapors as they are swept through the bed. Slow heat transfer through the bed cross section may then become a limiting factor, but simply stopping the flow during the initial phase of the heating cycle should minimize band spreading from this factor. Backflushing reduces band spreading due to residual vapor-adsorbent interactions at high temperature. Therefore, Eq. (5.10) provides a useful framework for considering the effects of various design and operating options on the adsorbent bed residence times and consequent breakthrough volumes.

Direct Measurement of Breakthrough

Based on Eq. (5.2) and (5.3), BTV of analytes on a sorbent trap can be determined. However, large extrapolation is required to estimate BTV values at lower temperatures or lower concentrations. Two direct methods can be used to obtain the BTV value in a single injection [44,199]. They are frontal analysis and GC injection method. In frontal analysis, an analyte standard of known concentration is passed continuously at a flow rate through the adsorbent bed, maintained at a constant temperature. Sample breakthrough is monitored by a flame ionization detector (FID). The direct BTV is determined by measuring the time passing between the disappearance of the analyte signal due to the adsorption of the organics in the trap and the inflexion point of the curve when the BTV has been attained. In GC injection method, the sorbent trap is connected to the injection and detection ports of a conventional GC with FID. A conventional injection is made and the effluent is monitored by FID. Multiplying the retention time of the analyte by the

flow rate through the trap produces the retention volume [200]. These two direct methods agree with each other for the light compounds, but not for the heavier compounds [199]. Generally, frontal analysis correlates well with the indirect method based on Eq. (5. 2), while the indirect method tends to underestimate the actual BTV by a factor of ~2 for the worse case [44].

Two methods have been studied previously to measure the breakthrough of the microtrap [122,201-203]. They are the t-method and the pulse interval method. In the t-method a series of pulses are first made to remove all organics from the microtrap, while the sample continues to flow through the trap. Then a pulse is made to desorb the retained substances. First, a desorption peak is seen. This is followed by a negative peak. The duration of the negative peak is the breakthrough time (t_b). In the pulse interval method, the sample stream continuously flows through the microtrp. For each interval, an electrical pulse is applied to release the analyte from the microtrap. The peak area is recorded for each pulse. A plot of peak area against pulse interval is made. The time at the point of inflexion within the curve is the breakthrough time (t_b). The breakthrough and desorption characteristics of the microtrap have been studied with different sorbents: Tenax-TA, Anasorb 747, Carbopack C, Carbopack B and Carbosieve SIII [204].

Safe Sampling Volume (SSV)

It is clear that the BTV is a volume threshold value above which the sampling operation is no longer quantitative. It is generally recommended to remain well below this value during sampling. A safe sampling volume (SSV) has been defined for this purpose, corresponding to a certain percentage of the actual BTV value. In earlier research, SSV

was set as high as 80% of BTV [192,205]. However, this only ensured 99% sampling efficiency. So, lower percentage of BTV was suggested by other researchers, such as two thirds of BTV [20,38,188,190,193], 70% of BTV [206], or even as low as 50% to ensure no sample loss [200].

Multi-bed Adsorbent trap

Since no single material can individually handle the complete range of VOCs encountered in the environment, a combination of sorbents is necessary. The best approach is to make sorbent tubes containing layers of different materials to attain the desired collection and desorption efficiency [38,199,200]. Sequential trapping takes place in these so-called multi-bed sorbents, where the air sample passes progressively through the weakest sorbent to the strongest. The materials would ideally have the ability to stand up to repeated use and heating without changing their characteristics and should additionally give a low background on the analysis. It is also desirable that they would have a low affinity for water.

In recent years, various combinations of carbonaceous and non-carbonaceous sorbents for trapping organic pollutants from air and other environmental samples are reported [24,38,44,125,199,202]. It was shown in scientific and commercial literature that combination of carbon sorbents allows the sampling of a large variety of compounds differing in polarity (non-polar/polar compounds) and volatility (C_2-C_{15}) at various concentration levels.

Since humidity affects the adsorption phenomena and/or the chromatography (GC-MS), selection of the proper adsorbent with a lower affinity for water is very

important [23,24,38,199,202]. Betz et al. [183] systematically evaluated nine molecular sieves and activated charcoal. The largest water breakthrough volume was noted for activated charcoal. Whereas, the hydrophobic properties of the sieves were a function of the pyrolysis temperature used to prepare them and of the subsequent non-specific surface interactions. For example, compared to Carbosieve S-III and Carboxen-563, Carboxen-569 and Carboxen-564 possessed the smallest breakthrough volumes for water. The hydrophobic properties of these sieves are, therefore, a function of the tailorability of the CMS, as stated by Matisova and Skrabakova [37].

In a previous study [123], a two-stage microtrap was developed for making sharp injections while increasing the breakthrough volume. The first stage comprised a large retention trap containing more sorbent, and the small second stage was used to achieve a narrow injection band. A multi-bed microtrap was also made with Carbotrap C, Carbotrap and Carbosieve S-III. The effect of delay time on its trapping efficiency was studied for methanol, acetone, hexane, dichloromethane, ethylbenzene and chlorobenzene [203]. This multi-bed microtrap was also applied to the C-NMOC analyzer for the on-line monitoring of air emissions [94]. Due to the small thermal mass, this kind of multi-bed microtrap would allow rapid heating of the sorbent and immediate on-line injection of the trapped VOCs into an analytical system [94,96-98,122,131].

5.1.2.3 Configuration of the Microtrap Systems. Microtrap can be used stood alone or in combination with other sampling techniques, such as valve or membrane. The combination is chosen to obtain high sensitivity, selectivity, complete separation, and to minimize/eliminate interferences [92,94-98,125-128,131]. Previously studied

configurations, on-line microtrap (OLMT), sequential sampling valve/microtrap combinations (SVM), and on-line microtrap in backflush mode (OLMT-BF), are compared in Table 5.4. It is clear that each of the three configurations has specific advantages and limitations.

5.1.3 Research Objective

The NMOC is an ideal technique for monitoring total organic emissions during polymer processing. It can be put on-line to a wide range of equipment (e.g., extruder, injection molder) and for a variety of polymers. Emissions from different polymers can be directly compared based on their total carbon emissions. With this in mind, an improved version of the C-NMOC analyzer was developed.

Two new configurations of microtrap system were developed to meet different practical sampling needs. In the first one, a sampling loop and a backflushed microtrap were sequentially connected with two valves. The sampling valve can inject a fixed volume of sample for multiple times to the microtrap before the thermal desorption. Thus, this system is referred to as multi-injection sequential valve with backflushed microtrap (MSV-BM) shown in Figure 5.7. It combines the advantages of SVM and OLMT-BF. Not only can the microtrap be backflushed, the total sampling volume can also be fixed. The latter is important when two or more sources are monitored using one instrument; or, when emission stream flow rates are very high and unstable. However, due to the use of two valves, the MSV-BM is a complicated set-up. So, another novel configuration was also developed with one ten-port valve, to which both a sampling loop and a microtrap are connected. Thus, the flow directions inside the loop and the microtrap

Table 5.4 Comparison of the microtrap systems

Microtrap system	Feature	Advantages	Disadvantages	Ref.
On-line microtrap (OLMT)	Microtrap directly placed in a sample stream	• Preconcentration ability, sensitive and selective device; • Continuous monitoring	• Sample matrix is not separated from analytical systems; • Difficulty in switching between different sampling lines; • Pressurized sample or pump needed; • Analyte breakthrough may contribute to the baseline of detection.	122, 96, 97, 203
Sequential valve microtrap (SVM)	Microtrap combined with sampling valve	• Large injection volume (up to 40 ml), so lower detection limit; • Sample stream isolated from analytical system	• Effects of sample matrix due to large volume injection; • No information during microtrap injections; • Lower sensitivity than OLMT in a fixed injection cycle time.	96, 203
On-line microtrap with backflush desorption (OLMT-BF)	Microtrap replacing the loop of a gas sampling valve	• Sample stream is completely isolated from the analytical system; • Some interferences eliminated; • High sensitivity and selectivity; • Backflush mode allowing the use of multi-bed microtrap	• No information during injections	94, 199, 124

are switched simultaneously. This configuration is referred to as sequential valve with backflushed microtrap (SV-BM).

In addition, selection of a proper adsorbent is critical in improving the performance of a microtrap sampling system. Given the lack of a universal sorbent, multi-bed microtrap is the best approach to collect organics with various volatilities and polarities [37,38,44]. Considering the BTV value from the literature results and the effect of humidity (as listed in Table 5.5), Carboxen 564, instead of the common Carbosieve S-III which has high affinity to moisture, was chosen. Then, a multi-bed microtrap was constructed with a combination of Carboxen 564, Carbotrap C and Carbopack B. This multi-bed microtrap and the two new sampling configurations were applied to the C-NMOC analyzer. The corresponding breakthrough and characteristics of these systems were studied with the highly volatile (i.e., propane) and polar (i.e., methanol) organic molecules. Because of their polarity and high volatility, propane and methanol are difficult to trap on most common sorbents, especially Carbotrap C.

Methanol is also designed as a pollutant to be regulated by the Title III of the 1990 Clean Air Act Amendments (CAAA) [59]. Whereas, propane is on the top list of anthropogenically generated VOCs. It is mainly produced by fossil fuel combustion and industrial processes [27,29,99]. In this study, both methanol and propane were chosen as the probe molecules to study breakthrough on the multi-bed microtrap during C-NMOC analysis.

Table 5.5 Physical characteristics of several most common adsorbents [37,46,183,184,200]

Adsorbent	Carbotrap C	Carbotrap	Carbopack B	Carboxen -563	Carboxen - 564	Carboxen -569	Carbosieve S III
Mesh size	20/40	60/80	60/80	20/45	20/45	20/45	60/80
BET surface area (m^2/g)	10	100	86	510	400	485	820
Density (g/ml)	0.72	N/A	N/A	0.53	0.60	0.58	0.61
BTV (methane)	2	N/A	N/A	N/A	N/A	$3.5x10^1$	$9.0x10^1$
BTV (ethane)	3	$1.73x10^1$	N/A	$3.67x10^2$	$8.17x10^2$	$5.15x10^2$	$9.80x10^2$
BTV (propane)	7	$5.49x10^1$	N/A	N/A	N/A	$4.49x10^3$	$8.5x10^3$
BTV (vinyl chloride)	N/A	N/A	N/A	$7.62x10^3$	$1.01x10^4$	$1.65x10^4$	$6.98x10^4$
BTV (methanol)	6	$2.5x10^2$	N/A	N/A	N/A	$9.5x10^2$	$7.5x10^3$
BTV (benzene)	$1.99x10^2$	$1.17x10^4$	$2.59x10^3$	N/A	N/A	N/A	N/A
BTV (toluene)	$7.77x10^2$	$6.50x10^5$	$3.35x10^4$	N/A	N/A	N/A	N/A
BTV (water)	low	low	low	$3.20x10^3$	$4.17x10^2$	$2.24x10^2$	$1.28x10^3$

Note: BTV: breakthrough volume at 20°C (ml/g).

5.2 Experimental

C-NMOC Analyzer: The schematic diagram of the microtrap based C-NMOC system is shown in Figure 5.1. The sampling and injection systems were developed with a backflushed multi-bed microtrap. The oxidizing unit in the NMOC analyzer was an about 5 inch long, 1/8 inch diameter stainless steel tubing packed with 1.0 g 80/100 mesh 19 wt% Chrome supported with γ-Al_2O_3 (Engelhard, Iselin, NJ). The oxidizing unit was put in a furnace at 650°C (Lindbergh, Watertown, WI). The reducing unit was a 2 inch long, 1/4 inch diameter stainless steel tubing packed with 1.0 g 80/100 mesh pure nickel. The reducing unit was installed in a GC injection port and heated to 360°C. All transfer lines were heated to 110°C to prevent the condensation of analytes. The temperatures were monitored with K-type thermocouples. A flame ionization detector (FID) from a Hewlett Parkard 5890 Series II gas chromatograph (Hewlett Packard, Avondale, PA) was used as the final detector.

Nitrogen (zero dry, Matheson Gas Co., East Rutherford, NJ) was used as the carrier gas to elute and inject the air sample from the microtrap sampling systems into the NMOC analyzer. The deactivation of the oxidizing and reducing catalysts was tested with 110 ppm CH_4 and 99 ppm CO_2 (certified standard gases, Matheson Gas Co., East Rutherford, NJ).

Multi-bed Microtrap: 3.3 mg Carbotrap C, 22.7mg Carbopack B and 64.5 mg Carboxen 564 (Supelco Inc., Bellefonte, PA) were packed into a 10 cm long, 1.3 mm I.D. thin wall stainless steel tubing (HTX-16TW, Small Parts Inc., Miami Lakes, FL). Silanized fiberglass was used to hold these adsorbents in place. The adsorbents were

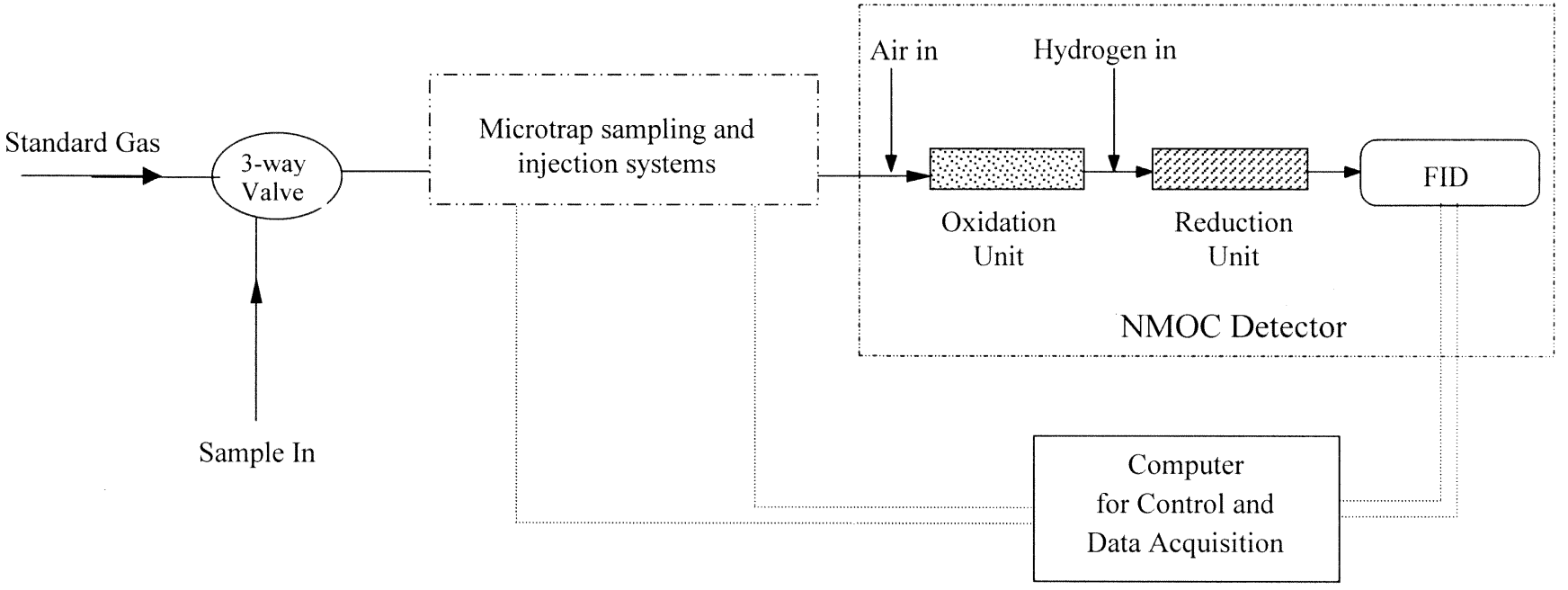

Figure 5.1 Schematic diagram of C-NMOC system.

arranged in order of increasing affinity to organics, as shown in Figure 5.2. Thus, the smallest molecules went through the weakest sorbent and were trapped on the stronger sorbents. It is important that during sample collection, the sample stream enters the microtrap at the least active layer and leave through the most tenacious layer. Whereas, the flow should be reversed during desorption to backflush the multi-bed sorbent trap. This also keeps the heat energy needed for volatilization to a minimum, as each component is trapped on a sorbent from which it is easily released.

The microtrap was conditioned by flowing a high purity carrier gas (nitrogen) while it was heated at a ramp rate of 7°C/min to 350°C. It was kept at 350°C for 3 hours with nitrogen on. Then the trap was cooled to room temperature, and sealed for use.

Microtrap Configurations: The multi-bed microtrap was configured in several ways with a six-port and a ten-port gas sampling valves (Valco Instruments Co. Inc., Houston, TX). These sampling systems were combined with the C-NMOC analyzer to study the breakthrough of propane and methanol. The performances of these systems were also evaluated with propane, methanol and high level background gases (8% CO_2 + 120ppm CH_4, balanced in air).

In all modes, the organic components were selectively retained by the adsorbents packed inside the microtrap. Then desorption and injection was performed by heating the microtrap with a pulse of electric current. Seven to ten amperes of current was supplied using a Varian. A microprocessor-based timer was used to control the current at a short pulse time of 4 seconds. Each electric pulse generated an analyte concentration pulse that was analyzed with the NMOC analyzer.

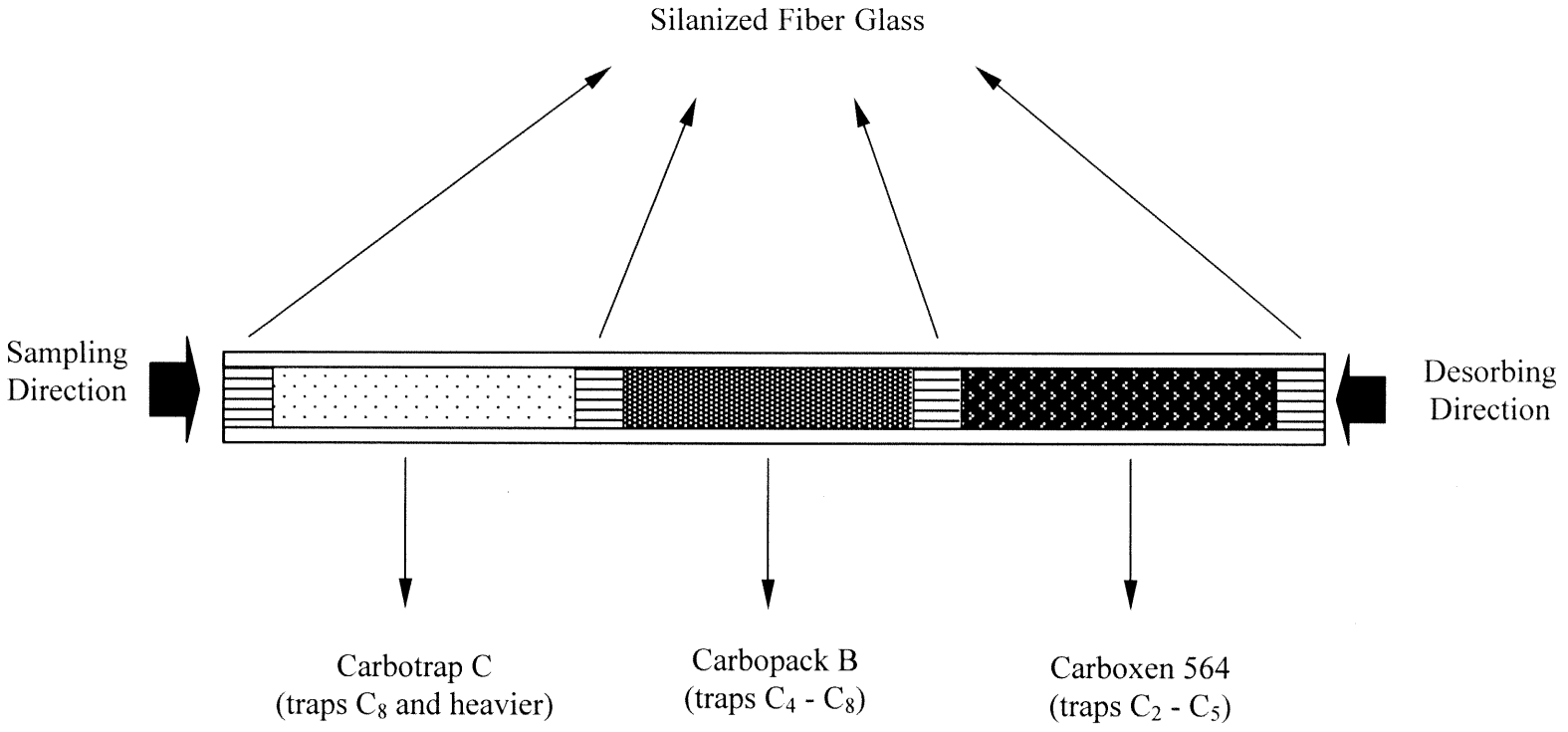

Figure 5. 2 Schematic diagram of multi-bed microtrap.

Analytes and Standards: The breakthrough studies were carried out with 8.1 ppm propane, 106 ppm propane, 231 ppm methanol and a mixture (5.5 ppm propane + 4.8 ppm methanol). The methanol was a calibrated sample. All other gases were certified standards from Matheson Gas Co., East Rutherford, NJ.

The C-NMOC analyzer was tested to see its ability to separate background gases from NMOC. This was done using methanol and a mixture (8% CO_2 + 120 ppm CH_4, balanced in air, Matheson Gas Co.). In addition, the new sampling systems were tested to trap both small molecules (e.g., methanol) and large molecules (e.g., toluene).

5.3 Results and Discussion

5.3.1 Importance of Backflushing

In this research, a ten-port valve was configured with a backflushed microtrap. This configuration allows the use of a multi-bed trap, where small molecules can be adsorbed efficiently whereas large molecules can be desorbed quantitatively. At the same time, background gases such as CO_2, CO and H_2O can be eliminated or separated. One backflushed configuration developed here is shown in Figure 5.3. It uses a ten-port valve and a multi-bed microtrap. The diagrams of this valve in loading and injection positions are illustrated in Figure 5.3. In the loading position, the sample loop filled with the air sample while the carrier gas, nitrogen, flowed through the multi-bed microtrap. The flow is from the stronger sorbent (Carboxen-564) to the weaker one (Carbotrap C). During this period, the microtrap was heated to desorb/inject the organics into the analyzer. This ensures that no irreversible adsorption takes place. Then the ten-port valve was switched to its injection position, where nitrogen carried the sample out of the loop, and injected it into the microtrap from the Carbotrap C end. So heavier compounds were trapped by the

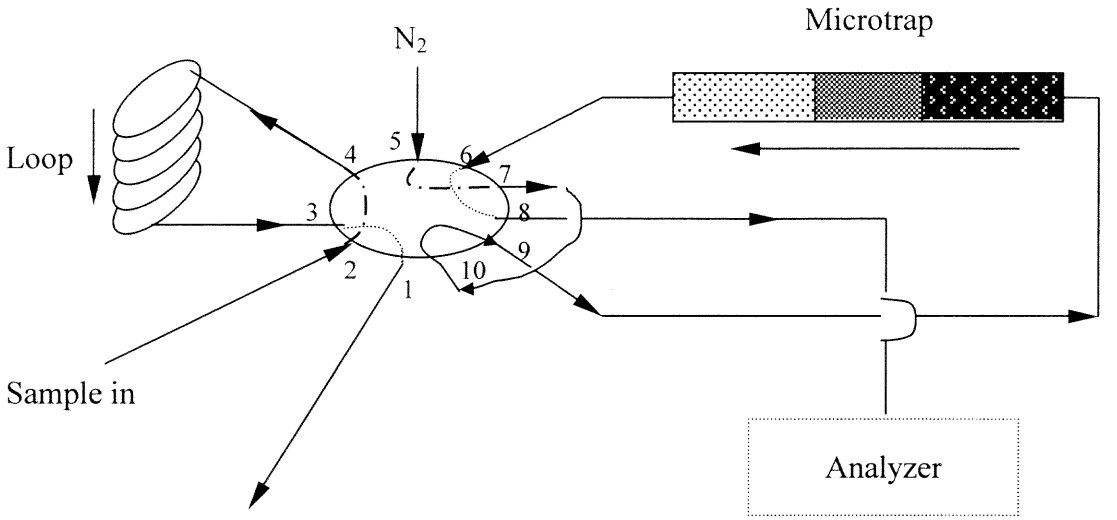

A: Loading of sample into the valve and desorption of microtrap

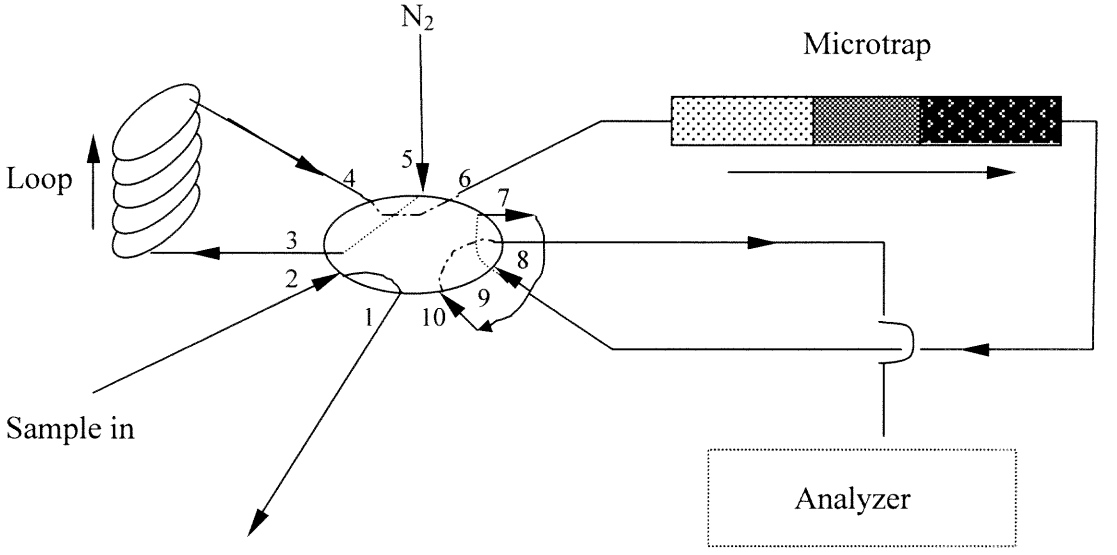

B. Injection of sample into the microtrap

Figure 5.3 Schematic diagram of the SV-BM mode with a ten-port valve.

weaker sorbent, while the light compounds went through to the stronger sorbents. The switching of the flow direction allowed the trap to be backflused. This configuration is referred to as sequential valve with backflushed microtrap (SV-BM). It was combined with the C-NMOC analyzer (as shown in Figure 5.1) to analyze both small and large molecules.

Trapping of small molecules and desorption of large molecules

Figure 5.4 represents the C-NMOC response in the SV-BM mode of a mixture of 99 ppm CH_4 and 231 ppm methanol in N_2. The excellent reproducibility in peak height showed that the SV-BM system could effectively trap small polar molecule such as methanol. Similar results were obtained using propane as a probe molecule. In previous studies where the trap was not backflushed, both methanol and propane had broken through.

Quantitative desorption of toluene was studied. The C-NMOC responses of 16.6 ppm toluene, 8.1 ppm and 106 ppm propane were illustrated in Figure 5.5. Their concentrations respectively corresponded to 116.2 ppm_C, 24.3 ppm_C and 318 ppm_C. The linear responses, as shown in the box in Figure 5.5, showed that the SV-BM/C-NMOC system not only effectively trapped small molecules (propane), but also quantitatively desorbed large molecules (toluene).

It should be noted that in the microtrap used here, only a small amount of Carbotrap C (3.3mg) was used. Since the toluene was to be retained in this sorbent, careful attention was given to ensure that there was no breakthrough. In this experiment, the optimal time period at injection position, where the toluene sample was injected from the sample loop to the microtrap, was found to be 25-30 seconds. After the valve was

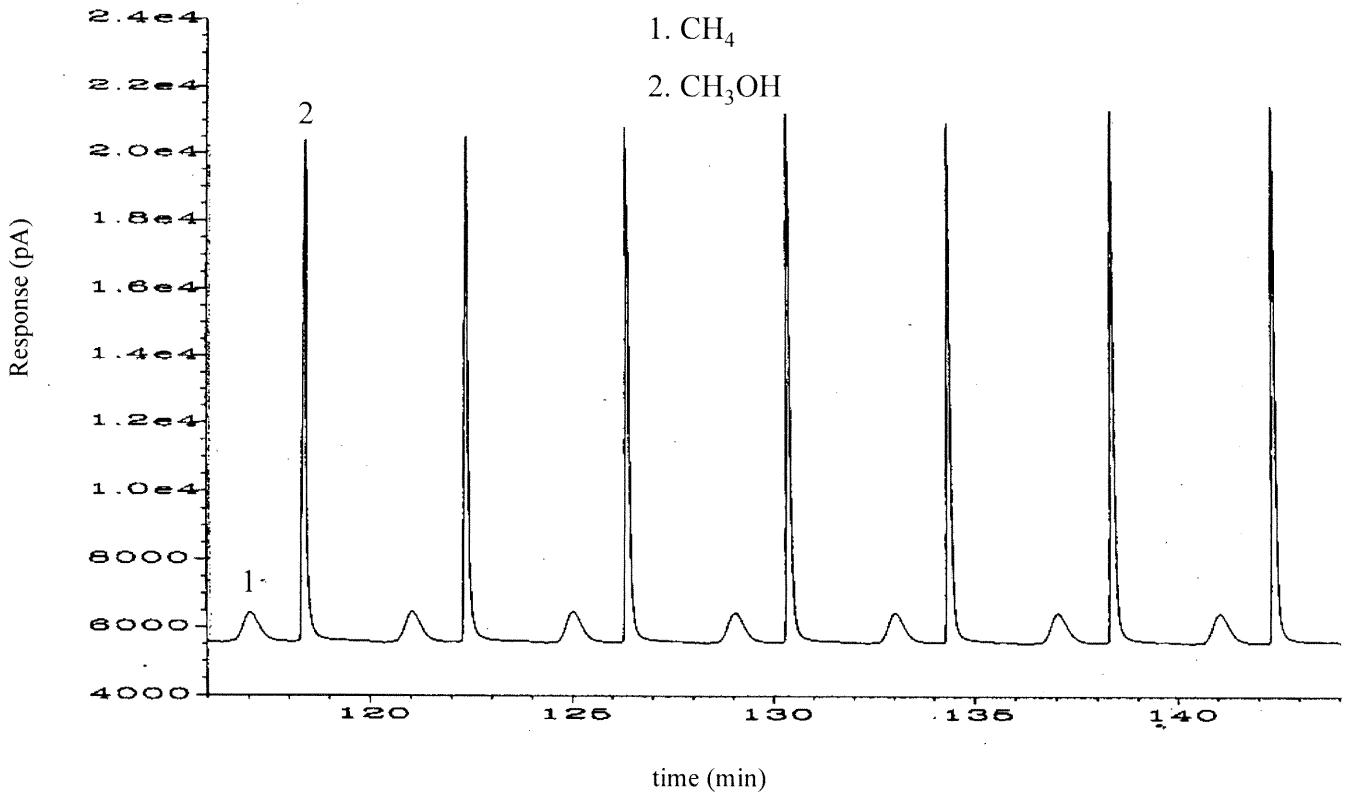

Figure 5.4 Adsorption of small molecules with the SV-BM mode
(Sampling loop: 5 ml. Based on Figure 5.3, load position 2 min and injection position 2 min.)

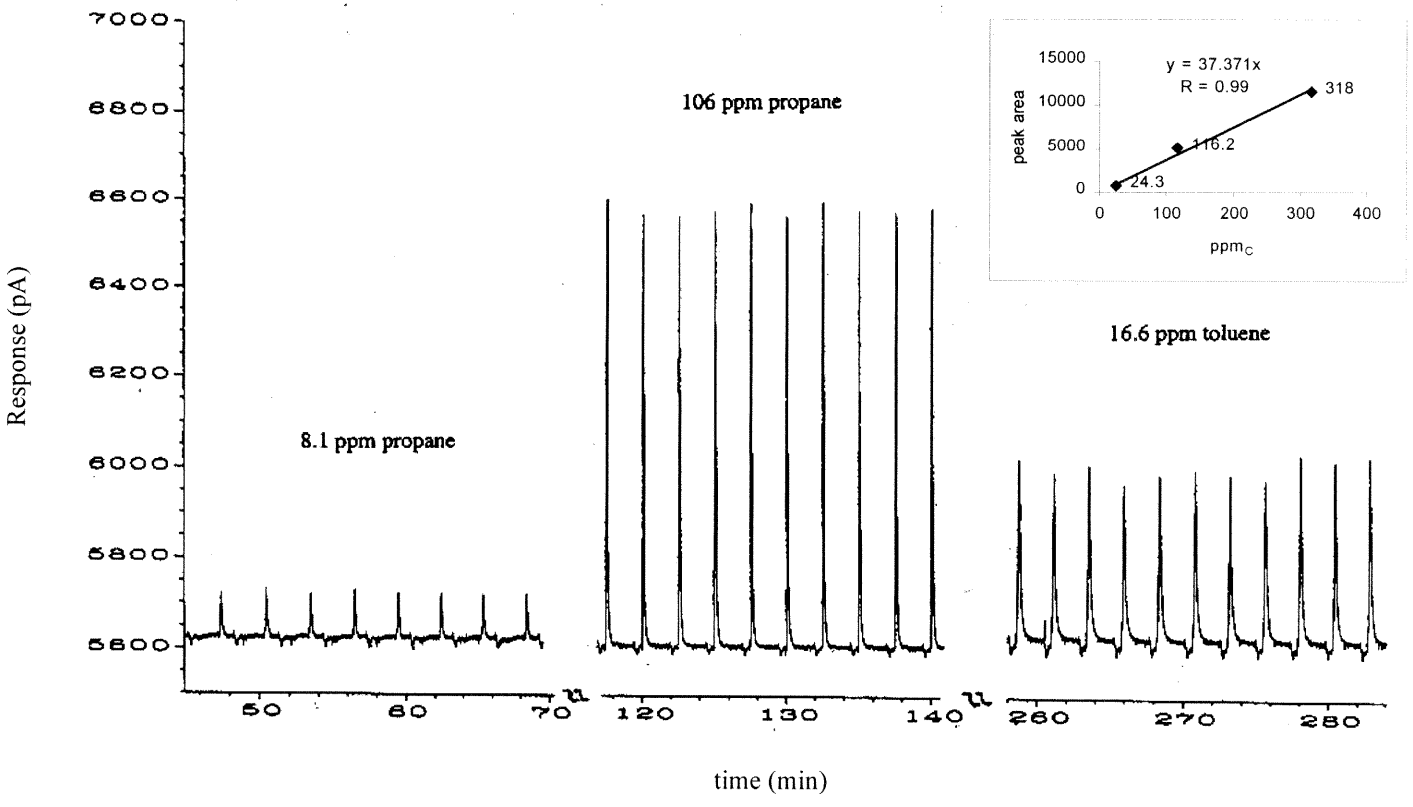

Figure 5.5 Desorption of large molecules with the SV-BM mode.
(Sampling loop: 1ml. Based on Figure 5.3, load position 2 min, injection position 1 min for propane and 25 sec for toluene)
The box shows the linear response (peak area) from propane and toluene at different concentrations (ppm_C).

switched to the load position for desorption, the microtrap was heated with only one second delay (this delay was for purging the trap). Larger amount of Carbotrap C would be needed if the breakthrough time of toluene on it is to be increased. Since the brakthrough volume of methanol and propane was relatively high on this multi-bed microtrap, the amount of carboxen 564 could be reduced. For example, 40mg of Carboxen 564, 20 mg of Carbopack B and 30 mg of Carbotrap C may efficiently analyze both small and large molecules. Optimization of these quantities may be done based on the application of interest.

Separation of background gases from NMOC

In a previous study [94], NMOC monitoring with SVM and OLMT-BF modes demonstrated good separation of NMOC from the background gases such as CO_2, CO and CH_4. As noted in Figure 5.4, the novel multi-bed microtrap with SV-BM mode could also separate NMOC from background gases. It could actually handle the background gases as high as (8% CO_2 + 120 ppm CH_4). This is clearly shown in Figure 5.6.

These high concentration background gases needed time to elute completely from the microtrap. In addition, hating the microtrap at the "load" position of the ten-port valve (see Figure 5.3) backflushes the microtrap. The separation of background gases from the NMOC is optimized by adjusting the load/injection time of the valve. For example, in Figure 5.6A, the time at the injection position was set as 9 min. During this period, the background gases and the NMOC were injected into the multi-bed microtrap at the direction from the weak to the stronger sorbents. The NMOC were selectively trapped, while the background gases eluted and it took about 7 minutes for their complete elution.

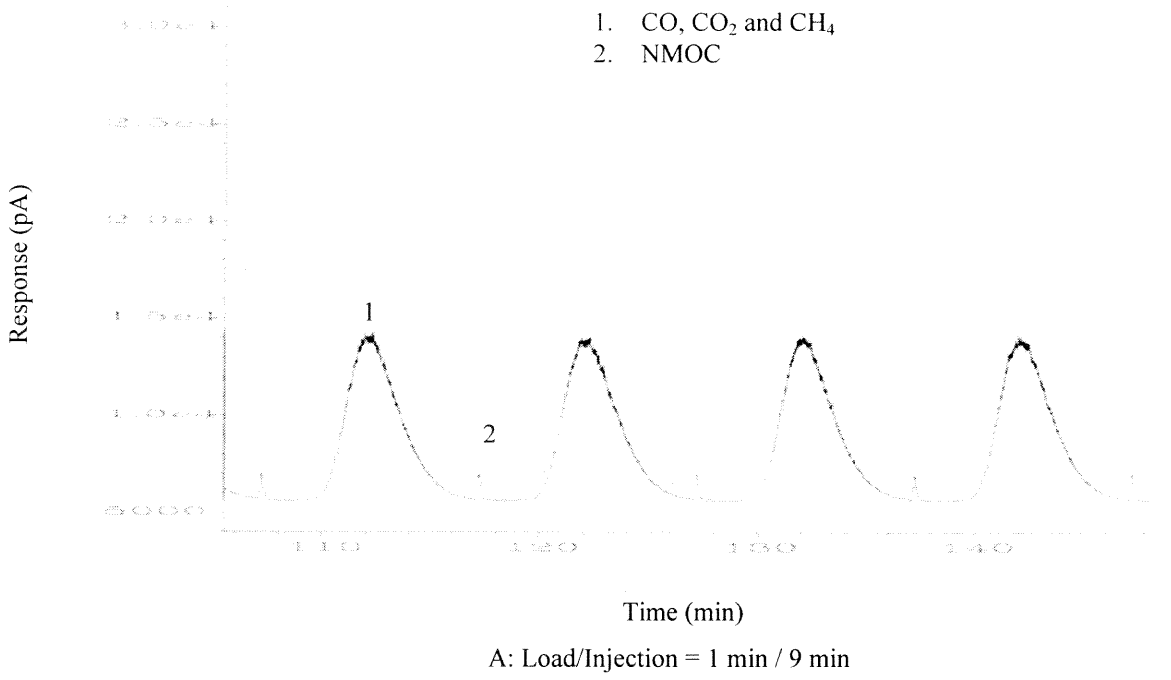

A: Load/Injection = 1 min / 9 min

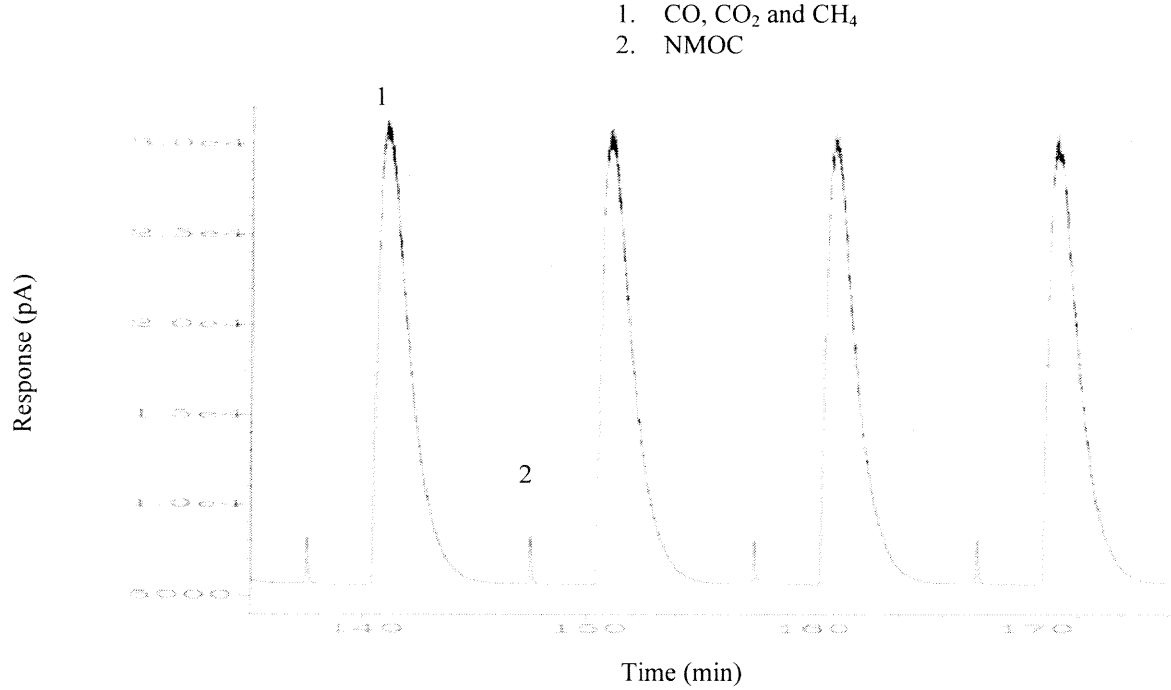

B: Load/Injection = 9 min / 1 min

Figure 5.6 Separation of NMOC from background gases with SV-BM system (sampling loop: 1 ml, NMOC: 231 ppm methanol, Background gases: 8% CO_2 + 120 ppm CH_4, balanced in air).

In Figure 5.6B, the time for injection was set as 1 min, while that for load was 9 min. At the load position (for 9 min), the microtrap was backflushed. It took about 6 minutes for the background gases to elute out of the multi-bed microtrap. In the latter time settings, not only the elution of the background gases became faster by one minute, but also the peaks from both NMOC and the background gases became higher and sharper. This meant that higher sensitivity was obtained from the C-NMOC system. This optimization is of significance for the situations when estimation of the background gases is needed, e.g., monitoring emissions from vehicle exhaust and polymer processing.

The background gases could be completely eliminated using another valve in series with the ten-port one. This configuration is shown in Figure 5.7, and is referred to as MSV-BM (multi-injection sequential valve with backflushed microtrap) mode. Its capability and the importance of performing multi-injection are discussed later. The two valves in the MSV-BM system were arranged in such a way that when the loop was in sampling position, the microtrap was in injection position, or vice versa, i.e., when the loop was in the injection position, the microtrap was in the sampling position. Thus in each cycle, a fixed volume of air sample was injected into the microtrap from the loop first, the organics were selectively preconcentrated by the microtrap. Then the microtrap was heated to desorb/inject the trapped organics (backflushed). Figure 5.8 shows that this MSV-BM mode could completely eliminate background gases in C-NMOC analysis. In this case, the MSV-BM had the same function as the OLMT-BF mode. However, the advantage of MSV-BM mode was that the total sampling volume could be fixed during each injection. This is important when two emission sources are compared directly with the analyzer response; or, when emission stream flow rates are high or unstable.

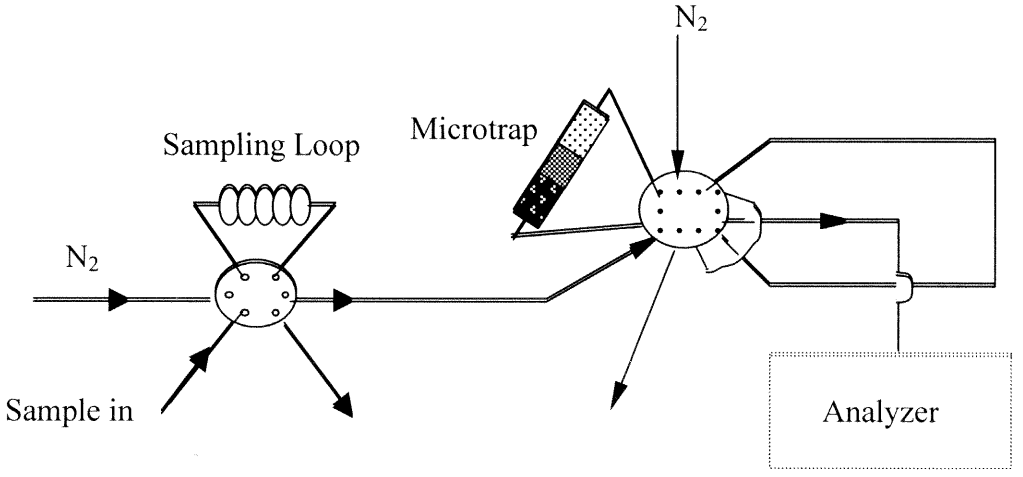

Figure 5.7. Multi-injection sequential valve with backflushed microtrap (MSV-BM).

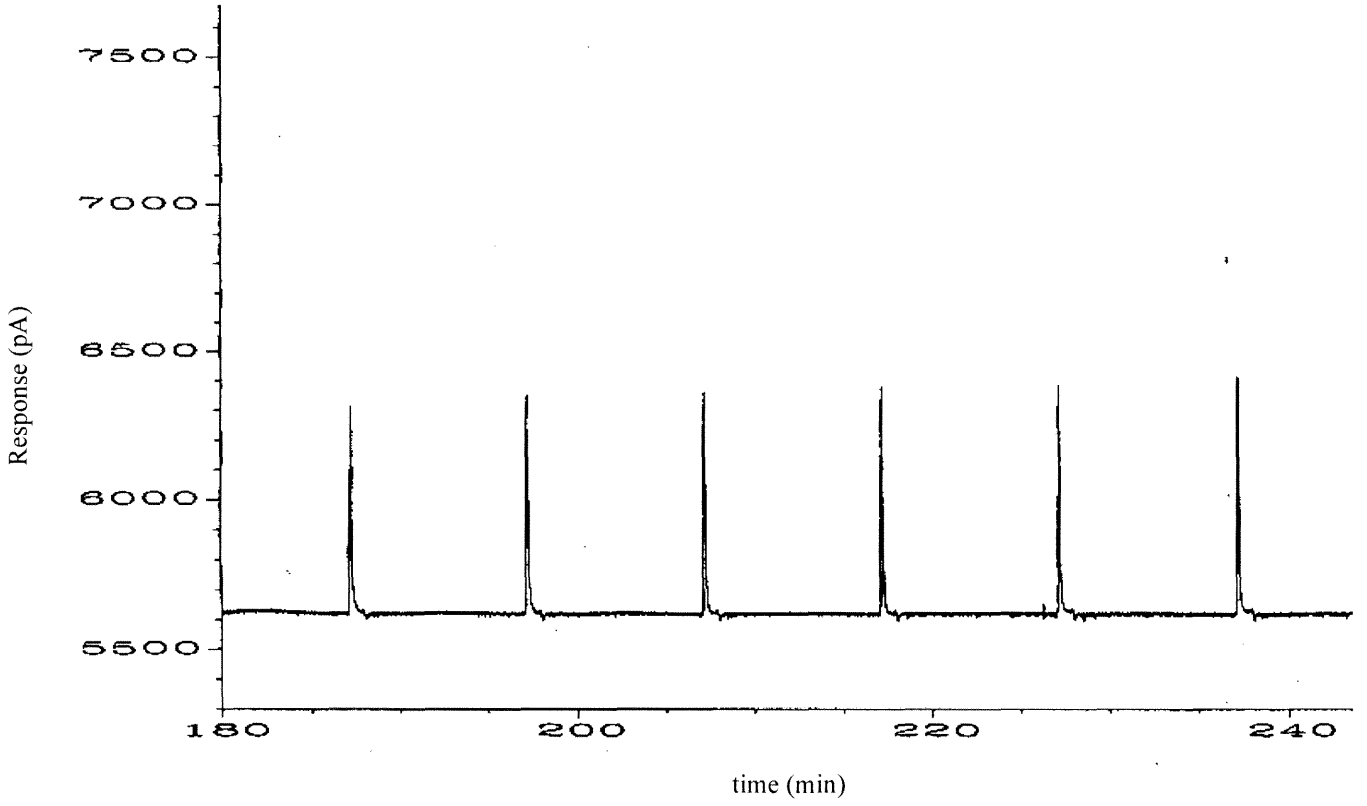

Figure 5.8 Elimination of background gases with the MSV-BM system (sampling loop: 1 ml, load position for 9 min, injection position for 1 min).

Compared to the SV-BM, the SVM mode can also separate and quantify background gases [203]. However, a multi-bed microtrap could not be used since there was no provision for back flushing. In contrast, the OLMT-BF and MSV-BM modes vent the background gases out of the analytical system. So in some cases, the capabilities to be backflushed and to quantify background gases are major advantages of the SV-BM system.

5.3.2 Calibration Curves

Calibration characteristics were studied with the SV-BM and MSV-BM modes. Figure 5.9 presents the calibration curves obtained from different analytes at the lower mass range (less than 1 μg) with these two sampling configurations. The asterisks stand for the responses from the mixture standard of 5.5 ppm propane+4.8 ppm methanol (21.3 ppm_C) after multiple injections with the MSV-BM configuration. The other two curves were obtained with the MSV-BM and SV-BM modes from the three standards: 8.1 ppm propane (24.3 ppm_C, multiple injected), the mixture standard (multiple injected) and 106 ppm propane (318 ppm_C). The results showed that these two modes gave similar responses, without regarding the composition of the standards. This meant that the SV-BM and the MSV-BM modes had identical calibration characteristics.

Two other configurations, OLMT and OLMT-BF (as shown in Figure 5.10), were also studied for their calibration characteristics. For the small molecules studied here, the OLMT mode demonstrated the similar performance as the OLMT-BF mode, except that the OLMT-BF system had better reproducibility. That was because the microtrap in the backflush mode was isolated from the sample stream during its heating. Whereas, in the

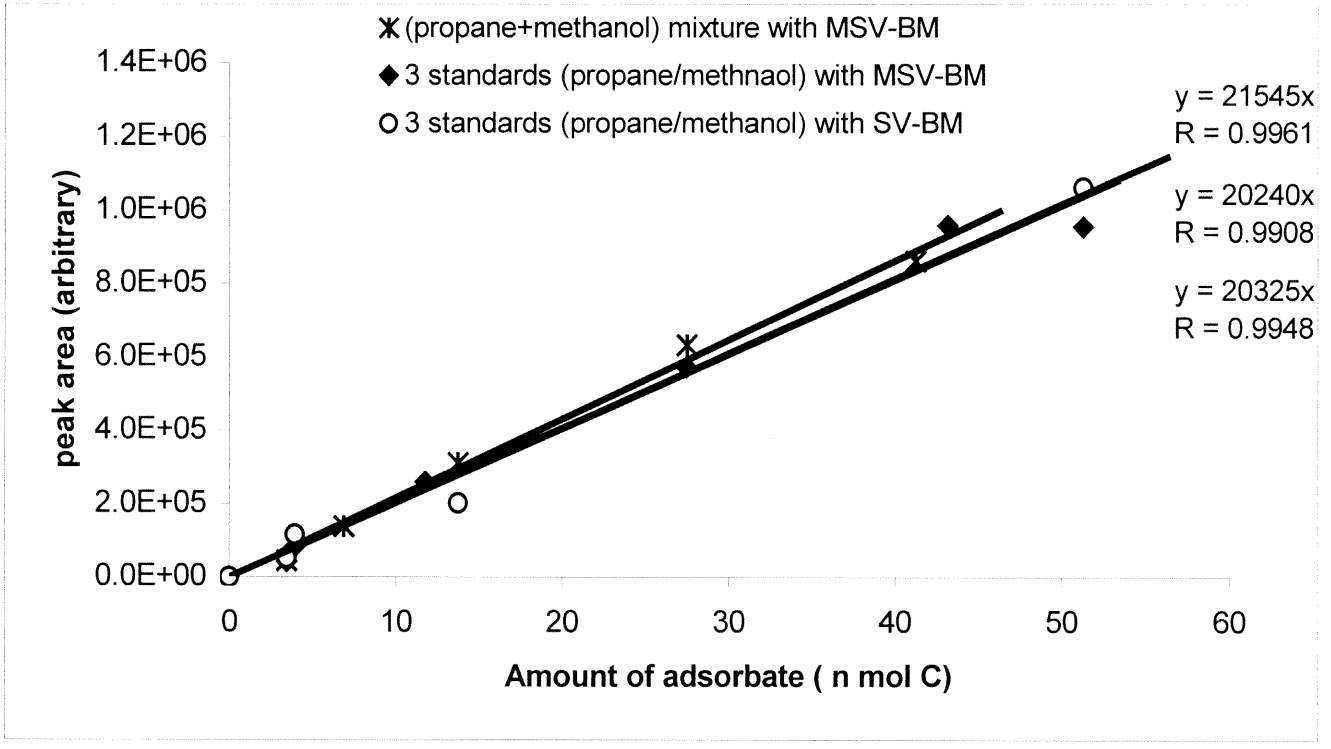

Figure 5.9 Calibration curves with different sampling configurations (sample volume per injection: 5 ml).

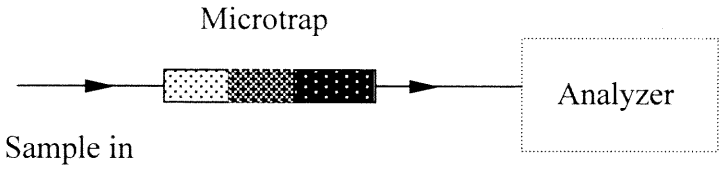

A: OLMT

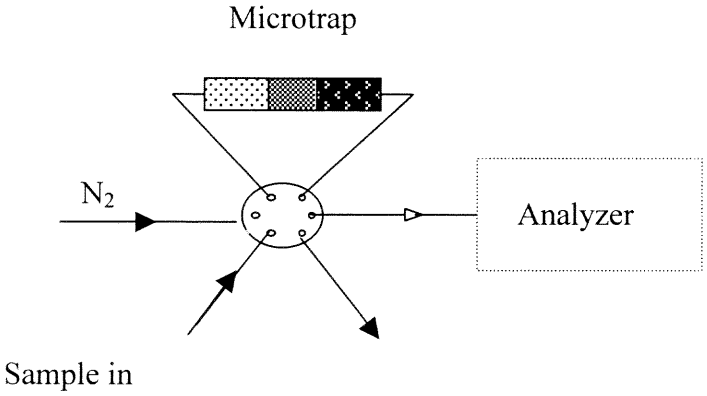

B: OLMT-BF

Figure 5.10 Configurations of on-line microtrap (OLMT) and on-line microtrap backflushed (OLMT-BF).

OLMT mode, the gas sample flowed continuously through the microtrap. After the trap was heated to desorb and inject the trapped materials, it could not quantitatively trap the analytes in the first few seconds due to the increased temperature. So as expected, the OLMT mode gave lower and less reproducible responses. In addition, it must be pointed out that multi-bed microtraps can not be effectively used in the OLMT system, because irreversible adsorption of heavier compounds may take place on the strong sorbents. Thus, tailing and incomplete desorption (or re-adsorption) are common problems for the OLMT system when organics with a wide range of volatility are encountered.

5.3.3 Multi-injection

Owing to their sampling loop configurations, both MSV-BM and SV-BM modes can be used to make multiple injections. This is of practical significance as by increasing the injection volume, the detection limits can be lowered. Multiple injections are also needed in the situations when higher concentration standards are required but not available for on-site immediate data. In Figure 5.11A, the C-NMOC response is presented as a function of number of injections. Linear increase in response with number of injection (proportional to sample volume) was observed in both MSV-BM and SV-BM modes. The results show some differences depending upon the mode. This was more obvious when the curves were expressed as mole number of carbon as shown in Figure 5.11B. It can be seen that the C-NMOC responses depended upon the mode. For example, the MSV-BM mode yielded the same results using standards with different composition and concentration. Whereas, the SV-BM mode gave a lower and lower response with the increase of injection number, compared to the MSV-BM mode with the same standard.

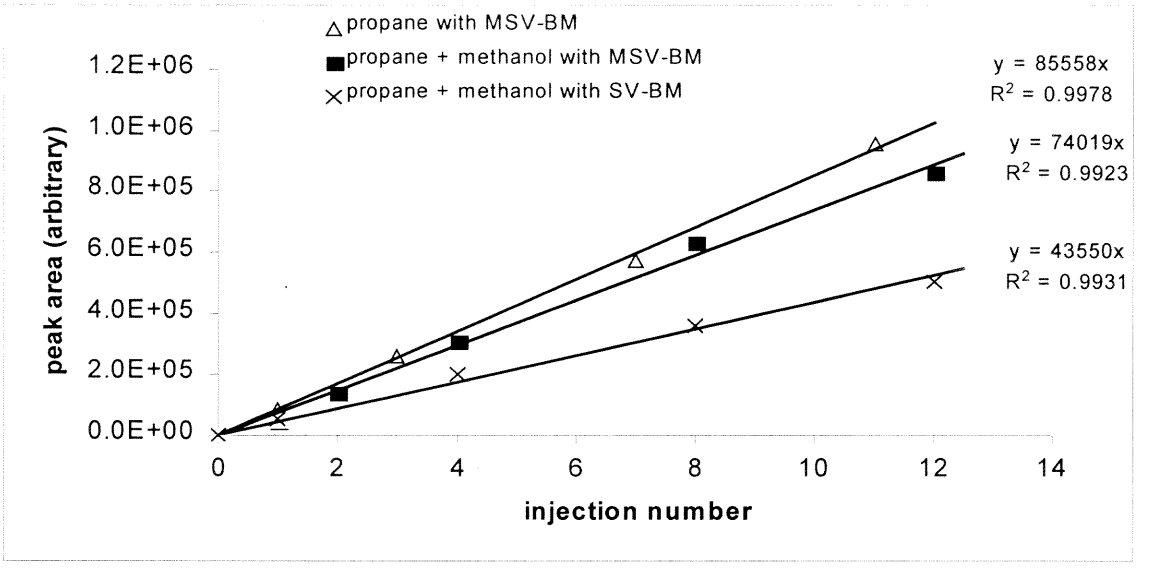

A: as a function of injection number

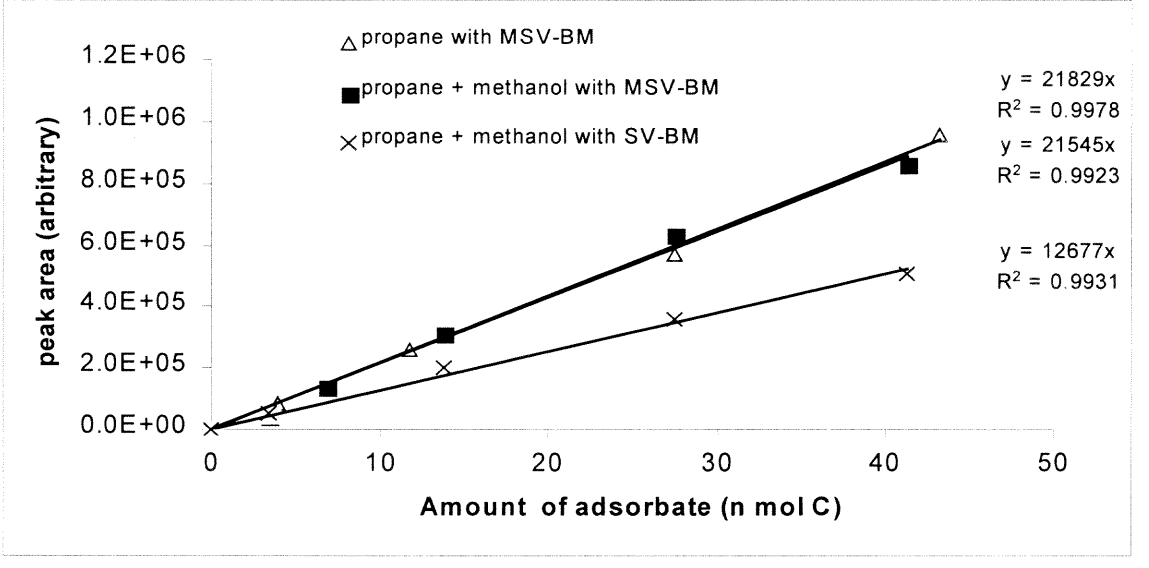

B: as a function of adsorbate amount

Figure 5.11 Comparison of multiple injection with different sampling configurations (sample volume per injection: 5 ml).

The MSV-BM appears to have higher sensitivity than the SV-BM mode. In the MSV-BM mode, the second valve for the microtrap was kept in the "load" position, while the first valve with the sample loop was switched several times from "load" to "inject" to make multiple injections. Then the valve for the microtrap was switched to "inject" position, while the microtrap was heated to release all the analytes. In contrast, in the SV-BM mode, only one 10-port valve was used. In order to make multiple injections, this valve was repeatedly switched from "load" to "inject" position. Simultaneously, the microtrap was repeatedly loaded with sample then backflushed by the carrier gas. The trapped analytes were partially blown out of the microtrap by the backflushing carrier gas. So, fewer analytes were trapped after multiple injections. With the increase of injection number, more analytes were blown out of the microtrap. Thus, decrease in the detector response (peak area) became more significant, as seen in Figure 5.11. Therefore, the MSV-BM mode is found to be more suited for multiple injections.

5.3.4 Breakthrough Characteristics of the Microtrap

The OLMT-BF and OLMT configurations (see Figure 5.10) were used to study the breakthrough volume of small molecules on the multi-bed microtrap. The adsorption curves for propane and methanol on the multi-bed microtrap were obtained at different concentrations and at different sampling temperature. The amount trapped as a function of sampling volume is shown in Figures 5.12A-D. According to Simon et al [193], BTV is defined as the sampled volume corresponding to the end of the linear domain. It can be seen that breakthrough volume depended on the analyte, its concentration and the sampling temperature of the sorbent. For instance, at 24^{o}C, 8.1 ppm propane started to

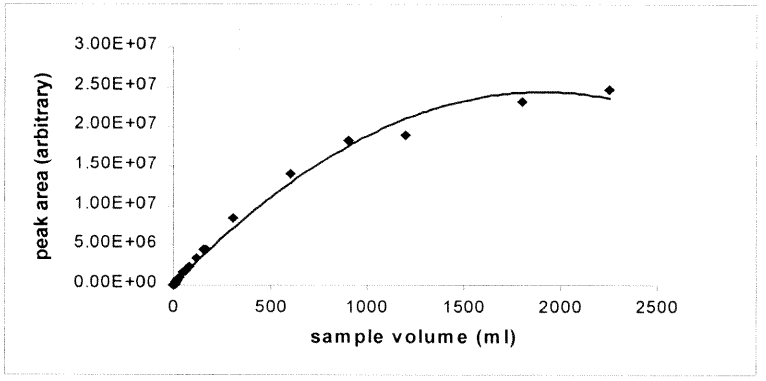

A: 8.1 ppm propane at 24°C with OLMT-BF.

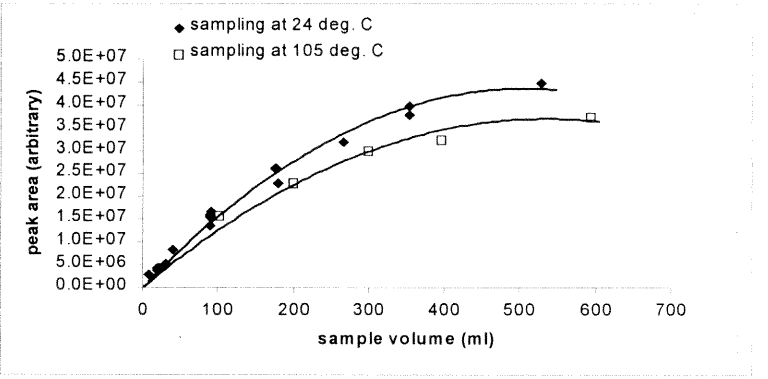

B: 106 ppm propane at different temperature with OLMT-BF.

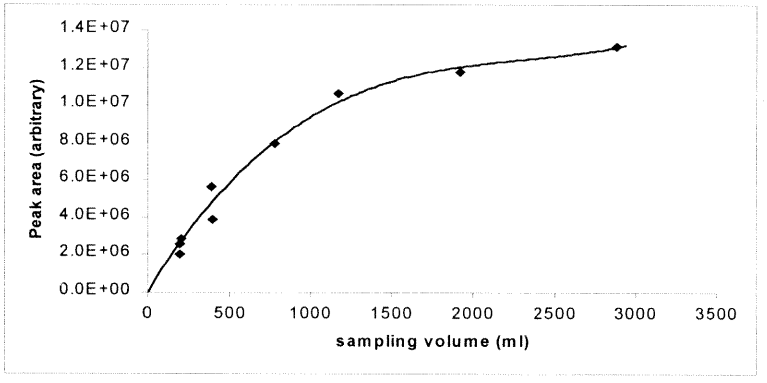

C. Mixture standard (5.5 ppm propane + 4.8 ppm methanol) at 105°C with OLMT-BF

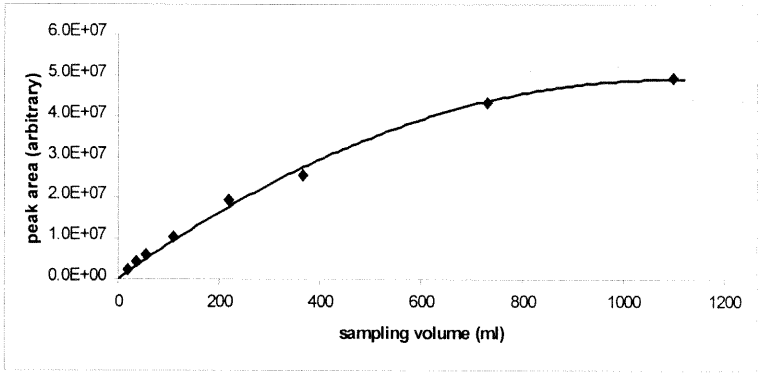

D: 231 ppm methanol at 105°C with OLMT

Figure 5.12 Adsorption curves from different analytes at different sampling temperatures.

break through at a sampling volume of 850 ml, while the same for 106 ppm propane was 220 ml. At 105°C, the BTV for the 106 ppm propane dropped to 150 ml. According to the Figures 5.12C and D, the standard mixture containing 5.5 ppm propane and 4.8 ppm methanol showed that, at 105°C, the breakthrough started around a sampling volume of 800 ml. Whereas, the BTV for 231 ppm methanol at 105°C was around 300 ml. It is evident that the BTV decreased with the increase in sample concentration and sampling temperature.

These breakthrough volumes were consistent with those for propane and methanol in literature (as seen in Table 5-5). It is safe to estimate that the multi-bed microtrap was able to trap these small molecules efficiently. First, the concentration level studied here (ppm levels) was at the high end of what is encountered in real environmental analysis. BTV values increase with the decrease of analyte concentration (Eq. 5-10). Second, only a few milliliters of the gas sample are necessary for ppb level detection limits, which is significantly lower than the corresponding BTV value. Third, the retention time of these small molecules on the microtrap was reasonably long, and no sample loss was expected. For instance, the breakthrough data in this study were obtained under a relatively high sampling rate, 75 ml/min. For the breakthrough volume of 850 ml (for 8.1 ppm propane), the multi-bed microtrap could retain it for as long as 11 minutes. These results were comparable to those reported in previous study [94].

As expected, the higher the analyte concentration, the lower was the breakthrough volume. For example, when the analyte concentration, expressed in total ppm_C, increased from 21.3 ppm_C (5.5 ppm propane+4.8 ppm methanol) to 24.3 ppm_C (8.1 ppm propane),

the BTV decreased from 850 ml to 800 ml. For a similar increase from 231 ppm_C (methanol) to 318 ppm_C (106 ppm propane), the BTV decreased from 300 ml to 150 ml.

Figure 5.12B shows that sampling temperature had a noticeable effect on the adsorption of analyte on the multi-bed microtrap. The high sampling temperature changed the properties of sorbents (such as surface area, pore size) and the adsorbent/adsorbate interactions (e.g., mass transfer rate, diffusion rate, affinity between gas and solid phases, etc.). Consequently, the sorption mechanisms also might have changed, and less propane was trapped by the multi-bed microtrap at higher temperature. The decrease in BTV agreed well with the Eq. (5.1) and (5.2).

The adsorption curves were compared as a function of sampling volume and mole of analyte. These are shown in Figure 5.13–5.14. In order to accommodate the sampling volumes in such a wide range, a logarithm scale was used in Figure 5.13. These curves approximately paralleled to each other. As expected, at the same sample volume, higher concentration (ppm_C) gave a higher peak area. In Figure 5.14, the peak area was plotted as a function of adsorbate amount (expressed in μ mole carbon). It is evident that identical response for the same number of moles of carbon was observed from these analytes irrespective of their chemical structure. That was because the NMOC detector generated a response directly proportional to the number of carbon atoms. Consequently, the curves in Figure 5.14 could not show a difference in breakthrough associated with different concentrations and components. It would be much clearer to express breakthrough using sampling volume. This allowed direct comparison of various analytes at different concentrations. It would also facilitate the process of choosing adsorbent and operational conditions for sampling. Additionally, sampling volume could be easily

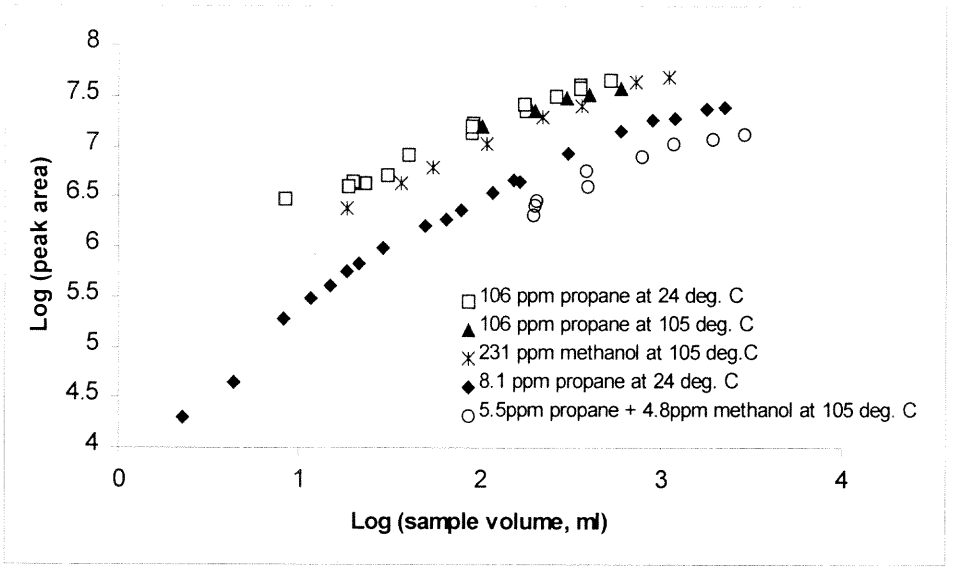

Figure 5.13 Comparison of the adsorption curves from different adsorbates as a function of sampling volume (ml).

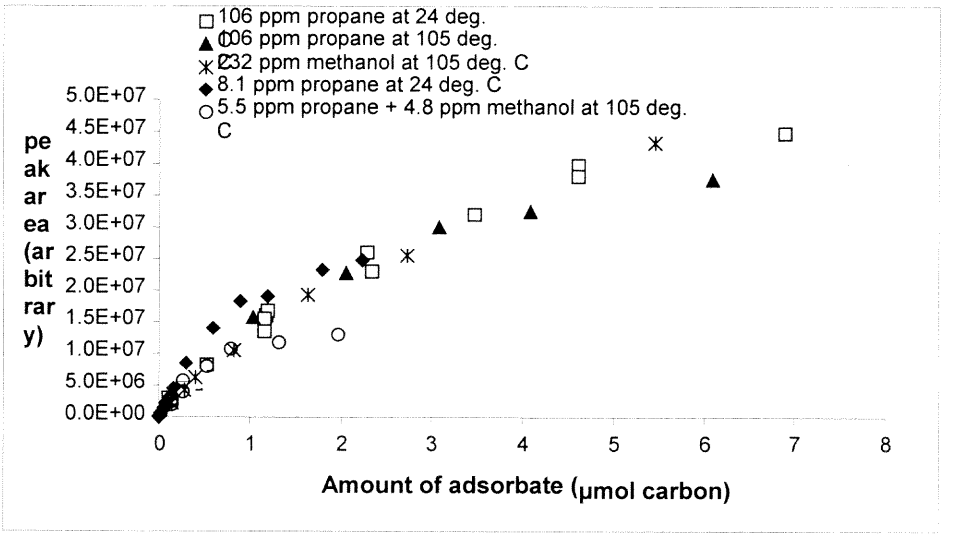

Figure 5.14 Comparison of the adsorption curves from different adsorbates as a function of the quantity of adsorbate (expressed in µmol carbon).

controlled by adjusting flow rate and/or sampling time. Therefore, breakthrough data in volume is of more importance in practice than other parameters such as retention time, number of moles, or mass of adsorbate.

5.4 Summary

The multi-bed microtrap, constructed with the first combination of Carboxen-564, Carbotrap C and Carbopack B, demonstrated adequate sorption capacity for small molecules such as propane and methanol. By combining this microtrap with the developed SV-BM and MSV-BM configurations, ideal performances were obtained in terms of linearity, multiple injection and separation of background gases. Both small molecules and large molecules could be effectively collected and desorbed with optimal amount of these adsorbents.

CHAPTER 6

CONCLUSIONS

In this study, analytical methods were developed for VOCs monitoring. The first method was based on direct flame ionization detector (FID) measurement. It was used to evaluate the potential environmental impact resulting from VOCs emissions during polymer processing and recycling. Compared to the conventional thermal analytical techniques, this direct FID method provided a more sensitive and accurate measure of VOCs.

Both virgin polymer resins and commingled post-consumer streams were studied. Significant VOCs emissions were observed around polymer processing temperatures, especially from recycled streams. For example, the total VOCs emissions from auto shredder residue were over 0.6% at 150°C for an hour. The processing parameters strongly influenced the amount of emissions, e.g., the increase in processing temperature and residence time remarkably promoted more emissions, whereas, the increase in heating rate decreased the total emissions.

Owing to the high sensitivity of the FID, the VOCs evolution traces were obtained from all the studied polymers during low temperature degradation. Each polymer showed unique VOCs evolution characteristics, including onset temperature, evolution rate, peak shape and peak temperature (T_m), etc. With the combination of this direct FID method and non-isothermal technique, the generation kinetics of these emissions was studied. Since the polymer degradation was focused at low temperature range in this research, correspondingly, lower values of kinetic parameters (E_a, k_0) were obtained. This was due to the presence of weak bonds in polymer matrix, particularly, in recycled polymers.

Consequently, less energy was needed to break these weak links, from which the emissions mainly originated. The results here were consistent with data from literature.

The direct FID method was also employed to study the total VOCs emitted from polypropylene (PP) during multiple melt reprocessing. The effects of stabilizer and processing conditions were examined by measuring VOCs generated from unstabilized PP (U-PP) after multiple injection molding, and stabilized PP (S-PP) after multiple extrusion. The results demonstrated that the effects of processing methods overcame the expected ones of stabilizers on the total VOCs. For both U-PP and S-PP, the maximum VOCs from each cycle did not change significantly. However, the cumulative emissions increased with the increase in number of processing cycle. The variations in the cumulative total VOCs agreed well with the changes in chemical structure and rheological properties. For U-PP, significant oxidative degradation was observed after the 7^{th} injection molding cycle, as evidenced by a rapid increase in carbonyl concentration and formation of new functional group. This was also accompanied by a rapid increase in Melt Flow Index and cumulative VOCs. For S-PP, predominant oxidative degradation was observed after the 4^{th} extrusion cycle, as evidenced by increase in carbonyl group strength and VOCs, and by decrease in M_w. The two screw configurations of extrusion (CON vs. KB45) did not result in much difference in VOCs generation. However, the FTIR results showed that the higher shear level in KB45 caused higher carbonyl concentration, standing for more oxidative degradation. Similarly, at the equivalent cycle number, the S-PP after multiple extrusion (with higher shear level) demonstrated more oxidative degradation than the injection molded U-PP.

To better understand the extent of polymer degradation at different gaseous atmospheres, simulation was performed by multiple heating/cooling of a single U-PP sample. The total VOCs emissions (with FID) or weight loss (with DSC) were measured in different atmospheres (nitrogen, air and oxygen). The results indicated that the emissions generated during actual reprocessing conditions were closer to those produced from a mild thermo-oxidative process rather than a pure thermal degradation.

The continuous non-methane organic carbon (C-NMOC) analysis is an excellent technique for monitoring organic emissions during polymer processing. First, the variable response factors associated with FID are eliminated. Second, methane, which is neither toxic nor is it involved in tropospheric ozone formation, is not counted to the total organic carbon in the NMOC measurements. This allows the comparison of different emission sources in terms of total carbon. Third, it can be connected on-line to a wide range of equipment (e.g., extruder, injection molder, etc) and for a variety of polymers. In this research, the C-NMOC system was further improved by combining a multi-bed microtrap with two novel sampling configurations (SV-BM and MSV-BM). Carboxen-564, Carbotrap C and Carbopack B were chosen to develop the multi-bed microtrap. With its backflushed mode, SV-BM and MSV-BM demonstrated excellent figures of merit. i.e., both small molecules and large molecules could be effectively collected and desorbed. Background gases could be completely separated or eliminated.

The major advantages of MSV-BM system are as follows: 1) it could be used for multiple sample injections; 2) the exact sampling volume was known; 3) the carrier gases for the two valves could be adjusted independently to get optimal performance. For example, the carrier gas of the first valve containing the sampling loop could be low in

order to avoid breakthrough of analytes. Whereas, the carrier of the second valve (for the trap) could be set higher to ensure complete desorption of the analytes from the trap.

Both the MSV-BM and SV-BM systems could separate background gases such as CO, CO_2 and CH_4, from the NMOC. However, only the SV-BM system could quantify these background gases as total carbon, while the MSV-BM configuration eluted them out of the system. When the background gases needed to be separated and quantified, the SV-BM system was the configuration of choice.

Future Studies

Nearly all polymers used in practice contain some kind of stabilizers in different concentrations. During polymer recycling, these stabilizers play an important role to retain the desired mechanical and rheological properties. However, they may also have complicated effects on the total VOCs emissions. In future, these effects can be further studied to correlate the VOCs emissions, structural/rheological properties and multiple processing. Furthermore, the improved C-NMOC system can be used in collecting and desorbing both small and large molecules generated during polymer processing. It will be of great interest to attach this system on-line to polymer processing equipment, so that real-time data can be generated for effective pollution prevention and control.

REFERENCES

1. Indoor Air Quality (IAQ), Office of Radiation and Indoor Air (ORIA), the US EPA, "Organic Gases (Volatile Organic Compounds – VOCs)", *EPA Intranet, http://www.epa.gov/iaq/voc.html*, last modified: November 9, 2000.

2. Westberg, H. and Zimmerman, P., "Analytical methods used to identify nonmethane organic compounds in ambient atmosphere", *Measurement Challenges in Atmospheric Chemistry*, Chapter 10, pp. 275-290, 1993.

3. Office of Air Quality Planning & Standards, the US EPA, "Smog – Who Does It Hurt? ", *EPA-452/K-99-001*, July 1999; "Ozone: Good Up High, Bad nearby", *EPA/451/K-97-002*, October 1997; "The Plain English Guide To The Clean Air Act", *EPA-400-K-93-001*, April 1993.

4. Fehsenfeld, F., Calvert, J., Fall, R., Goldan, P., Guenther, A.B., Hewitt, C. Nicholas, Lamb, B., Liu, S., Trainer, M., Westberg, H. and Zimmerman, P., "Emissions of Volatile Organic Compounds from vegetation and the implication for atmospheric chemistry", *Global Biogeochemical Cycles*, vol. 6, pp. 389-430, 1992.

5. Ashley, D. L., Bonin, M. A., Cardinali, F. L., McCraw, J. M., Holler, J. S., Meedham, L. L. and Patterson, D. G. Jr., "Determining volatile organic compounds in human blood from a large sample population by using purge and trap gas chromatography/mass spectrometry", *Analytical Chemistry*, vol. 64, no. 9, pp. 1021-1029, 1992.

6. Kim, Y. M., Harrad, S. and Harrison, R. M., "Concentrations and sources of VOCs in urban domestic and public microenvironments", *Environ. Sci. Technol.*, vol. 35, no. 6, pp. 997-1004, 2001.

7. Office of Air Quality Planning & Standards, the US EPA, *Compilation of Air Pollutant Emission Factors (AP-42)*, the 5th Edition.

8. US EPA, *EPA 2000 Strategic Plan,* submitted to Congress in September 2000, as required under the Government Performance and Results Act (GPRA), pp. 7-18.

9. Aragon, P., Atienza, J. and Climent, M. D., "Analysis of organic compounds in air: A review", *Critical Reviews in Analytical Chemistry*, vol. 30, issues 2-3, pp. 121-151, 2000.

10. Clement, R. E., Yang, P. W. and Koester, C. J., "Environmental Analysis", *Analytical Chemistry*, ASAP, 2001; vol. 71, no. 12, pp. 257R-292R, 1999; vol. 69, no. 12, pp. 251R-287R, 1997; Clement, R. E., Eicemen, G. A. and Koester, C. J., vol. 67, no. 12, pp. 221R-255R, 1995; Clement, R. E., Langhorst, M. L. and Eicemen, G. A., vol. 63, no. 12, pp. 270R-292R, 1991.

11. Koziel, J., Jia, M., Khaled, A., Moah, J. and Pawliszyn, J., "Field air analysis with SPME device", *Analytical Chimica Acta*, vol. 400, pp. 153-162, 1999.

12. US EPA, *Compendium of Methods for the Determination of Toxic Organic Compounds in Ambient Air, EPA-600/4-84-041*, April 1984.

13. National Institute for Occupational Safety and Health, *NIOSH Manual of Analytical Methods*, 2nd edition, DHEW (NIOSH) pub.no. 77-157, NIOSH, Cincinnati, OH, 1977.

14. US Department of Labor, Occupational Safety and Health Administration, *OSHA Manual of Analytical Methods,* OSHA Analytical Laboratory, Salt Lake City, UT.

15. US EPA, Method 18, *Code of Federal Regulations*, Part 60; Title 40; Appendix A; US GPO: Washington, DC, July 1987.

16. Kebbekus, B. B. and Mitra, S., *Environmental Analytical Chemistry*, Chapman Hall, Inc., Chapter 8, "Methods for Air Analysis", 1995.

17. Hsu, J. P., Miller, G. and Moran, V. III, "Analytical method for determination of trace organics in gas samples collected by canisters", *J. of Chromatogr. Sci.*, vol. 29, pp. 83-88, 1991.

18. Peters, R. J. B., *Analyst*, vol. 119, paper 3/03199C, 1994.

19. Walling, J. f., Bumgarner, J. E., Driscoll, D. J., Morris, C. M., Riley, A. E. and Wright, L. H., *atmospheric Environment*, vol. 20, pp. 51-57, 1986.

20. Harper, M., Kimberland, M. L., Orr, R. J. and Gulld, L. V., "An evaluation of sorbents for sampling ketones in workplace air", *Appl. Occup. Environ. Hyg.*, vol. 8, no. 4, pp. 293-304, 1993.

21. Batterman, S. A., Zhang, G. and Baumann, M., "Analysis and stability of aldehydes and terpenes in electropolished canisters", *Atmospheric Environment*, vol. 32, no. 10, pp. 1647-1655, 1998.

22. Wang, Y., Raihala, T. S., Jackman, A. P. and John, R. St., "Use of Tedlar bags in VOC testing and storage: evidence of significant VOC losses", *Environmental Science & Technology*, vol. 30, no. 10, pp. 3115-3117, 1996.

23. Dewulf, J. and Langenhove, H. V., "Anthropogenic volatile organic compounds in ambient air and natural waters: a review on recent developments of analytical methodology, performance and interpretation of field measurements", *Journal of Chromatography A*, vol. 843, pp. 163-177, 1999.

24. Dewulf, J. and Langenhove, H. V. "Analytical techniques for the determination and measurement data of 7 chlorinated C1- and C2-hydrocarbons and 6 monocyclic aromatic hydrocarbons in remote air masses: an overview", *Atmospheric Environment*, vol. 31, no. 20, pp. 3291-3307. 1997.

25. Bayne, C. K., Schmoyer, D. D. and Jenkins, R. A., "Practical reporting times for environmental samples", *Environmental Science & Technology*, vol. 28, no. 8, pp. 1430-1436, 1994.

26. Mugica, V., Vega, E., Chow, J., Reyes, E., Sanchez, G., Arriaga, J., Egami, R. and Watson, J., "Speciated non-methane organic compounds emissions from food cooking in Mexico", *Atmospheric Environment*, vol. 35, pp. 1729-1734, 2001.

27. Fukui, Y. and Doskey, P. V. "Identification of nonmethane organic compound emissions from grassland vegetation", *Atmospheric Environment*, vol. 34, pp. 2947-2956, 2000.

28. Park, H., Kim, Y., Lee, D. and Lee, K., "Evaluation of natural crab shell as an adsorbent for preconcentrating airborne volatile organic compounds collected in a canister", *Journal of Chromatography A*, vol. 829, pp. 215-221, 1998.

29. Na, K. and Kim, Y. P., "Seasonal characteristics of ambient volatile organic compounds in Seoul, Korea", *Atmospheric Environment*, vol. 35, pp. 2603-2614, 2001.

30. US EPA, *Compendium Method TO-15; Determination of volatile organic compounds (VOCs) in air collected in specially prepared canisters and analyzed by gas chromatography/mass spectrometry (GC/MS)*. Center for Environmental Research Information, Office of Research and Development, US EPA, Cincinatti, Ohio, 1997.

31. Woolfenden, E. A., McClenny, W. A., *Compendium Method TO-17; Determination of volatile organic compounds (VOCs) in ambient air using active sampling onto sorbent tubes, EPA/625/R-96/010b,* US EPA, Research Triangle Park, NC, 1997.

32. McClenny, W. A. and Colón, M., "Measurement of volatile organic compounds by the US Environmental Protection Agency Compendium Method TO-17, Evaluation of performance criteria", *Journal of Chromatography A*, vol. 813, pp. 101-111, 1998.

33. Shojania, S., Oleschuk, R. D., McComb, M. E., Gesser, H. D. and Chow, A., "The active and passive sampling of benzene, toluene, ethyl benzene and xylenes compounds using the inside needle capillary adsorption trap device", *Talanta*, vol. 50, pp. 193-205, 1999.

34. Otson, R. and Cao, X., "Evaluation of a small prototype passive sampler for airborne volatile organic compounds", *Journal of Chromatography A*, vol. 802, pp. 307-314, 1998.

35. Uchiyama, S., Asai, M., and Hasegawa, S., "A sensitive diffusion sampler for the determination of volatile organic compounds in ambient air", *Atmospheric Environment*, vol. 33, pp. 1913-1920, 1999.

36. Ma, C. Y., McCorkle, D. L., Ding, W. and Pinnaduwage, L. A., "Methodology for gas chromatographic-mass spectral analysis of volatile organic compounds emerging from a low-pressure, flow-through reaction cell", *Journal of Chromatography A*, vol. 844, pp. 217-224, 1999.

37. Matisova, E., Skrabakova, S., "Carbon sorbents and their utilization for the preconcentration of organic pollutants in environmental samples", *Journal of Chromatography A*, vol. 707, pp. 145-179, 1995.

38. Harper, M., "Novel sorbents for sampling organic vapours", *Analyst*, vol. 119, pp. 65-69, 1994.

39. Simpson, E. J., Koros, W. J. and Schechter, R. S., "An emerging class of volatile organic compound sorbents: Friedel-Crafts modified polystytenes. 1. Synthesis, characterization, and performance in aqueous and vapor-phase applications. 2. Performance comparison with commercially-available sorbents and isotherm analysis", *Ind. Eng. Chem. Res.*, vol. 35, no. 4, pp. 1195-1205; no. 12, pp. 4635-4645, 1996.

40. Brancaleoni, E., Scovaventi, M., Frattoni, M., Mabilia, R. and Ciccioli, P., "Novel family of multi-layer cartridges filled with a new carbon adsorbent for the quantitative determination of volatile organic compounds in the atmosphere", *Journal of Chromatography A*, vol. 845, pp. 317-328, 1999.

41. Zhao, X. S., Lu, G. Q. and Hu, X., "Organophilicity of MCM-41 adsorbents studied by adsorption and temperature-programmed desorption", *Colloids and Surface A: Physicochem. Eng. Aspects*, vol. 179, pp. 261-269, 2001.

42. Burg, P., Fydrych, P., Abraham, M. H., Matt, M. and Gruber, R. "The characterization of an active carbon in terms of selectivity towards volatile organic compounds using an LSER approach", *Fuel*, vol. 79, pp. 1041-1045, 2000.

43. Chen, C., Chen, J., Wang, X., Liu, S., Sheng, G. and Fu, J., "Fullerenes-extracted soot: a new adsorbent for collecting volatile organic compounds in ambient air", *Journal of Chromatography A*, vol. 886, pp. 313-317, 2000.

44. Simmonds, P. G., O'Doherty, S., Nickless, G. , Sturrock, G. A., Swaby, R., Knight, P., Ricketts, J., Woffendin, G. and Smith, R., "Automated gas chromatograph/mass spectrometer for routine atmospheric field measurements of the CFC replacement compounds, the hydrofluorocarbons and hydrochlorofluorocarbons", *Analytical Chemistry*, vol. 67, no. 4, pp. 717-723, 1995.

45. Bianchi, A. P. and Varney, M. S., *Journal of Chromatography*, vol. 643, pp. 11, 1992.

46. *Sample handing Bulletin 850A*, Bellefonte, PA: Supelco, Inc., 1991; "Carbotrap™ • an excellent adsorbent for sampling many airborne contaminants", *Supelco Reporter, GC Bulletin 846C*, vol. V, no. 1, pp. 5-7, Supelco, Inc., 1986.

47. Helmig. D. and Greenberg, J. P., *Journal of chromatography*, vol. 677, pp. 123-132, 1994; D. Helmig, *Journal of Chromatography*, vol. 732, pp. 414-417, 1996.

48. Gawlowski, J. and Niedzielski, J., *Analyst*, vol. 125, pp. 2112-2117, 2000.

49. Helmig, D. and Vierling, L., *Analytical Chemistry*, vol. 67, pp. 4380-4386, 1995.

50. Llompart, M., Li, K. and Fingas, M. "Headspace solid phase microextraction (HSSPME) for the determination of volatile and semivolatile pollutants in soils", *Talanta,* vol. 48, pp. 451-459, 1999.

51. Li, K., Santilli, A., Goldthorp, M., Whiticar, S., Lambert, P. and Fingas, M., "Solvent vapor monitoring in work space by solid phase micro extraction", *Journal of Hazardous Materials*, vol. 83, pp. 83-91, 2001.

52. Pawliszyn, J., *Solid Phase Microextraction – Theory and Practice*, Wiley-VCH, New York, 1997.

53. Yassaa, N., Meklati, B. Y. and Cecinato, A. "Analysis of volatile organic compounds in the ambient air of Algiers by gas chromatography with a ß-cyclodextrin capillary column", *Journal of Chromatography A*, vol. 846, pp. 287-293, 1999.

54. Baltussen, E., Davis, F., Sandra, P., Janssen, H. G. and Cramers, C., *Analalytical Chemistry,* vol. 71, no. 22, pp. 5193-5198, 1999.

55. Lopez-Avila, V., "Trends in environmental analysis", *Journal of AOAC International*, vol. 82, no. 1, pp. 217-222, 1999.

56. Lewis, A. C. "New directions: Novel separation technique in VOC analysis pose new challenges to atmospheric chemistry", *Atmospheric Environment*, vol. 34, pp. 1155-1156, 2000.

57. Wang, J., Chen, W., Lin, Y. and Tsai, C., "Cryogen free automated gas chromatography for the measurement of ambient volatile organic compounds", *Journal of Chromatography A,* vol. 896, pp. 31-39, 2000.

58. Oliver, K. D., Adams, J. R., Daughtrey, E. H. Jr., McClenny, W. A., Yoong, M. J., Pardee, M. A., Almasi, E. B. and Kirshen, N. A., "Technique for monitoring toxic VOCs in air: Sorbent preconcentration, closed-cycle cooler cryofocusing, and GC/MS analysis", *Environmental Science & Technology*, vol. 30, no. 6, pp. 1939-0945, 1996.

59. Current, R. W., Kozliak, E. I. and Borgerding, A. J., "Monitoring biodegradation of VOCs using high-speed gas chromatography with a dual-point sampling system", *Environmental Science and Technology,* Vol. 35, no. 7, pp. 1452-1457, 2001.

60. Daughtrey, E. H., Adams, J. R., Oliver, K. D., Kronmiller, K. G. and McClenny, W. A., "Performance characteristics of an automated gas chromatograph-ion trap mass spectrometer system used for the 1995 southern oxidants study field investigation in Nashville, Tennessee", *Journal of Geophysical Research D: Atmospheres,* vol. 103, no. D17, pp. 22,375-22,386, 1998.

61. Grall, A. J., Zellers, E. T. and Sacks, R. D., "High-speed analysis of complex indoor VOC mixtures by vacuum-outlet GC with air carrier gas and programmable retention", *Environmental Science and Technology*, vol. 35, no. 1, pp. 163-169, 2001.

62. Begerow, J., Jermann, E., Keles, T., Koch, T. and Dunemann, L., "Screening method for the determination of 28 volatile organic compounds in indoor and outdoor air at environmental concentrations using dual-column capillary gas chromatography with tandem electron-capture-flame ionization detection", *Journal of Chromatography A*, vol. 749, pp, 181-191, 1996.

63. Ryan, J. V., Lemieux, P. M. and Preston, W. T., "Near-real-time measurement of trace volatile organic compounds from combustion process using an on-line gas chromatography", *Waste Management*, vol. 18, pp. 403-410, 1998.

64. Yamamoto, N., Okayasu, H., Hiraiwa, T., Murayama, S., Maeda, T., Morita, M. and Suzuki, K., "Continuous determination of volatile organic compounds in the atmosphere by an automated gas chromatographic system", *Journal of Chromatography A*, vol. 819, pp, 177-186, 1998.

65. Zielinska, B., Sagebiel, J. C., Harshfield, G., Gertler, A. W. and Pierson, W. R., "Volatile organic compounds up to C_{20} emitted from motor vehicles; Measurement methods", *Atmospheric Environment*, vol. 30, no. 12, pp. 2269-2286, 1996.

66. Tuan, H. P., Janssen, H., Cramers, C. A., Mussche, P., Lips, J., Wilson, N. and Handley, A., "Novel preconcentration technique for on-line coupling to high-speed narrow-bore capillary gas chromatography: sample enrichment by equilibrium (ab)sorption – II. Coupling to a portable micro gas chromatograph", *Journal of Chromatography A*, vol. 791, pp. 187-195, 1997.

67. Ross, A. B., Junyapoon, S., Bartle, K. D., Jones, J. M. and Williams, A. "Development of pyrolysis-GC with selective detection: coupling of pyrolysis-GC to atomic emission detection (py-GC-AED)", *Journal of Analytical and Applied Pyrolysis*", vol. 58-59, pp. 371-385, 2001.

68. Schweigkofler, M. and Niessner, R., "Determination of siloxanes and VOC in landfill gas and sewage gas by canister sampling and GC-MS/AES analysis", *Environmental Science and Technology,* vol. 33, no. 20, pp. 3680-3685, 1999.

69. Wong, P. S. H., Cooks, R. G., Cisper, M. E. and Hemberger, P. H., "On-line, in situ analysis with membrane introduction MS", *Environmental Science & Technology*, vol. 29, no. 5, pp. 215A-218A, 1995.

70. Wise, M. B. and Guerin, M. R., "Direct sampling MS for environmental screening", *Analytical Chemistry News & Features*, January 1, pp. 26A-32A, 1997.

71. Ouyang, S., Chen, Y. H. and Xu, Y., "Enhancing the performance of membrane introduction mass spectrometry by organic carrier and liquid chromatographic separation", *Analytica Chimica Acta*, vol. 337, pp. 165-172, 1997.

72. Mendes, M. A., Sparrapan, R. and Eberlin, M. N., "Headspace membrane introduction mass spectrometry for trace level analysis of VOCs in soil and other solid matrixes", *Analytical Chemistry*, vol. 72, no. 9, pp. 2166-2170, 2000.

73. Ketola, R. A., Ojala, M., Sorsa, H., Kotiaho, T. and Kostiainen, R. K., "Development of a membrane inlet mass spectrometric method for analysis of air samples", *Analytica Chimica Acta,* vol. 349, pp. 359-365, 1997.

74. Cisper, M. E., Gill, C. G., Townsend, L. E. and Hemberger, P. H. "On-line detection of volatile organic compounds in air at parts-per-trillion levels by membrane introduction mass spectrometry", *Analytical Chemistry*, vol. 67, no. 8, pp. 1413-1417, 1995; vol. 68, pp. 2097-2101, 1996.

75. Lindinger, W., Hansel, A. and Jordan, A., "On-line monitoring of volatile organic compounds at pptv levels by means of proton-transfer-reaction mass spectrometry (PTR-MS) medical applications, food control and environmental research", *International Journal of Mass Spectrometry and Ion Processes*, vol. 173, no. 3, pp. 191-241, 1998.

76. Karl, T., Fall, R., Jordan, A. and Lindinger, W., "On-line analysis of reactive VOCs from urban lawn mowing", *Environmental Science & Technology*, in press, 2001.

77. Fall, R., Hansel, A., Jordan, A. and Lindinger, W., "Volatile organic compounds emitted after leaf wounding: On-line analysis by proton-transfer-reaction mass spectrometry", *Journal of Geophysical Research D: Atmosphere*, vol. 104, no. 13, pp. 15,963-15,974, 1999.

78. Holzinger, R., Sandoval-Soto, L., Rottenberger, S., Crutzen, P. J. and Kesselmeier, J., "Emissions of volatile organic compounds from Quercus ilex L. Measured by proton transfer reaction mass spectrometry under different environmental conditions", *Journal of Geophysical Research D: Atmosphere,* vol. 105, no. 16, pp. 20,573-20,579, 2000.

79. De Gouw, J., Howard, C. J., Custer, T. G., Baker, B. M. and Fall, R., "Proton-transfer chemical-ionization mass spectrometry allows real-time analysis of volatile organic compounds released from cutting and drying of crops", *Environmental Science & Technology*, vol. 34, no. 12, pp. 2640-2648, 2000.

80. Rieder, J., Lirk, P., Ebenbichler, C., Gruber, G., Prazeller, P., Lindinger, W. and Amann, A., "Analysis of volatile organic compounds: Possible applications in metabolic disorders and cancer screening", *Wiener Klinische Wochenschrift*, vol. 113, no. 5-6, pp. 181-185, 2001.

81. Roberts, K. P., Jankiwiak, R. and Small, G. J., "High-performance liquid chromatography interfaced with fluorescence line-narrowing spectroscopy for on-line analysis", *Analytical Chemistry*, vol. 73, no. 5, pp. 951-956, 2001.

82. Godejohann, M., Preiss, A., Mugge, C. and Wunsch, G., "Application of on-line HPLC-1H NMR to environmental samples: Analysis of groundwater near former ammunition plants", *Analytical Chemistry*, vol. 69, no. 18, pp. 3832-3837, 1997.

83. Granby, K., Christensen, C. S. and Lohse, C., "Urban and semi-rural observations of carboxylic acids and carbonyls", *Atmospheric Environment*, vol. 31, no. 10, pp. 1403-1415, 1997.

84. Borrego, C., Gomes, P., Barros, N. and Miranda, A. I., "Importance of handling organic atmospheric pollutants for assessing air quality", *Journal of Chromatography A*, vol. 889, pp. 271-279, 2000.

85. Schleibinger, H. and Ruden, H., "Air filters from HVAC systems as possible source of volatile organic compounds (VOC) – laboratory and field analysis", *Atmospheric Environment,* vol. 33, pp. 4571-4577, 1999.

86. Nakamura, K., Nakamoto, T. and Moriizumi, T., "Classification and evaluation of sensing films for QCM odor sensors by steady-state sensor response measurement", *Sensors and Actuators B*, vol. 69, pp. 295-301, 2000.

87. Ricco, A. J., Crooks, R. M. and Osbourn, G. C., "Surface acoustic wave chemical sensor arrays: New chemically sensitive interfaces combined with novel cluster analysis to detect volatile organic compounds and mixtures", *Accounts of Chemical Research*, vol. 31, no. 5, pp. 289-296, 1998.

88. Getino, J., Horrillo, M. C., Gutierrez, J., Ares, L., Robla, J. I., Garcia, C. and Sayago, I., "Analysis of VOCs with a tin oxide sensor array", *Sensors and Actuators B*, vol. 43, pp. 200-205, 1997.

89. Lee, D., Jung, J., Lim, J., Huh, J., Lee, D., "Recognition of volatile organic compounds using SnO2 sensor array and pattern recognition analysis", *Sensors and Actuators B,* vol. 77, pp. 228-236, 2001.

90. Ulmer, H., Mitrovics, J., Noetzel, G., Weimar, U. and Gopel, W., "Odors and flavors identified with hybrid modular sensor systems", *Sensors and Actuators B,* vol. 43, pp. 24-33, 1997.

91. Wessa, T., Kuppers, S., Rapp, M. and Reibel, J., "Validation of an industrial analytical sensor procedure realized with a SAW-based sensor system", *Sensors and Actuators B,* vol. 70, pp. 203-213, 2000.

92. Yu, T.-C., Mitra, S. and McAllister, G. "Monitoring effluents from an air toxic control device using continuous nonmethane organic carbon analyzer", *American Industrial Hygiene Association Journal,* vol. 61, no. 1, pp. 16-21, 2000.

93. Emission Measurement Branch, Technical Support Division, OAQPS, US EPA, "Method 25 – Determination of total gaseous nonmethoane organic emissions as carbon", *Emission measurement technical information center NSPS Test Method*, EMTIC TM-25, June 18, 1993.

94. Mitra, S., Xu, Y., Chen, W. and McAllister, G. "Development of instrumentation for continuous on-line monitoring of non-methane organic carbon in air emissions", *Journal of Air & Waste Management Association*, vol. 48, pp. 743-749, 1998.

95. Mitra, S., Xu, Y., Chen, W. and McAllister, G., "Instrumentation for on-line monitoring of non-methane organic carbon in air", *Proceedings of the EPA/AWMA Conference on Measurement of Toxic and Related Compounds in Air*, Durham, NC, May 1997.

96. Mitra, S. and Lai, A. " A sequential valve-microtrap injection system for continuous, on-line gas chromatographic analysis at trace levels", *Journal of Chromatographic Science*, vol. 33, pp. 285-289, 1995.

97. Mitra, S., Xu, Y., Chen, W. and Lai, A., " Characteristics of microtrap-based injection systems for continuous monitoring of volatile organic compounds by gas chromatography", *Journal of chromatography A*, vol. 727, pp. 111-118, 1996.

98. Mitra, S. and Feng, C., "Development and field testing of a continuous NMOC (C-NMOC) monitor for VOCs in air emissions", *Measurement of Toxic and Related Air Pollutants, Symposium Courses*, Gary, NC, September 1998

99. Kang, D., Aneja, V. P., Zika, R. G., Farmer, C., Ray, J. D., "Nonmethane hydrocarbons in the rural southeast United States national parks", *Journal of Geophysical Research D: Atmospheres,* vol. 106, no. 3, pp. 3133-3155, 2001.

100. Patel, S.H. and Xanthos, M. "Special Report Volatile Emissions During Thermoplastics Processing – A Review", *Advances in Polymer Technology*, vol. 14, no. 1, pp. 67-77, 1995.

101. Chiantore, O. and Guaita, M., "Experimental and methodological aspects in the characterization of polymers undergoing degradation", *Journal of Applied Polymer Science*: Applied Polymer Symposium 52, pp. 1-10, 1993.

102. Haines, P. J., *Thermal Methods of Analysis - Principles, Applications and Problems*, Blackie Academic & Professional, UK, pp. 4, 22-23, 64-65, 1995.

103. Wendlandt, W. Wm., *Thermal Analysis*, third edition, John Wiley & Sons, pp. 190-200, 424-442, 1986.

104. Wu, C.H., Chang, C.Y. and Lin, J.P., "Effects of moisture on pyrolysis of polypropylene", *J. Environ. Eng.*, vol. 124, no. 9, pp. 892-896, 1998.

105. Dollimore, D. and Phang, P., "Thermal analysis", *Analytical Chemistry*, vol. 72, no. 12, pp. 27R-36R, 2000; D. Dollimore adn S. Lerdkanchanaporn, "Thermal analysis", *Analytical Chemistry*, vol. 70, no. 12, pp. 27R-35R, 1998; D. Dollimore, "Thermal analysis", *Analytical Chemistry*, vol. 68, no. 12, pp. 63R-71R, 1996.

106. Smith, P. B., Pasztor, A. J. Jr., McKelvy, M. L., Meunier, D. M., Froelicher, S. W. and Wang, F. C.-Y., "Analysis of synthetic polymers and rubbers", *Analytical Chemistry*, vol. 69, no. 12, 95R-121R, 1997.

107. Ballice, L., Yuksel, M., Saglam, M., Reimert, R. and Schulz, H., "Classification of volatile products from the temperature-programmed pyrolysis of low- and high-density polyethylene", *Energy & Fuels*, vol. 12, no. 5, pp. 925-928, 1998.

108. Adams, K., J. Bankston, A. Barlow, M. W. Holdren, J. Meyer and V. J. Marchesani, "Development of emission factors for polypropylene processing", *J. Air & Waste Manage. Assoc.*, vol. 49, pp. 49-56, 1999.

109. Barlow, A., D.A. Contos, M.W. Holdren, P.J. Garrison, L.R. Harris and B. Janke, "Development of emission factors for polyethylene processing", *J. Air & Waste Manage. Assoc.*, vol. 46, pp. 569-580, 1996.

110. Barlow, A., P. Moss, E. Parker, T. Schroer, M.W. Holdren and K. Adams, "Development of emission factors for ethylene-vinyl acetate and ethylene-methyl acryltate copolymer processing", *J. Air & Waste Manage. Assoc.*, vol. 47, pp. 1111-1118, 1997.

111. Zhu, J., Zhang, J. and Shaw, C., "Chemical composition analysis and its application in estimation of VOC emission rates from hydrocarbon solvent-based indoor materials", *Chemosphere*,, vol. 39, no. 14, pp. 2535-2547, 1999.

112. Lytle, C. A., Bertsch, W. and McKinley, M., "Determination of novolac resin thermal decomposition products by pyrolysis-gas chromatography-mass spectrometry", *Journal of Analytical and Applied Pyro*lysis, vol. 45, pp. 121-131, 1998.

113. Wolf, M., Riess, M., Heitmann, D., Schreiner, M., Thoma, H., Vierle, O. and Van Eldik, R. "Application of a purge and trap TDS-GC/MS procedure for the determination of emissions from flame retarded polymers", *Chemosphere*, vol. 41, pp. 693-699, 2000.

114. Villberg, K., Veijanen, A., Gustafsson, I., Wickstrom, K., "Analysis of odour and taste problems in high-density polyethene", *Journal of Chromatography A,* vol. 791, pp. 213-219, 1997.

115. Villberg, K. and Veijanen, A., "Analysis of a GC/MS thermal desorption system with simultaneous sniffing for determination of off-odor compounds and VOCs in fumes formed during extrusion coating of low-density polyethylene", *Analytical Chemistry*, vol. 73, no. 5, pp. 971-977, 2001.

116. Hodgson, S. C., Casey, R. J., Bigger, S. W. and Scheirs, J., "Review of volatile organic compounds derived from polyethylene", *Polymer-Plastics Technology and Engineering,* vol. 39, no. 5, pp. 845-874, 2000.

117. Patel, S. H. and Xanthos, M., "Environmental issues in polymer processing: A review on volatile emissions and material/energy recovery options", *Advances in Polymer Technology*, vol. 20, no. 1, pp. 22-41, 2001.

118. Xiang, Q., Mitra, S., Xanthos, M. and Dey, S.K., "Evolution and kinetics of volatile organic compounds (VOCs) generated during low temperature polymer degradation", *J. Air & Waste Manage. Assoc.*, in press, 2001.

119. Tolnai, B., Hlavay, J., Möller, D., Prümke, H., Becker, H. and Dostler, M., "Combination of canister and solid adsorbent sampling techniques for determination of volatile organic hydrocarbons", *Microchemical Journal*, vol. 67, pp. 163-169, 2000.

120. Schumacher, B. A. and Ward, S. E., "Quantitation reference compounds and VOC recoveries from soil by purge-and trap GC/MS", *Environmental Science & Technology*, vol. 31, no. 8, pp. 2287-2291, 1997.

121. Moore, J. Jr., "Barriers to using field analytical technology instrumetns as an example adoption", *Environ. Sci. Technol.,* vol. 28, no. 4, pp. 193A-195A, 1994. McDonald, W. C., Erickson, M. D., Abraham, B. M. and Robbat, A. Jr., "Developments and applications of field mass spectrometers", *Environ. Sci. Technol.,* vol. 28, no. 7, pp. 336A-343A, 1994. Poppiti, J., "The role of field testing in environmental measurements", *Environ. Sci. Technol.,* vol. 28, no. 12, pp. 536A-539A, 1994.

122. Mitra, S. and Yun, C., "Continuous gas chromatographic monitoring of low concentration sample streams using an on-line microtrap", *Journal of Chromatography*, vol. 648, pp. 415-421, 1993.

123. Feng, C. and Mitra, S., "Two-stage microtrap as an injection device for continuous on-line gas chromatographic monitoring", *Journal of Chromatography A*, vol. 805, pp. 169-176, 1998.

124. Chen, W., Xu, Y. H., Mitra, S., *Journal of Microcolumn Separations*, vol. 11, no. 3, pp. 239-245, 1999.

125. Xu, Y. and Mitra, S., "Continuous monitoring of volatile organic compounds in water using on-line membrane extraction and microtrap gas chromatography system", *Journal of Chromatography A*, vol. 688, pp. 171-180, 1994.

126. Mitra, S., Zhu, N., Zhang, X. and Kebbekus, B., "Continuous monitoring of volatile organic compounds in air emissions using an on-line membrane extraction–microtrap–gas chromatographic system", *Journal of Chromatography A*, vol. 736, pp. 165-173, 1996.

127. Mitra, S., Zhang, L., Zhu, N. and Guo, X., "Characteristic of on-line membrane microtrap GC system as applied to air and water monitoring", *Journal of microcolumn Separations*, vol. 8, no. 1, pp. 21-27, 1996.

128. Zhang, L., Guo, X. and Mitra, S., "Using a composite membrane for enhanced sensitivity and faster response in on-line membrane extraction microtrap gas chromatography", *Environmental Monitoring and Assessment*, vol. 44, pp. 529-540, 1997.

129. Overton, E. B., Stewart, M., Carney, K. R., "Instrumental considerations for reliable fieldable VOC analyses", *Journal of Hazardous Materials*, vol. 43, pp. 77-89, 1995.

130. Hart, K. J., Dindal, A. B. and Smith, R. R., "Monitoring volatile organic compounds in flue gas using direct sampling ion trap mass spectrometry", *Rapid Communications in Mass Spectrometry*, vol. 10, pp. 352-360, 1996.

131. Mita, S., Feng, C., Zhang, L., Ho, W. and McAllister, G., "Microtrap interface for on-line mass spectrometric monitoring of air emissions", *Journal of Mass Spectrometry*, vol. 34, pp. 478-485, 1999.

132. Goldthorp, M. D. and Lambert, P., "Use of a portable infra-red analyzer for low-level hydrocarbon emissions", *Journal of Hazardous Materials*, vol. 83, pp. 135-152, 2001.

133. Bisio, A.L. and Xanthos, M. eds. *How to Manage Plastics Waste*, Carl Hanser Verlag, New York, pp. 69-78, 83-90, 145,165,1994.

134. Westerhout, R. W. J., Waanders, J., Kuipers, J. A. M. and van Swaaij, W. P. M., "Kinetics of the low-temperature pyrolysis of polyethene, polypropene, and polystyrene modeling, experimental determination, and comparison with literature models and data", *Ind. Eng. Chem. Res.*, vol. 36, pp. 1955-1964, 1997.

135. Chan, J. H. and Balke, S. T., "The thermal degradation kinetics of polypropylene: Part III. Thermogravimetric analyses", *Polym. Degrad. Stab.*, vol. 57, pp. 135-149, 1997.

136. Bockhorn, H., Hornung, A., Hornung, U. and Schawaller, D., "Kinetic study on the thermal degradation of polypropylene and polyethylene", *J. Anal. Appl. Pyrolysis*, vol. 48, pp. 93-109, 1999.

137. Sezgi, N. A.; Cha, W.S., Smith, J. M. and McCoy, B. J., "Polyethylene pyrolysis: Theory and experiments of molecular-weight-distribution kinetics", *Ind. Eng. Chem. Res.*, vol. 37, no. 7, pp. 2582-91, 1998.

138. Kao, C. Y., B. Z. Wan and W. H. Cheng, "Kinetics of hydrolytic depolymerization of melt poly(ethylene terephthalate)", *Ind. Eng. Chem. Res.*, 1998, 37:4, 1228-34.

139. Lin, J. P. and Chang, C. Y., "Pyrolytic treatment of rubber waster: Pyrolysis kinetics of styrene-butadiene rubber", *J. Chem. Technol. Biotechnol.*, vol. 66, pp.7-14, 1996.

140. Chen, K. S., Yeh, R. Z. and Chang, Y. R., "Kinetics of thermal decomposition of styrene-butadiene rubber at low heating rates in nitrogen and oxygen", *Combust. Flame*, vol. 108, pp. 408-418, 1997.

141. Oh, S.C., Lee, H. P., Yi, S. and Yoo, K. O., "Kinetics of the nonisothermal degradation of styrene-butadiene rubber", *J. Fire Sci.*, vol. 17, pp. 362-377, 1999.

142. Howe, G. B., Sherrill, S.T. and Jayanty, R. K., *Method 25 – Varian Instrument Evaluation*, RTI/5960/195-01D, USEPA, 1993.

143. Koch, E., *Nonisothermal Reaction Analysis*, Academic Press Inc., New York, USA, 1977.

144. Dunkerton, L. V., Mitra, S., Phillips, J. B., Smith, G. V., Hinckley, C. C. and Wiltonwska, T., "Migration of sulphur from organic to the inorganic phase under hydrodesulphurization conditions", *Fuel*, vol. 67, pp. 967–972, 1988.

145. Narh, K A., Xanthos, M., Li, Z., Dey, S. K., Yilmazer, U. and Li, Y., "Simulation of the intrusion process for thick walled thermoplastics – Product and process characteristics", *Proc. 56th SPE ANTEC,* vol. 44, pp. 1767, 1998.

146. Yilmazer, U., Xanthos, M., Dey, S. K., Mitra, S. and Feng, C., "Mechanical and thermal properties and leachate analysis of carpet residue / polyethylene prototypes for building and construction applications", *Proc. 57th SPE ANTEC*, vol. 45, pp. 3265, 1999.

147. Rodriguez, F., *Principles of Polymer Systems,* 4th Edition, Taylor & Francis, pp. 55-75, 1996.

148. Kato, M. and Osawa, Z. "Effects of stereoregularity on the thermo-oxidative degradation of polypropylenes", *Polym. Degrad. Stab.*, vol. 65, pp. 457-461, 1999.

149. Gambiroza-Jukic, M. and Cunko, R., "Kinetics of the thermal degradation of polypropylene fibres", *Acta Polym.*, vol. 43, pp. 258-260, 1992.

150. Verdu, S. and Verdu, J., "A new kinetic model for polypropylene thermal oxidation at moderate temperatures", *Macromolecules*, vol. 30, pp. 2262-2267, 1997.

151. Waldman, W. R. and De Paoli, M. A., "Thermo-mechanical degradation of polypropylene, low-density polyethylene and their 1:1 blend", *Polym. Degrad. Stab.*, vol. 60, pp. 301-308, 1998.

152. Cooney, J. D., Day, M. and Wiles, D. M., "Thermal degradation of poly(ethylene terephthalate): A kinetic analysis of thermogravimetric data", *Journal of Applied Polymer Science*, Vol. 28, pp. 2887-2902, 1983.

153. Jellinek, H. H., *Polymer Science*, Vol. 3, pp. 850, 1948.

154. Amelin, A. V., Pozdnyakow, O. F., Regel, V. R. and Sanfirova, T. P., *Soviet Physics-Solid State*, vol. 12, 9 2034, 1971.

155. La Mantia, F.P., Capizzi, L., "Recycling of compatibilized and uncompatibilized nylon/polypropylene blends", *Polymer Degradation and Stability*, vol. 71, no. 2, pp. 285-291, 2001..

156. Wyser, Y., Leterrier, Y. Manson, J.-A.E., "Effect of inclusions and blending on the mechanical performance of recycled multilayer PP/PET/SiOx films", *Journal of Applied Polymer Science*, vol. 78, no. 4, pp. 910-918, Oct, 2000.

157. Tall, S., Karlsson, S., Albertsson, A.-Ch., "Improvements in the properties of mechanically recycled-thermoplastics", *Polymers & Polymer Composites*, vol. 6, no. 5, pp. 261-267, 1998.

158. Charbonneau, Mark T., "Effects of recycle history on the mechanical characteristics of long glass fiber reinforced polypropylene", Annual Technical Conference – ANTEC, *Conference Proceedings Special Areas Proceedings of the 1997 55th Annual Technical Conference, ANTEC. Part 3*, April 27 – May 2 1997, vol. 3, pp. 2920-2923, 1997,Toronto, Canada.

159. Bied-Charreton, B., "Closed loop recycling of lead/acid batteries", *Journal of Power Sources*, vol. 42, no. 1-2, pp. 331-334, Jan 29, 1993.

160. Tomlins, Paul, Scoggins, Clive, "Saving more waste plastics from the scrap heap", *Materials World*, vol. 7, no. 3, pp. 137-138, 1999.

161. Czvikovszky, T., Hargitai, H., "Compatibilization of recycled polymers through radiation treatment", *Radiation Physics and Chemistry*, vol. 55, no. 5, pp. 727-730, 1999.

162. Marrone, M., La Mantia, F.P., "Re-stabilisation of recycled polypropylenes", *Polymer Recycling*, vol. 2, no. 1, pp. 17-26, 1996.

163. Czvikovszky, T., Hargitai, H , "Electron beam surface modifications in reinforcing and recycling of polymers", *Nuclear Instruments & Methods in Physics Research, Section B: Beam Interactions with Materials and Atoms*, vol. 131, no. 1-4, pp. 300-304, 1997.

164. Schwarzenbach, K. In: Gachter, R, Muller H, editors. *Plastics Additives*. Munich: Carl Hanser Verlag, pp. 1-70, 1983.

165. Ryu, SH, Gogos, CG, Xanthos, M. "Parameters affecting process efficiency of peroxide initiated controlled degradation of polypropylene", *Adv Polym Technol* vol. 11, no. 2, pp.121, 1991/92..

166. Canevarolo, S. V., "Chain scission distribution function for polypropylene degradation during multiple extrusions", *Polym Degrad Stab* vol. 70, no.1, pp.71-76, 2000.

167. Hinsken, H, Moss, S, Pauquet, JR, Zweifel, H. "Degradation of polyolefins during melt processing" *Polym Degrad Stab*, vol. 34, pp. 279-293, 1991.

168. Gonzalez-Gonzalez, VA, Neira-Velazquez, G, Angulo-Sanchez, JL. "Polypropylene chain scissions and molecular weight changes in multiple extrusion", *Polym Degrad Stab*, vol. 60, pp. 33-42, 1998.

169. Stadler, U., "Impact of stabilization additives on the controlled degradation of polypropylene", *The International Conference on Polyolefins, Polyolefins 2001*, pp. 521-542, February 25-28, 2001. Houston, TX.

170. Staicu, Doina, Banica, Gabriela, Stoica, Stela, "Photo-oxidative resistance of reprocessed polypropylene", *Polymer Degradation and Stability*, vol. 46, no.2, pp. 259-262, 1994.

171. Guerrica-Echevarria, G, Eguiazabal, JI, Nazabal, J. "Effects of reprocessing conditions on the properties of unfilled and talc-filled polypropylene", *Polym Degrad Stab,* vol. 53, pp. 1-8, 1996.

172. Incarnato, Loredana, Scarfato, Paola, Gorrasi, Giuliana, Vittoria, Vittoria, Acierno, Domenico, "Structural modifications induced by recycling of polypropylene", *Polymer Engineering and Science*, vol. 39, no. 9, pp. 1661-1666, 1999.

173. Incarnato, Loredana, Scarfato, Paola, Acierno, Domenico, "Rheological and mechanical properties of recycled polypropylene", *Polymer Engineering and Science,* vol. 39, no. 4, pp. 749-755, 1999.

174. Tiganis, B.E., Shanks, R.A., Long, Yu, "Effects of processing on the microstructure, melting behavior, and equilibrium melting temperature of polypropylene", *Journal of Applied Polymer Science*, vol.59, no4, pp. 63-671, Jan 24, 1996.

175. Waldman, W. R., De Paoli, M. A., "Thermo-mechanical degradation of polypropylene, low-density polyethylene and their 1:1 blend", *Polym. Degrad. Stab.*, vol. Pp. 01-308, 1998.

176. Chan, J. H., Balke, S. T., "The thermal degradation kinetics of polypropylene: Part I. Molecular weight distribution", *Polym. Degrad. Stab.*, vol. 57, pp.113-125, 1997.

177. George, G. A., Celina, M., Vassallo, A. M., Cole-Clarke, P. A., "Real-time analysis of the thermal oxidation of polyolefins by FT-IR emission", *Polym. Degrad. Stab.*, vol. 48, pp.199-210, 1995.

178. Kato, M., Osawa, Z., "Effects of stereoregularity on the thermo-oxidative degradation of polypropylenes", *Polym. Degrad. Stab.*, vol. 65, pp. 457-46, 1999.

179. Garton, A., Carlsson, D. J., Wiles, D. M., "Role of polymer morphology in the oxidation of polypropylene", *Journal of Polymer Science: Polymer Chemistry Edition*, vol. 16, pp.33-40, 1978.

180. Weber, W. J., "Adsorption", Chapter 5 *in Physical Processes for Water Quality Control*, John Wiley & Sons, Inc., New York, pp. 199, 1977.

181. Conder, J. R. and Young, C. L., *Physicochemical Measurement by Gas Chromatography*, John Wiley & Sons, Inc., New York, 1979.

182. Kiselev, A. V. and Yashin, Y. I., *Gas Adsorption Chromatography*, Plenum Press, New York, 1969.

183. Betz, W. R., Maroldo, S. G., Wachob, G. D. and Firth, M. C., "Characterization of carbon molecular sieves and activated charcoal for use in airborne contaminant sampling", *Am. Ind. Hyg. Assoc. J.*, vol. 50, no. 4, pp. 181-187, 1989.

184. Betz, W. R. and Supina, W. R., "Use of thermally modified carbon black and carbon molecular sieve adsorbents in sampling air contaminants", *Pure & Appl. Chem.*, vol. 61, no. 11, pp. 2047-2050, 1989.

185. Betz, W. R. and Lambiase, S. J., "Dynamic gas-solid chromatographic techniques for characterizing carbon molecular sieves", *Journal of Chromatography*, vol. 556, pp. 433-440, 1991.

186. Betz, W. R., Ho, K. S., Hazard, S. A. and Lambiase, S. J., "Dynamic gas chromatographic techniques for the characterization of carbon-based adsorbents utilized in air sampling", Chapter 6 *in Sampling and Analysis of Airborne Pollutants*, pp. 91-100, Lewis Publishers, 1993.

187. Chiang, Y.-C., Chiang, P.E., Chiang, P.-C., Chang, P.E. and Chang, E.-E., "Effects of surface characteristics of activated carbons on VOC adsorption", *Journal of Environmental Engineering*, vol. 127, issue 1, pp. 54-62, 2001.

188. Harper, M., Coyne, L. S. and Florito, D. L., "Validation of sorbent sampling methods for methylene chloride", *Appl. Occup. Environ. Hyg.*, vol. 9, no. 3, pp. 198-205, 1994.

189. Lu, C. J. and Zellers, E. T., "A dual-adsorbent preconcentrator for a portable indoor-VOC microsensor system", *Analytical chemistry*, ASAP, 2001.

190. Harper, M., "Evaluation of solid sorbent sampling methods by breakthrough volume studies", *Ann. Occup. Hyg.,* vol. 37, no. 1, pp. 65-88, 1993.

191. Zaranski, M. and Bidleman, T., "High volume elution chromatography of dichlorobenzenes on a polyurethane foam-Tenax sandwich cartridge", *Journal of Chromatography*, vol. 409, pp. 235-242, 1987.

192. Vidal-Madjar, C., Gonnord, M., Benchanh, F. and Guiochon, G., "Performances of various adsorbents for the trapping and analysis of organohalogenated air pollutants by gas chromatography", *Journal of Chromatographic Science*, vol. 16, pp. 190-196, 1978.

193. Simon, V., Riba, M., Waldhart, A. and Torres, L., "Breakthrough volume of monoterpenes on Tenax TA: influence of temperature and concentration for α-pinene", *Journal of Chromatography A*, vol. 704, pp. 465-471, 1995.

194. Liteanu, C., Popescu, I. C. and Hopirtean, E., *Analytical Chemistry*, vol. 48, pp. 2010, 1976,

195. Wood, G. O. and Moyer, E. S., "A review and comparison of adsorption isotherm equations used to correlate and predict organic vapor cartridge capacities", *American Industrial Hygiene Association Journal*, vol. 52, pp. 235-242, 1991.

196. Yoon, Y. H. and Nelson, J. H., "Effects of humidity and contaminant concentration on respirator cartridge breakthrough", *American industrial Hygiene Association Journal*, vol. 51, no. 4, pp. 202-209, 1990.

197. Cohen, H. J., Briggs, D. E. and Garrison, R. P., "Development of a field method for evaluating the service lives of organic vapor cartridges – Part III: Results of laboratory testing using binary organic vapor mixtures", *American Industrial Hygiene Association Journal,* vol. 52, pp. 34-43, 1991.

198. Zellers, E. T., Morishita, M. and Cai, Q. Y., *Sensors and Actuators B*, vol. 67, no. 3, pp. 244-253, 2000.

199. Bertoni, G., Bruner, F., Liberti, A. and Perrino, C., "Some critical parameters in collection, recovery and gas chromatographic analysis of organic pollutants in ambient air using light adsorbents", *Journal of Chromatography*, vol. 203, pp. 263-270, 1981.

200. Manura, J. J., "Calculation and use of breakthrough volume data"; "Selection and use of adsorbent resins for purge and trap thermal desorption applications"; "Preparation and conditioning of desorption tubes and resin beds", *SISWEB™ Application Note*, 32, Scientific Instrument Services, Inc., NJ.

201. Mitra, S., *Ph.D. Dissertation*, Southern Illinos University, Casrbondale, IL, 1987.

202. Chen, Y., "A thermal desorption modulator for continuous monitoring of volatile organic compounds" *MS Thesis*, New Jersey Institute of Technology, Newark, NJ, January 1993.

203. Xu, Y., "Continuous monitoring of volatile organic compounds using microtrap based gas chromatographic systems", *Ph.D. Thesis*, New Jersey Institute of Technology, Newark, NJ, May 1996.

204. Feng, C. and Mitra, S. "Breakthrough and desorption characteristics of a microtrap", *Journal of microcolumn Separations*, vol. 12, no. 4, pp. 267-275, 2000.

205. Cropper, F. R. and Kaminsky, S., "Determination of toxic organic compounds in admixture in the atmosphere by gas chromatography", *Analytical Chemistry*, vol. 35, no. 6, pp. 735-743, 1963.

206. Health and Safety Executive, *Methods for the Determination of Hazardous Substances, Laboratory Method Using Pumped Solid Sorbent Tubes, Thermal Desorption and Gas Chromatography*, MDHS 72, HSE, London, 1992.